

**LUBRICATION AND TRIBOLOGICAL  
PERFORMANCE OPTIMIZATIONS FOR MICRO-  
ELECTRO-MECHANICAL SYSTEMS**

BY

**LEONG YONGHUI, JONATHAN**  
*B. Eng (Hons), NUS*

**A THESIS SUBMITTED  
FOR THE DEGREE OF NUS-IMPERIAL COLLEGE  
JOINT DOCTOR OF PHILOSOPHY  
DEPARTMENT OF MECHANICAL ENGINEERING  
NATIONAL UNIVERSITY OF SINGAPORE**

2012

## Preface

This thesis is submitted for the Joint Degree of Doctor of Philosophy with National University of Singapore and Imperial College London, under the supervision of Dr. Hugh Alexander Spikes and Dr Sujeet Kumar Sinha. The works presented in this thesis have been submitted, under review for publication or have been published for publication as listed below:

### Journal Papers and Patents:

1. **Jonathan, L. Y., Harikumar, V., Satyanarayana, N. and Sinha, S. K.** (2010). "Localized lubrication of micromachines: A feasibility study on Si in reciprocating sliding with PFPE as the lubricant." *Wear* **270**(1-2): 19-31.
2. **Sinha, S. K., Jonathan, L. Y., Satyanarayana, N., Yu, H., Harikumar, V. and Zhou, G.** (2010). "Method of applying a lubricant to a micromechanical device." U.S. Provisional Patent, 61/314,627. Filing date: 17 March 2010
3. **Hongbin, Y. Guangya Z., Sinha S. K. Leong J. Y. Fook Siong Chau,** "Characterization and Reduction of MEMS Sidewall Friction Using Novel Microtribometer and Localized Lubrication Method", Journal of Microelectromechanical Systems, 2011. **20**(4): p. 991-1000.
4. **J. Y. Leong, T. Reddyhoff, S. K. Sinha, A. S. Holmes, H. A. Spikes,** *Hydrodynamic Friction Reduction in a MAC-Hexadecane Lubricated MEMS Contact*, Tribology Letters, 2013, **49**, p. 217-225, ISSN:1023-8883
5. **Leong Y. Jonathan, N. Satyanarayana and Sujeet K. Sinha,** *A tribological study of Multiply-Alkylated Cyclopentanes and Perfluoropolyether lubricants*

*for application to Si-MEMS devices, Tribology Letters, In Press*

6. **J. Y. Leong, T. Reddyhoff, S. K. Sinha, H. A. Spikes, A. S. Holmes**, *Liquid Containment on Silicon Surfaces*, Manuscript prepared
7. **J. Y. Leong, Tian Feng, Loy Xing Zheng Keldren, N. Satyanarayana, Sujeet K. Sinha**, *Localized Lubrication on sidewalls of reciprocating MEMS contacts using PFPE and MAC lubricants*, Submitted to Tribology Letters

#### **Book Chapters:**

1. L. Y. Jonathan, N. Satyanarayana and S. K. Sinha., “Localized Lubrication of Micromachines – A Novel Method of Lubrication on Micromechanical Devices”, in “Nano-Tribology and Materials Issues in MEMS” (Eds: S. K. Sinha, N. Satyanarayana and S. C. Lim), Springer-Verlag, Berlin, Germany, 2012, in press.

#### **Conference Papers/Presentations:**

TriboUK 2012, Southampton

- Poster Presentation, “Lubricant Additives to Reduce Boundary and Hydrodynamic Friction in Silicon MEMS”, *J. Y. Leong, L. Tonggang, T. Reddyhoff, S. K. Sinha, A. S. Holmes, H. A. Spikes*, Imperial College London, UK & National University of Singapore, Singapore

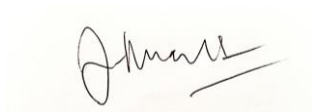
STLE 2010, Atlanta

- Paper presentation, “Localized Lubrication of Micro-Machines”, *J. Leong, H. Vijayan, N. Satyanarayana, S. Sinha*, National University of Singapore, Singapore
- Poster Presentation, “Localized Lubrication – A Novel Method of Lubricant Application to MEMS Devices”, *J. Leong, H. Vijayan, N. Satyanarayana, S. Sinha*, National University of Singapore, Singapore

## **Declaration**

I hereby declare that the thesis is my original work and it has been written by me in its entirety. I have duly acknowledged all the sources of information which have been used in the thesis.

This thesis has also not been submitted for any degree in any university previously.

A handwritten signature in black ink, appearing to read 'Jonathan', is centered on a light-colored rectangular background.

---

Leong Yonghui, Jonathan

10 October 2012

## **Acknowledgements**

First of all, I would like to express my deep thanks to my supervisors Sujeet Sinha Kumar and Hugh Spikes, and also to Tom Reddyhoff for their patience and guidance throughout the research and dissertation writing. I have been honoured to work with each of you and have learned much indeed.

I also wish to express my gratitude to the academic and technical staff in Materials Lab, National University of Singapore, and in the Tribology Lab, Imperial College London.

I am extremely thankful to all my labmates in Imperial College for providing me a conducive and warm environment in which we could learn and have fun together! Thank you for the times we had working, playing and chatting together – special mention goes to Oana, “Ponjac”, Jason and Jessika; who have become true friends during my short time in London.

I am grateful for all the guidance showered upon me by my elders and betters through the years of education, and I thank each of my teachers and mentors who have influenced me along the way.

I am deeply indebted to my family and loved ones, without whom this PhD would have been much more difficult. Your support and encouragement has driven me all these years. Thanks go to my wife-to-be for being strong during this time.

And lastly, to God Almighty, for His mercy and grace through this season.

## Table of Contents

Preface .....	i
Declaration .....	iv
Acknowledgements .....	v
Table of Contents.....	vi
List of Figures.....	ix
List of Tables .....	xv
List of Equations.....	xvii
Abstract.....	1
Chapter 1 - Introduction .....	3
1.1 Introduction to Tribology.....	4
1.2 Introduction to MEMS.....	4
1.3 Objectives of study .....	6
1.4 Scope of thesis .....	7
Chapter 2 - Literature Review .....	10
2.1 Issues with MEMS reliability and difficulties in lubrication .....	11
2.1.1 Release Stiction.....	12
2.1.2 In-use Stiction.....	14
2.1.3 Friction, Wear and Lubrication .....	14
2.2 Surface energy, surface tension and hydro/oleophobicity.....	16
2.3 Studies on solutions to MEMS Tribology .....	19
2.3.1 Surface Films and Treatments .....	20
2.3.2 Vapour Phase.....	23
2.3.3 Liquid lubrication.....	23
2.3.4 The “Half-Wetted Bearing” .....	26
2.4 Liquid Spreading and Starvation .....	28
2.5 Obstacles with current methods of lubrication.....	31
2.6 Lubricants for MEMS Tribology.....	33
2.6.1 Perfluoropolyether (PFPE) .....	33
2.6.2 Multiply Alkylated Cyclopentanes (MACs).....	35
Chapter 3 - Materials and Experimental Methodology .....	40
3.1 Materials .....	41
3.1.1 Silicon.....	41

3.1.2	Perfluoropolyether (PFPE) .....	41
3.1.3	Hexadecane .....	42
3.1.4	Multiply Alkylated Cyclopentanes (MAC) .....	43
3.1.5	Octadecylamine.....	43
3.2	Surface analysis equipment and techniques .....	44
3.2.1	Contact angles .....	44
3.2.2	Surface Profiling.....	44
3.2.3	Microscopy.....	45
3.2.4	Friction and wear tests .....	46
Chapter 4	- Localized Lubrication (“Loc-Lub”) – A Novel Method .....	57
4.1	Introduction and Objective.....	58
4.2	Materials and Methodology .....	58
4.3	Experimental Results .....	60
4.3.1	Water contact angle measurements .....	60
4.3.2	Optical Profiling and Ellipsometry .....	61
4.3.3	Friction and Wear Life.....	64
4.3.4	Surface analysis and film morphology.....	69
4.4	Conclusion .....	79
Chapter 5	- Comparison of MAC and PFPE Lubricants under “Loc-Lub” .....	81
5.1	Introduction and Objective.....	82
5.2	Materials and methodology.....	82
5.3	Experimental results.....	82
5.3.1	Contact Angle Measurements .....	82
5.3.2	Spreading of lubricant.....	83
5.3.3	Reciprocating Wear Tests .....	87
5.3.4	Optical Microscopy.....	90
5.3.5	FESEM and EDS analysis .....	96
5.4	Discussion .....	97
5.5	Conclusion .....	101
Chapter 6	- “Localized Lubrication” on Reciprocating MEMS Contacts .....	102
6.1	Introduction.....	103
6.2	Results.....	104
6.2.1	Wear Tests.....	104
6.2.2	Surface analysis .....	107
6.3	Discussion .....	114
6.3.1	Error in friction measurements.....	114



6.3.2	Effect of Roughness on Tribological Behaviour.....	116
6.3.3	Differences in Lubricant Life and Behaviour .....	118
6.4	Conclusions.....	122
Chapter 7	- Hydrodynamic Lubrication in MEMS.....	124
7.1	Introduction.....	125
7.2	Materials and Experimental Procedures .....	125
7.3	Experimental Results .....	126
7.3.1	Test lubricants and additives.....	126
7.3.2	Friction tests.....	126
7.4	Discussion .....	135
7.4.1	Possible origins of observed friction reduction .....	135
7.5	Conclusion .....	137
Chapter 8	- Barrier Coatings for Local Containment of Lubricant.....	139
8.1	Introduction.....	140
8.2	Materials and Experimental Procedures .....	141
8.3	Results .....	142
8.3.1	Contact Angle Measurements .....	142
8.3.2	Spin tests .....	144
8.3.3	Lubricant additives for non-spreading .....	147
8.4	Discussion .....	158
8.4.1	Differences between liquid behaviour in spin tests .....	158
8.4.2	Practical use of additives for non-spreading liquids .....	159
8.5	Conclusion .....	160
Chapter 9	- Conclusions and Future Work .....	161
9.1	Conclusions.....	162
9.1.1	“Localized Lubrication” Method.....	162
9.1.2	Reduction of Hydrodynamic friction.....	162
9.1.3	Lubricant Containment .....	163
9.2	Future work.....	164
9.2.1	“Localized Lubrication” on MEMS devices .....	164
9.2.2	Hydrodynamic friction reduction in MEMS .....	165
9.2.3	Anti-spreading methods and lubricant containment.....	165
References	.....	167

## List of Figures

Figure 1-1: Schematic of deep reactive ion etching (DRIE) fabrication process for MEMS.....	5
Figure 2-1: Direction of Laplace pressure for hydrophobic and hydrophilic surfaces .....	13
Figure 2-2: Contact angles of hydrophobic and hydrophilic surfaces.....	13
Figure 2-3: Failure of a micro-bearing after 91 seconds at 1720 Hz.....	15
Figure 2-4: Wetting states showing the a) apparent contact angle, b) contact angle from Wenzel’s model, and c) contact angle from the Cassie-Baxter model .....	18
Figure 2-5: Stribeck curve, showing coefficient of friction as a function of viscosity, speed and load .....	20
Figure 2-6: Schematic of a stepped pad bearing with stick of lubricant on the surfaces, resulting in separation of the contacts due to entrainment .....	25
Figure 2-7: Velocity profiles of fluid-lubricated gaps with the top surface sliding at a velocity, (top) normal conditions and (bottom) slip conditions .....	26
Figure 2-8: Map of occurrence of slip for a fully flooded, infinitely long linear slider bearing. ....	28
Figure 2-9: Oil droplets on plates of stainless steel, encircled within a fluorinated coating painted on with a brush.....	29
Figure 2-10: Nano-friction and nano-adhesion forces measured for treated and untreated silicon surfaces. ....	37
Figure 3-1: Schematic of the Loc-Lub setup for reciprocating sliding wear testing....	47
Figure 3-2: A video still capture of the Loc-Lub method applied to a reciprocating MEMS tribometer.....	47
Figure 3-3: Images of Loc-Lub setup for feasibility verification a) from the side, b) from the front and c) a schematic of the reciprocating wear tester .....	49
Figure 3-4: Schematic of the reciprocating tribometer.....	50
Figure 3-5: Schematic of the displacement sensing mechanism, with rotational grating .....	51
Figure 3-6: Closeup schematic of tribometer showing springs and loading .....	53

Figure 3-7: Screenshot of LabView VI used in motor control and data acquisition.....	54
Figure 3-8: Dimensions of etched stepped pad bearing used in experiments .....	54
Figure 3-9: Picture of the rotating MEMS Tribometer, with the laser path indicated with red arrows.....	55
Figure 3-10: Schematic for spin tests conducted on a spinning disc, with a silicon specimen and a drop of lubrication placed at the tested distance .....	56
Figure 4-1: Optical profile images of a) bare unpolished silicon, b) dip-coated unpolished silicon and c) unpolished silicon with localized lubrication, with their respective line profiles taken across the centre of the scan.....	62
Figure 4-2: Summary of results from Reciprocating Sliding Wear (R.S.W.) and Ball-On-Disc Tests, showing the initial and stable coefficient of friction (top) and wear lives of samples (bottom) .....	64
Figure 4-3: CoF data, taken over the duration of the test, with respect to the number of reciprocation cycles for different lubrication methods and PFPE concentrations for both a) polished and b) unpolished Si surfaces.....	65
Figure 4-4: Optical images at (a) lower magnification (50x) and (b) higher magnification (200x) for bare polished silicon.....	70
Figure 4-5: Optical Images for unpolished bare Si at (a) lower magnification (50x) and (b) higher magnification (200x) .....	70
Figure 4-6: Optical images for unpolished Si LL 4.0% at (a) lower magnification (50x) and (b) higher magnification (200x). .....	70
Figure 4-7: EDS element maps of fluorine (F) for unpolished Si samples lubricated with 4.0 wt% PFPE under a) dip-coating, b) localized lubrication, and c) vapour deposition.....	72
Figure 4-8: a) FESEM image and b) EDS mapping for the presence of fluorine (F), which is representative of PFPE lubricant .....	74
Figure 4-9: EDS mapping of element fluorine (F) for (a) area near wear track that has an overflow of lubricant, (b) area in the centre of the wear track, both after 540,000 cycles.....	74
Figure 4-10: EDS fluorine mapping for wear tracks of unpolished dip-coated Si samples (a) before and (b) after a 6 hour wear test; and samples undergone localized lubrication (c) before and (d) after a 6 hour wear test .....	76
Figure 4-11: a) SEM and b) EDS mapping for fluorine (F) of polished dip-coated Si surface.....	77

Figure 5-1: Spreading of MAC and PFPE lubricant with droplets outlined, showing the spreading of MAC lubricant a) upon dispense, b) 1 hour after dispense, c) 24 hours after dispense and PFPE lubricant d) upon dispense and e) 1 hour after dispense with no discernible shape, on cleaned Si surfaces .....84

Figure 5-2: Initial coefficient of friction for various lubricated Si surfaces under dip-coating (DC) and “Loc-Lub” (LL), conducted with the reciprocating wear test machine at a speed of 5 mm s<sup>-1</sup> and 50 g load.....87

Figure 5-3: Final coefficient of friction for samples that did not fail after 54,000 cycles (6 hour wear test), under dip-coating (DC) and "Loc-Lub" (LL) at a reciprocating speed of 5 mm s<sup>-1</sup> and 50 g load .....87

Figure 5-4: Wear lives (vertical log scale) of various Si samples lubricated via dip-coating (DC) and “Loc-Lub” method (LL), at a reciprocating speed of 5 mm s<sup>-1</sup> and 50 g load.....88

Figure 5-5: Silicon surfaces lubricated via dip-coating before wear test; a) Polished Si dip-coated with MAC, b) Polished Si dip-coated with PFPE, c) Unpolished Si dip-coated with MAC, and d) Unpolished Si dip-coated with PFPE.....90

Figure 5-6: Optical images of Si samples dip-coated with MAC and PFPE lubricant at 4.0 wt% after 6 hours (54,000) cycles of reciprocating sliding wear, at a reciprocating speed of 5mm s<sup>-1</sup> and 50 g load.....91

Figure 5-7: Optical images of silicon surfaces lubricated with “Loc-Lub” method with MAC and PFPE lubricant at 4.0 wt%, after 60 hours (540,000) cycles of wear tests, at a reciprocating speed of 5 mm s<sup>-1</sup> and 50 g load.....91

Figure 5-8: Optical image of wear track on polished silicon surface tested at 70g load and lubricated via “Loc-Lub” with 0.4 wt% MAC, after 540,000 cycles of wear test at 5 mm s<sup>-1</sup> .....94

Figure 5-9: Optical images of wear tracks for polished silicon surfaces after testing for 54,000 cycles at 5 mm s<sup>-1</sup> and 70 g load for a) 0.4 wt% PFPE, b) 4 wt% PFPE, c) 0.4 wt% MAC and d) 4 wt% MAC .....95

Figure 5-10: FESEM (left) and EDS mapping (right) for element C on silicon surfaces dip-coated with MAC lubricant (4 wt%), untested, and taken at 200x magnification .....96

Figure 5-11: FESEM (left) and EDS mapping (right) for element C on silicon surfaces dip-coated with MAC lubricant, after 540,000 cycles (60 hours) of reciprocating wear tests at 5 mm s<sup>-1</sup> and 50 g load, taken at 200x magnification .....97

Figure 6-1: Graph of PSD displacement voltage versus cycles for a PFPE-lubricated MEMS reciprocating tribometer ..... 105

Figure 6-2: Graph of PSD Displacement voltage versus cycles for a MAC-lubricated MEMS reciprocating tribometer ..... 105

Figure 6-3: Device life of MEMS Reciprocating Tribometers when under dry conditions and lubricated via “Loc-Lub” with PFPE or MAC.....	106
Figure 6-4: FESEM images of the MEMS Tribometer device, showing a) contacts lubricated with PFPE (x400), b) sidewall of the flat contact at x450 magnification, c) x2000 magnification, and d) x4500 magnification .....	107
Figure 6-5: FESEM and EDS imaging scans on untested PFPE lubricated devices, with fluorine as the representative element of PFPE .....	108
Figure 6-6: FESEM and EDS imaging scans for tested PFPE lubricated devices, with fluorine as the representative element of PFPE .....	109
Figure 6-7: a) FESEM image for MAC-lubricated MEMS sidewalls, and EDS imaging scans for MAC lubricated devices, b) tested and c) untested .....	110
Figure 6-8: Meniscus bridge of MAC lubricant between (left) silicon nitride ball and polished silicon wafer and (right) silicon nitride ball and unpolished silicon wafer, both just in contact .....	112
Figure 6-9: Image of lubricant trails on a polished silicon surface (top) and an unpolished silicon surface (bottom), and a comparison of the two trails when placed together with an indicated starting line. ....	113
Figure 6-10: Schematic of the proposed mechanism of depletion between the ball and flat contact upon sliding.....	114
Figure 6-11: Capillary forces due to condensation between surface, plotted for various roughness values and over varying humidity levels.....	116
Figure 6-12: Schematic for liquid meniscus behaviour against a flat surface and against asperities in a rough surface. ....	117
Figure 6-13: Schematic of lubricant behaviour for PFPE (left column) and MAC (right column) under flat-on-flat reciprocal sliding.....	120
Figure 6-14: Schematic of point-on-flat sliding for PFPE coated (left) and MAC coated (right) specimens.....	121
Figure 7-1: Friction coefficient versus speed for MEMS contacts lubricated with neat hexadecane, neat MAC, and a blend of 3 wt% MAC in hexadecane.....	127
Figure 7-2: Repeatability of experimental results across tests, using different specimens.....	128
Figure 7-3: Friction coefficient versus speed for MEMS contacts lubricated with hexadecane with varying percentages of MAC as additive.....	129

Figure 7-4: Plot of minimum coefficient of friction, friction measured at 15000 rpm and dynamic viscosity, all versus concentration of MAC additive in hexadecane. ...	130
Figure 7-5: Coefficient of friction versus speed for neat hexadecane, and a blend of squalane and hexadecane of 3.3 cP dynamic viscosity to match the viscosity value of 3 wt% MAC in hexadecane .....	131
Figure 7-6: Coefficient of friction versus speed for individual blends of octadecylamine and 2 wt% MAC in hexadecane, including a blend with all three liquids.....	132
Figure 7-7: Coefficient of friction versus speed for MEMS contacts lubricated with pure hexadecane, hexadecane with 0.1 wt% octadecylamine (ODA), and a compound blend of hexadecane with 0.1 wt% ODA and 1 wt% MAC.....	133
Figure 7-8: Coefficient of friction versus speed for neat squalane and squalane blended with 2 wt% MAC as additive.....	134
Figure 8-1: Schematic of silicon surfaces (left to right) after cleaning, after OTS SAM coating, and after selective modification using PDMS masking and plasma treatment .....	143
Figure 8-2: 1 $\mu$ l water droplets on a) OTS coated silicon, and b) on the circle of plasma-treated silicon surface.....	143
Figure 8-3: 1 $\mu$ l hexadecane droplets on a) OTS coated silicon and b) on the plasma treated circle and c) on bare silicon.....	144
Figure 8-4: Throw-off Forces for Spin Tests conducted on cleaned bare Si, Si coated with an OTS SAM (Si-OTS), and Si with selective OTS removal after coating (Si-OTS-mod).....	145
Figure 8-5: Throw-off forces for spin tests conducted on cleaned bare Si, Si coated with an OTS SAM (Si-OTS), and Si with selective OTS removal after coating (Si-OTS-mod).....	145
Figure 8-6: Frame captures from video taken at 30 fps of 0.2wt% ODA in hexadecane on a silicon surface, showing a) the droplet at application (frame 391), b) start of retraction at frame 511, c) frame 531, d) frame 541, e) frame 551, f) frame 561, g) frame 571, h) frame 581, i) frame 591, and j) frame 601 .....	149
Figure 8-7: Frames from video taken at 30 fps of 1 wt% DDA in hexadecane on silicon, with a) droplet prior to retraction at frame 341, b) start of retraction at frame 441, c) continued retraction at frame 541, d) frame 641, e) frame 741, f) frame 841, g) frame 941, h) frame 1041, i) frame 1141, j) and approximate stabilization at frame 1241.....	151
Figure 8-8: Plot of spreading area of the droplet vs. time for various blends of additives in hexadecane .....	152

Figure 8-9: Plot of spreading area of the droplet vs.  $\log(\text{time})$  for various blends of additives in hexadecane ..... 153

Figure 8-10: Plot of stable spread area versus dynamic viscosity for various concentrations of squalane and 3wt% MAC in hexadecane ..... 157

## List of Tables

Table 2-1: Water Contact Angles on various modified silicon surfaces .....	37
Table 3-1: Physical properties of perfluoropolyether (PFPE) lubricant Fomblin Z-dol 4000 .....	42
Table 3-2: Physical properties of MAC Lubricant, Nye Synthetic Oil 2001A.....	43
Table 4-1: Water contact angles for various Si surfaces.....	60
Table 4-2: Optical images for the wear tracks of different surfaces under different lubrication methods, after 6 hours of R.S.W test .....	69
Table 4-3: Levels of Element F detected from EDS scans in Figure 4-10 .....	75
Table 5-1: Water contact angles for silicon surface lubricated with various methods and lubricants.....	83
Table 5-2: Spreading of lubricants during and after contact when applied with the “Loc-Lub” method, using a glass slide as the larger counterface and a diced silicon wafer as the smaller counterface .....	85
Table 5-3: Initial and final coefficients of friction for wear tests conducted at higher loads and with various lubricants under Loc-Lub.....	89
Table 5-4: Optical images of wear track on polished silicon surfaces for various concentrations and types of lubricants and loads, after 540,000 cycles (60 hours) of reciprocating wear tests at $5 \text{ mm s}^{-1}$ .....	93
Table 7-1: Viscosities of mixtures used in tests, measured with a Stabinger viscometer .....	126
Table 7-2: Contact angles of 1 $\mu\text{l}$ of liquid on various surfaces .....	136
Table 8-1: Contact angles performed on various silicon surfaces.....	142
Table 8-2: Categorization of the tested blends under the four types of spreading observed. ....	148
Table 8-3: Contact angles of various blends on silicon after droplet retraction. 5 $\mu\text{l}$ of liquid was used in each blend application.....	153
Table 8-4: Contact angles made when 1 $\mu\text{l}$ of test fluid is placed on bare and MAC-coated silicon wafers .....	155



Table 8-5: Dynamic viscosities of 3wt% MAC in hexadecane and various concentrations of squalane in hexadecane. .... 157

## List of Equations

Equation 2-1: Laplace Equation .....	12
Equation 2-2: Relation of surface energy with contact angles.....	16
Equation 2-3: Approximation of interfacial energy between the solid and liquid interface from respective surface energies .....	16
Equation 2-4: Wenzel’s equation accounting for roughness effects on contact angles .....	17
Equation 2-5: Cassie-Baxter model accounting for roughness and surface fraction effect on contact angles.....	17
Equation 3-1: Mechanical deflection of MEMS tribometer .....	51
Equation 3-2: Formula for centripetal force exerted on liquid droplet under spin tests .....	56
Equation 6-1: Adhesion force model for a capillary meniscus between a rough sphere and a flat surface .....	117
Equation 6-2: Free energy cost required of liquid bridge to overcome defects in a surface in capillary condensation on rough surfaces.....	118
Equation 7-1: Relation of hydrodynamic friction to dynamic viscosity according to Reynolds’s theory .....	135

## **Abstract**

Lubricants and lubrication have been of great interest to mankind since the introduction of machines with sliding/rolling surfaces into everyday life. With the recent trend of miniaturization, Micro-Electro-Mechanical Systems (MEMS) have taken centre stage, featuring components with scales in dimensions as small as nanometres. At this scale, friction depends less on inertial forces (e.g. gravity), and more on surface forces such as surface tensions and free energies, van der Waals forces, capillary forces and electrostatic forces. These strong surface influences on the phenomena of friction and wear at the micro- and nano-scale have spawned a new area of research in micro- and nano-tribology. In this PhD study, two approaches to solving MEMS tribology problems have been pursued. In the first approach, a direct lubrication method using well-known lubricants such as perfluoropolyether (PFPE) and multiply alkylated cyclopentane (MAC) was developed. Extensive tribological tests using reciprocating sliding and actual MEMS tribometry were conducted. The second approach utilized the concept of hydrodynamic lubrication and selective surface modification for MEMS. Brief descriptions of the two approaches are presented below.

A novel method of lubricating MEMS devices, termed “Localized Lubrication” or “Loc-Lub” for short, was investigated and compared to other methods of lubricating silicon surfaces. The “Loc-Lub” method involves depositing a small measured amount of lubrication onto a specific location of a MEMS device – hence the name. The method was found to be not only feasible but also more effective than conventional lubrication techniques in preventing wear of the surfaces and reducing friction. The technique was then used to compare PFPE and MAC lubricants’

tribological performances and their mechanisms – MAC was found to prevent wear more effectively than PFPE due to its cohesive nature. Finally, the technique, having been proven to work conceptually, was tested on a custom-made reciprocating MEMS tribometer, and found to reduce friction and adhesion of MEMS sidewalls, and to extend the device wear life by several orders of magnitude compared to dry, unlubricated samples. PFPE was found to be very effective in extending wear life for side walls and it was found that a well-spreading lubricant such as PFPE with lower surface tension has advantage over MAC when the surface is rough with sharp asperities.

In the interests of fluid-film liquid lubrication of MEMS, MAC was found to reduce the hydrodynamic friction of high-sliding MEMS when included as an additive in hexadecane at an optimum concentration. Upon investigation, this phenomenon is believed to be due to the “half wetted bearing” effect and not due to the change in viscosity. A compound blend of octadecylamine and MAC additives in hexadecane was found to reduce both boundary and hydrodynamic friction.

To combat spreading and starvation of lubricants in small contacts such as in MEMS, selective modification of the silicon surface with hydrophobic (non-wetting) and hydrophilic (wetting) portions was carried out and found to increase the force required to move a droplet of lubricant from a designated location on the surface. Octadecylamine and dodecylamine were also used as additives to successfully induce autophobicity in hexadecane, and the various spreading behaviours investigated.

In conclusion, several new approaches to tackling tribological problems in MEMS have been researched. These methods are easily adapted to suitable MEMS devices and greatly reduce adhesion and friction, and increase wear and device life by several orders of magnitude.

## **Chapter 1 - Introduction**

*This chapter introduces the general concepts of Tribology and an overview of MEMS, with references to the combining of the two disciplines, and concludes with a brief description of the scope of the thesis.*

## **1.1 Introduction to Tribology**

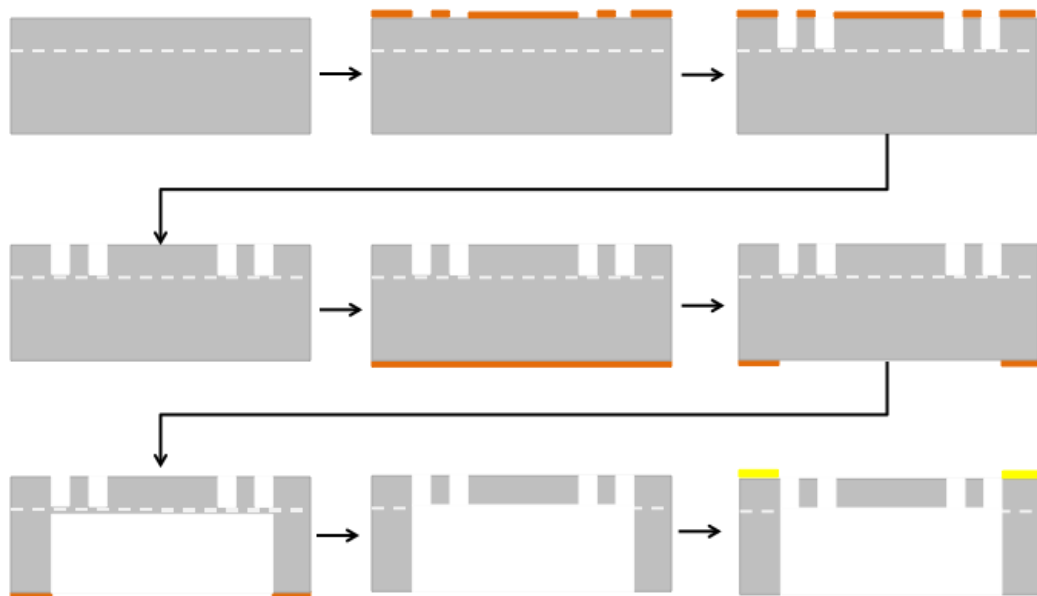
Tribology, the study of contacting surfaces in relative motion and the various surface interactions such as friction, wear and adhesion, is a universal issue – either preventing friction and surface damage in the case of most machine components, or enhancing it in practical ways such as in brakes, material processing, friction drives and so on. In his famous speech “There is plenty of room at the bottom” in 1959, Feynman spoke of the potential of micro-machines, and pointed out that the main obstacles to the practical and common usage of these machines were adhesion and friction. Bhushan also later pointed out that with decreasing scale, the forces that are proportional to area such as adhesion, friction, meniscus forces and viscous drag forces become much larger than forces proportional to volume, e.g. inertial and electromagnetic forces (Bhushan 2007).

Microtribology refers to the study of such interactions between surfaces at the micro-scale. At this level, the interactions as well as the consequences such as friction and wear are driven mainly by the magnitude of interfacial adhesion (Bhushan 1990). These issues are also the limiting factors for design of reliable and durable MEMS components (Mate 2007).

## **1.2 Introduction to MEMS**

Micro-Electromechanical Systems, commonly abbreviated as MEMS, have found their way as miniature sensors, actuators, motors and gears into today’s world. As MEMS are used primarily in the integrated circuit (IC) and semiconductor industry with silicon as the basic material, polycrystalline silicon is the most common material in surface micromachining (Maboudian et al. 2002). MEMS devices are now being looked to for integration of sensors, actuators and signal processing units into

miniature devices (Patton et al. 2001; Ku et al. 2011), particularly as MEMS devices can be mass produced, demonstrating low-cost potential and high throughput. With the small sizes, low energy supply required, and comparable performance to macro-scale counterparts, MEMS technology is a very viable option for many applications (Madou 1997). Devices have now found applications as pressure sensors (Eaton et al. 1997), RF switches (Girbau et al. 2007), gyroscopes (Syms et al. 2004) and have also been adopted into airbag systems in the automotive industry (Chau et al. 1998). MEMS are fabricated with various methods, one of which is Deep Reactive Ion Etching, known as DRIE for short (Figure 1-1). Surface etching and micro-machining are also other methods of fabrication.



**Figure 1-1: Schematic of deep reactive ion etching (DRIE) fabrication process for MEMS. Protective layers (indicated in orange) are coated prior to etching away of the silicon wafer (grey), and the final product is coated with pads (shown in gold) for electric conduction for the final device**

With MEMS technology advancing at such a fast pace, the industry has also faced the bottlenecks to widespread application of MEMS. With the shrinking of scale, the methods used against prevention of wear and high levels of friction at the

macro scale can no longer be applied effectively and new approaches must be undertaken (Kim et al. 2007). Commercially available MEMS sensors and actuators often avoid the tribological issues of contact by designing systems and the devices to avoid contact, using electrical capacitance for both sensing and actuating purposes, or including other methods of detection such as laser diffraction. Due to the low tolerances of the designs and the small scale, simple contact between components is sufficient to prevent the device from functioning. Any solution of tribological issues will require modification of the surfaces, selection of suitable lubricant(s) and development of appropriate methods of lubrication that are compatible with current MEMS fabrication processes.

### **1.3 Objectives of study**

The study elaborated in this thesis aims to do the following:

- Develop a novel method of applying lubricant onto a MEMS device at a particular location in sufficiently tiny quantities so as to not affect the functionality of the rest of the device (such as the pad for wiring),
- Compare this novel method of application with other current and common methods of lubrication, using both silicon surfaces as well as actual MEMS devices for comparison,
- Investigate possible improvements of liquid lubrication for MEMS and friction reduction in both the boundary and hydrodynamic regime,
- Study possible methods for confining lubricant under MEMS conditions to prevent starvation and contamination of other regions of the device, using the concept of barrier coatings



It is commonly recognised that reliability issues are the main obstacles to unleashing the full potential and practical use of MEMS devices. Up till now, attempts to improve the reliability of MEMS devices have shown that stiction and friction under various conditions can be decreased, but often require hermetic packaging (Potter 2005) or some form of replenishment during the use of the MEMS devices. This work will cover the progression of an investigation of lubricating MEMS devices; from the application of lubricant using a novel technique, the verification of its effectiveness under various conditions, and a form of modification of the lubricant and/or the surface for local containment of the lubricant. In order for these processes to be integrated successfully into the MEMS industry, these methods must show a substantial increase in the prolonged wear life of the MEMS devices, and also show compatibility with the materials and processes currently in use today.

Based on previous work involving surface modifications and both film and liquid lubrication under linear sliding and rotational conditions, as well as studies on hydrodynamic lubrication, the use of hydrophobic and oleophobic coatings, surface modifications and other novel methods will be explored. However, lubricant containment on MEMS devices as well as the novel technique of application are relatively new concepts and a number of studies are necessary to understand the underlying mechanisms as well as the practical applications and effects, in order to determine if the technology is a viable option for integration into processes and extension of the lifetimes of MEMS devices.

#### **1.4 Scope of thesis**

This thesis begins in Chapter 2 with a literature review and introduction to MEMS and tribology – including various factors that influence friction and wear

properties at the micro-scale, current methods and techniques of lubricating MEMS and their drawbacks, the issue of spreading on surfaces, and a brief summary of the various concepts which assist in explaining the behaviours in the chapters outlining experimental work.

Chapter 3 details the experimental methods and materials that are used in this study, including the reciprocating wear tests for feasibility testing and the various MEMS tribometers used in the course of this work. Analytical methods are also elaborated.

Chapter 4 introduces a novel method of lubrication, dubbed “Localized Lubrication” or “Loc-Lub” for short, which seeks to overcome some of the issues that we currently face with lubricating MEMS. A feasibility test is carried out on reciprocating sliding wear, and the friction and wear results are analysed and presented.

Chapter 5 compares the performance of two different lubricants – a perfluoropolyether and a multiply-alkylated cyclopentane – in a study of the “Loc-Lub” technique. The different behaviour of the lubricants are examined and accounted for in their varying tribological performances. Chapter 6 implements the “Loc-Lub” method on an actual MEMS reciprocating tribometer, and examines the friction and wear properties compared with dry conditions.

Chapter 7 investigates the possibility of using liquid lubrication of MEMS, and in particular how to reduce hydrodynamic friction in MEMS contacts to manageable values, which is thought to be one of the major drawbacks of liquid lubrication in this application. The mechanism of lubrication and lowering of hydrodynamic friction via additives is examined and described, and compared with other blends of lubricants.

Chapter 8 deals with the prevention of spreading of lubricant oils on surfaces, which has the potential to directly combat starvation in MEMS contacts by preventing loss of lubricant from the zone of interest. Two methods are tested – modification of the surface and modification of the lubricant itself to induce autophobicity. Experiments are introduced to test the containment ability of these methods, and to compare the spreading rates of the liquids.

Chapter 9 summarizes the conclusions in the thesis, and is followed by some suggestions for future research in this area.

## **Chapter 2 - Literature Review**

*This chapter presents current literature available at the time of writing, discussing tribology as a whole, methods of lubricating micro-devices and the factors affecting friction at that scale, in an attempt to understand them and reduce the overall friction. The concepts of hydrodynamic, boundary and mixed lubrication are presented, and current methods of lubricating MEMS devices are summarized, including novel techniques of surface modifications. Other analytical methods used are also introduced as a basis for the experimental results in subsequent chapters.*

## **2.1 Issues with MEMS reliability and difficulties in lubrication**

Due to the reduction in size, lubrication concepts commonly applied at the macro-scale cannot simply be adopted in MEMS devices – as the dimensions grow smaller, mass and inertial forces decrease by a cube of the dimensions, while surface area, and therefore surface forces, decrease only by the square of the dimensions. The increasing dominance of surface forces such as van der Waals forces and capillary effects, over inertial forces accounts for the well-known problem of stiction (Kim et al. 2007).

Lubrication of such devices often require advanced techniques such as vapour phase lubrication (Asay et al. 2008), as well as specialized packaging and storage of devices (Potter 2005). These procedures and processes add to the cost of MEMS devices and their manufacturing and usage, and thus cause some potential devices, which could involve large amounts of sliding, to become impractical.

The potential usefulness in practical applications of MEMS along with the tribological challenges faced in micro-devices has driven research into discovering means by which silicon surfaces can be lubricated, as silicon is the primary material used for MEMS device fabrication. One of the methods of creating surfaces where stiction and friction are controlled is to modify the surfaces directly with a coating. Friction and adhesion reduction has been explored in many areas, in liquid lubrication under boundary lubrication and hydrodynamic lubrication (Ku et al. 2011; Reddyhoff et al. 2011), as well as under specialized conditions and packaging of MEMS devices with vapour phase lubrication (Asay et al. 2008).

### 2.1.1 Release Stiction

Stiction refers to the adhesion of the microstructures in MEMS devices during the release process; this is primarily due to the capillary forces between the underlying substrate and the fabricated component surfaces during the final etching process of the sacrificial layer. Due to the very large capillary forces that will occur in the micro-scale under these conditions, the liquid used in the etching process cannot simply be allowed to evaporate on its own (Guckel et al. 1989; Mastrangelo et al. 1993; Legtenberg et al. 1994; Tanner et al. 1999), and instead the devices are stored until other methods can be used to dry them, avoiding the unwanted capillary forces. Such forces depend heavily on the hydrophobicity and hydrophilicity of the surfaces.

Capillary forces can be described using the Laplace Equation below:

$$P_L = P_1 - P_2 = \frac{2\gamma \cos \theta}{d} \quad (2-1)$$

**Equation 2-1: Laplace Equation**

Where  $P_L$  is the pressure difference across the fluid interface (obtained from the difference between  $P_1$  and  $P_2$ , which are the opposing interfacial pressures),  $\gamma$  is the surface tension,  $\theta$  the contact angle between the liquid and the solid, and  $d$  the distance between the parallel surfaces. Different conditions, depending on the value of contact angle, are illustrated in Figure 2-1 and Figure 2-2.

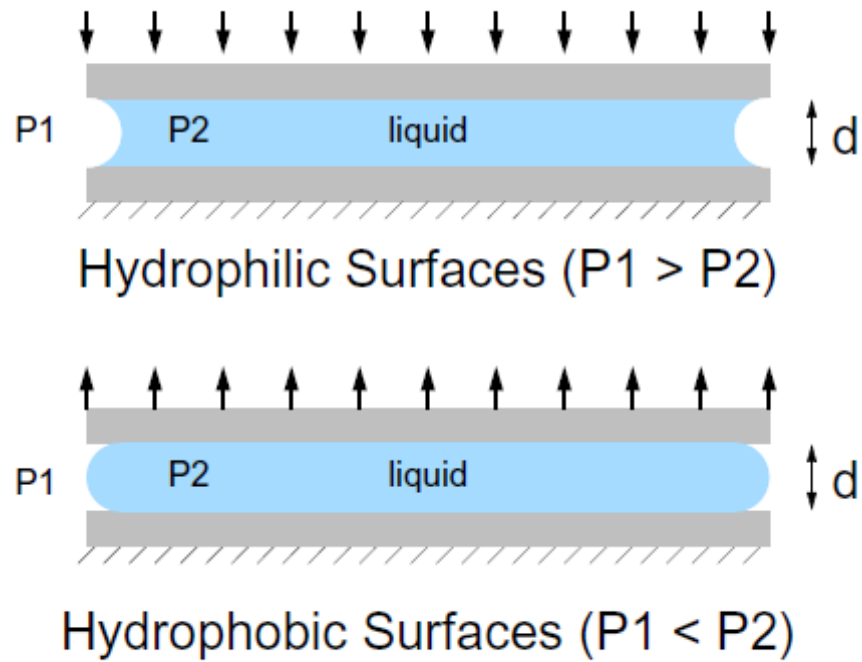


Figure 2-1: Direction of Laplace pressure for hydrophobic and hydrophilic surfaces (Ashurst 2003)

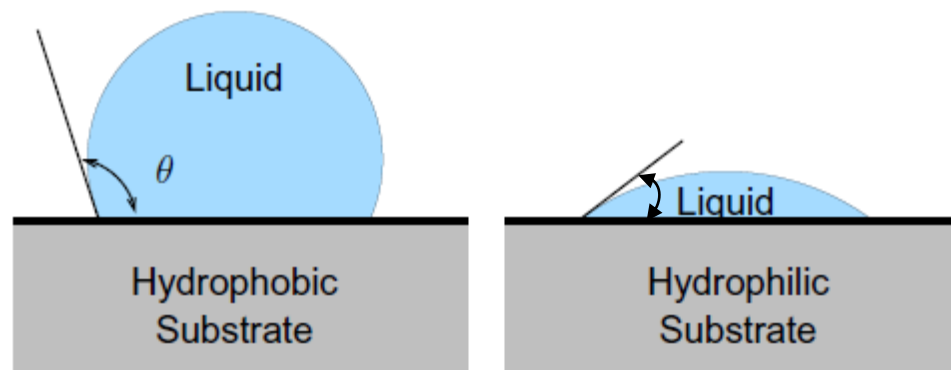


Figure 2-2: Contact angles of hydrophobic and hydrophilic surfaces (Ashurst 2003)

In the case of a hydrophilic surface, the contact angle is less than  $90^\circ$ , resulting in a net attractive force that pulls the surfaces together, leading to stiction between components. Conversely, for a hydrophobic surface with contact angle of more than  $90^\circ$ , the pressure calculated from the Laplace equation results in a force that pushes the two components apart, preventing stiction.

These capillary effects are almost unavoidable in the MEMS fabrication process since procedures such as cleaning and rinsing with water and other solvents lead to oxide layers being formed on the silicon surface. These layers are able to further adsorb water molecules due to their high surface energy (and hydrophilicity), which promotes meniscus formation and increases the level and propensity of stiction. Hydrophobic coatings or specialized treatments have therefore been used to reduce the amount of stiction.

### **2.1.2 In-use Stiction**

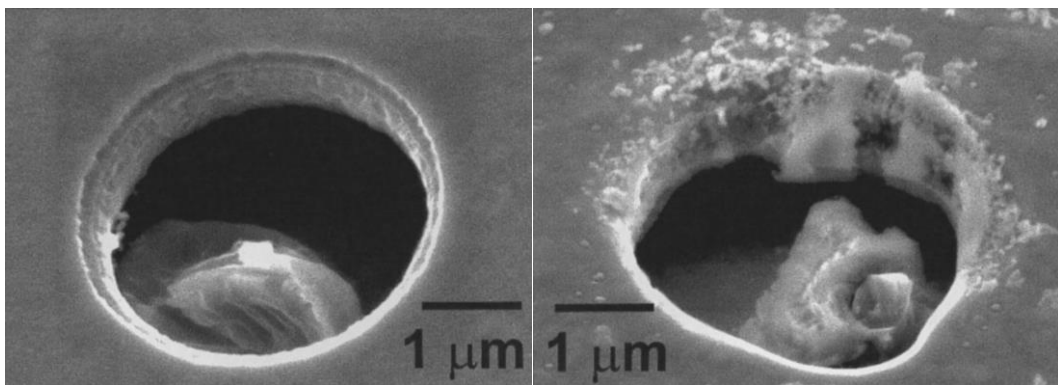
In-use stiction refers to the adhesion of the components while the device is in use. MEMS operation often requires contact between two components. Applications such as switches, with regular or intermittent contact, as well as gears, with continual contact with each other, are especially prone to this phenomenon. In addition to the surface free energies of the surfaces involved, the surface roughness also plays a part in increasing or decreasing the real contact area between the components, thereby affecting the actual adhesive or stiction force. In-use stiction has a direct effect on the friction between components, particularly in the rubbing of MEMS sidewalls.

### **2.1.3 Friction, Wear and Lubrication**

Due to the very small contact areas that occur typically in micro-devices, their components are often subjected to very large contact pressures, despite the very small loads involved (Tanner et al. 1999; Williams 2001; Wang et al. 2002). Upon sliding, the surfaces, particularly those with asperities, cause energy loss in the form of plastic deformation and wear debris generation. Hubs on micro-gears experience large amounts of wear (Tanner et al. 1999; Tanner 2000) as shown in Figure 2-3. Although



mechanical contact and environmental conditions such as humidity are known to be important, the mechanisms of wear are not entirely understood and are highly specific to each application (Tanner et al. 1999; Patton et al. 2002). Friction at the micro-scale is largely dependent on the adhesion forces between the components and hence the methods of reduction of friction are similar to those of reduction of stiction and adhesion. The adhesion between the surfaces causes one or both of the surfaces to wear upon sliding.



**Figure 2-3: Failure of a micro-bearing after 91 seconds at 1720 Hz (Tanner et al. 1999). Reprinted with permission.**

Lubrication of micro-devices is difficult due to the small scale and the very finely detailed components. Conventional methods such as dip-coating often do not work on many devices as the evaporation of the liquids under dip-coating cause the capillary forces to pull components into mutual contact. Furthermore, it has been difficult to lubricate the sidewalls of MEMS, as the gaps between the sidewalls can be as small as 10 - 40 nm. It has also been noted that, due to the different exposure to processing environments, the behaviour of sidewalls is likely to be very different from that of the plane surfaces (Ashurst et al. 2003b). High levels of friction and wear occur in such components, which emphasizes the need for proper lubrication. Various methods have been utilized to combat friction between MEMS surfaces. Vapour

phase lubrication has been explored as an option (Asay et al. 2008), and also hydrodynamic lubrication techniques to both prevent and study friction on MEMS (Ku et al. 2010; Ku et al. 2011; Reddyhoff et al. 2011). However, all these methods, unless used with particular packaging or in a bath, may undergo starvation of the lubricant.

## 2.2 Surface energy, surface tension and hydro/oleophobicity

The interfacial surface energies can easily be measured by its hydrophobicity and water contact angle, and are directly related by the Young's Equation as follows:

$$\gamma_L \cos \theta = \gamma_S - \gamma_{SL} \quad (2-2)$$

**Equation 2-2: Relation of surface energy with contact angles (Doms et al. 2008)**

where  $\theta$  is the contact angle of the fluid on the surface in question,  $\gamma_{SL}$  is the surface tension of the liquid or the interfacial energy between the solid and liquid surface, and  $\gamma_L$  and  $\gamma_S$  are the surface energies of the liquid and solid respectively.  $\gamma_{SL}$  can be approximately related to  $\gamma_L$  and  $\gamma_S$  by the following equation:

$$\gamma_{SL} = \gamma_S + \gamma_L - 2\sqrt{\gamma_S \cdot \gamma_L} \quad (2-3)$$

**Equation 2-3: Approximation of interfacial energy between the solid and liquid interface from respective surface energies (Doms et al. 2008)**

Based on the above equations 2-2 and 2-3, when the solid surface energy is higher than the energy at the solid-liquid interface (i.e.  $\gamma_S > \gamma_{SL}$ ), the contact angle of the liquid will be less than  $90^\circ$  and the solid surface is termed hydrophilic when polar liquids such as water are used. As silicon surfaces have very high surface free

energies, their surfaces are found to be extremely hydrophilic and have also been found to be oleophilic (Hurst 2010). Therefore, one method of modifying the surface energies of silicon surfaces is to chemically alter the surface, for example, by attaching a monolayer of a suitable molecule onto the surface.

The roughness of a surface has also been found to affect its surface energy and hydrophobicity. The real contact angle of the liquid can be measured as that between the surface of the asperities and the edge of the droplet (Wenzel 1936). Wenzel was the first to investigate this case, and found that if the interface is rough, the actual contact angle should be equal to the equilibrium contact angle on a smooth surface adjusted by a given roughness factor  $r$ , as shown in Equation 2-4, where  $r$  is the ratio of the actual surface area to the project surface area (i.e.  $r > 1$  for rough surfaces):

$$\cos \theta_w = r \cos \theta \quad (2-4)$$

**Equation 2-4: Wenzel's equation accounting for roughness effects on contact angles (Wenzel 1936)**

Cassie and Baxter later investigated hydrophobicity on rough surfaces, examining a model in which air is trapped between the liquid droplets and the rough surfaces (Cassie et al. 1944). This newer model builds on the previous Wenzel model by accommodating the fraction ( $\varphi < 1$ ) of the surface where a liquid droplet comes into contact with a surface. This is less than unity due to the presence of trapped air on the rough surface, and is described by Equation 2-5:

$$\cos \theta_{CB} = \varphi \cos \theta + (1 - \varphi) \cos \theta_G \quad (2-5)$$

**Equation 2-5: Cassie-Baxter model accounting for roughness and surface fraction effect on contact angles (Cassie et al. 1944).**

where  $\theta_G$  is the contact angle between the liquid droplet and the gas. Figure 2-4 illustrates the various models of contact angles and their respective wetting states.

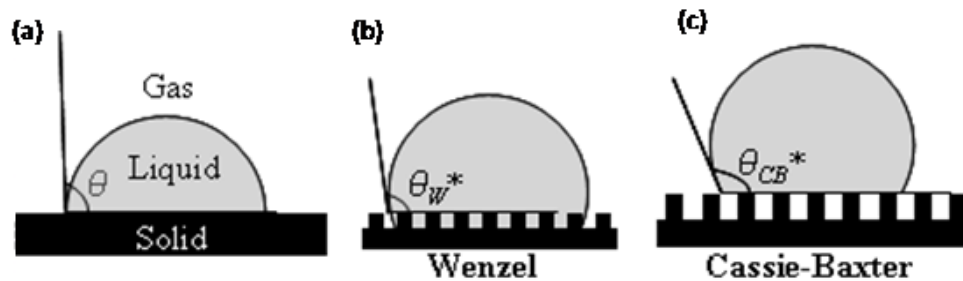


Figure 2-4: Wetting states showing the a) apparent contact angle, b) contact angle from Wenzel's model, and c) contact angle from the Cassie-Baxter model (Hurst 2010)

Hydrophobic surfaces have been used in the MEMS industry to prevent both release and in-use stiction via the reduction of adhesion forces between components. The same concept can be applied to prevent spreading and to contain lubricants on surfaces or sidewalls of MEMS, utilizing surface energy induced by surface coatings or self-assembled monolayers. Phenomena such as autophobicity – whereby a liquid forms a surface film which prevents the liquid from wetting the surface and hence reduces spreading – have been studied (Hare et al. 1955; Wade et al. 1971; Novotny et al. 1991; Biebuyck et al. 1994; Waltman et al. 2002) and provide a basis for some of the ideas explored in this thesis.

The interest in hydrophobicity, oleophobicity and the surface free energies of contact surfaces in tribology is due to the discovery that surfaces that exhibit a hydrophobic property also show low levels of stiction and friction, the former being the primary factor for the latter in the micro-scale. Modifying the surface of the materials does not interfere with the gap tolerance, and is therefore a viable option for improving the tribological properties of devices at the micro-scale. Super-

hydrophobic surfaces, where the water contact angle is greater than  $160^\circ$ , are often sought out as potential applications in MEMS tribology – such surfaces typically combine textured surfaces with low surface free energy materials (e.g. fluorinated compounds) to create this effect (Lacroix et al. 2005), which leads to a great reduction in the surface energies. This technology holds great potential in overcoming the difficulties faced in MEMS and microstructural surfaces.

### **2.3 Studies on solutions to MEMS Tribology**

To date, there are three main methods of reduction of friction on MEMS surfaces – dry coatings, surface treatments and deposited films (such as Self-Assembled Monolayers, or SAMs) on the surface, and vapour phase and liquid lubrication. These three methods also encompass the different regimes of friction, encountered during different speeds of sliding. The different regimes are best summarized in a Stribeck Curve illustrating the relationship between sliding speed, load and friction (Figure 2-5). Modification of the dry surfaces such as surface treatments and vapour deposition influence friction in the boundary regime by preventing excessive contact or interlocking asperities between the surfaces. Liquid lubrication, on the other hand, has been found to reduce friction in both the boundary and hydrodynamic regime (Ku et al. 2011; Ku et al. 2012).

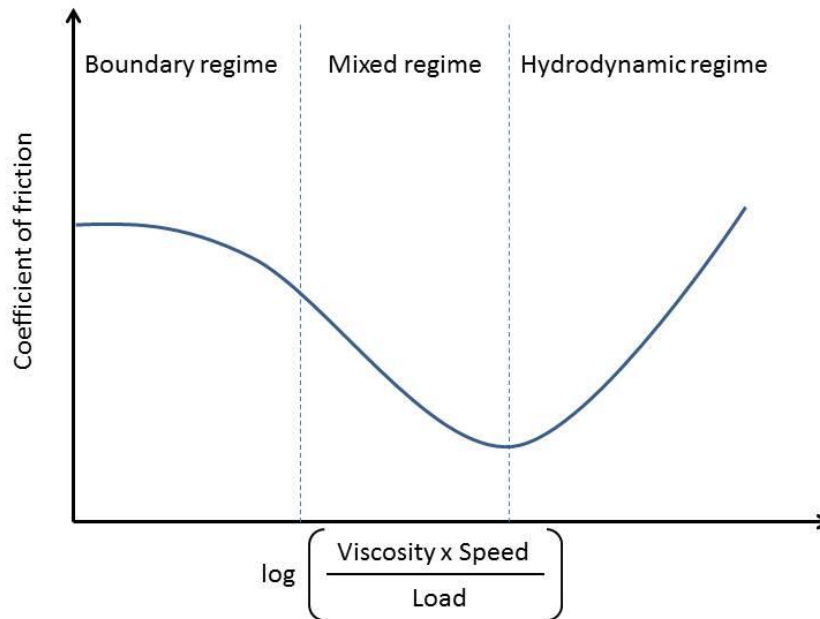


Figure 2-5: Stribeck curve, showing coefficient of friction as a function of viscosity, speed and load

### 2.3.1 Surface Films and Treatments

Ultra-thin organic layers have been suggested as possible lubricants for silicon MEMS (Bhushan et al. 1995; Komvopoulos 1996; Srinivasan et al. 1997; Srinivasan et al. 1998a; Rymuza 1999; Maboudian et al. 2000). Self-Assembled Monolayers (SAMs) have also garnered a lot of interest in MEMS application and tribology – the reduction of interfacial energies between the surface and liquid allows for a reduction in capillary and surface tension forces when liquids are being used, either in fabrication (in the case of release stiction) or in lubrication during use (for in-use stiction). The ease of deposition of SAMs on three-dimensional surfaces and the stronger covalent bonds compared to layers formed by the Langmuir-Blodgett method, which only utilizes van der Waals forces, make SAMs a more feasible solution to MEMS tribology (Koinkar et al. 1996). Properties of SAMs such as the

degree of crosslinking, the terminal group, hydrophobicity and the length of the chains can also be easily varied to a large degree (Ulman 1991). Such surface treatments modify the properties of the material surface and are therefore used to reduce both friction in the boundary regime, and release stiction by their various mechanisms.

One particular SAM, octadecyltrichlorosilane ( $\text{CH}_3(\text{CH}_2)_{17}\text{SiCl}_3$ ), commonly known as OTS, has been extensively studied and been found to be both hydrophobic and slightly oleophobic (Hurst 2010). This property originates from its behaviour of orientating its polar head groups toward the substrate and its non-polar tail groups away from the substrate – the tail groups then create a film of closely packed alkane chains with methyl termination, giving the film an extremely hydrophobic nature.

SAMs in general have been studied for possible hydrophobic coatings on MEMS components (Doms et al. 2008). These hydrophobic coatings, when integrated appropriately into MEMS fabrication processes, can help eliminate release stiction and reduce in-use stiction, as well as reduce the coefficient of friction in micro-machines (Deng et al. 1995; Srinivasan et al. 1997; Srinivasan et al. 1998a; Srinivasan et al. 1998b; Cabuz et al. 2000; Maboudian et al. 2000). As friction at the micro-scale is highly dependent on the adhesion between surfaces, applications of SAMs have been identified to be a possible solution for friction due to their ability to reduce adhesion through modification of surface energies. SAMs have also been used to provide an interfacial layer for bonding of polymers, utilizing their ability to modify the surface wettability of the substrate in promoting adhesion of the polymer coating onto the surface (Myo et al. 2008).

Ionic liquids (ILs) have been studied as ultra-thin films for silicon surfaces and MEMS devices (Palacio et al. 2008). ILs have been considered as viable

lubricants for MEMS devices due to excellent thermal and electrical conductivity (Bhushan et al. 2008; Palacio et al. 2008). Nainaparampil and co-workers have found that MEMS devices that have been coated with a thin film of IL have also shown an improvement in wear life, based on a developed method using atomic force microscopy (AFM) with a liquid cell (Nainaparampil et al. 2005; Nainaparampil et al. 2007) – these tests conducted show good correlation with the failure life span of MEMS motors. In testing two ILs in particular, 1-butyl-3-methylimidazolium hexafluorophosphate ([BMIM]PF<sub>6</sub>) and 1-butyl-3-methylimidazolium octylsulfate ([BMIM][OctylSO<sub>3</sub>]), it was found that thermally treated coatings which contained a mobile lubricant fraction were better able to protect the Si surfaces, compared to the fully bonded coatings – this enhanced protection has been attributed to the replenishment of lubricant from the mobile fraction (Bhushan et al. 2008; Palacio et al. 2008).

Another form of lubrication involves the formation of dry, solid films on the surface. In particular, diamond-like carbon (DLC) coatings have been shown to increase the hardness of the silicon surface and to reduce wear and friction in the process (Tagawa et al. 2004; Smallwood et al. 2006). Hydrogen termination has also been used to reduce adhesion (Tagawa et al. 2004).

These treatments have been effective at reducing adhesion and friction but do not provide prolonged protection against sliding wear as there are no means for protective film replenishment. As a result, liquid and vapour phase lubrication, as self-replenishing methods, have gathered interest for study and investigation.



### **2.3.2 Vapour Phase**

Vapour phase lubrication is achieved when the condensation of a vapour, usually a hydrocarbon or fluorocarbon, forms a film on the surfaces (Ashurst et al. 2003a; Asay et al. 2008). This has been shown to be effective in preventing wear, but requires special hermetic packaging (Potter 2005) and elaborate setups for operation.

Lubrication and replenishment using vapour phase lubricants can be extremely effective for MEMS devices as the gaps between components are in the micron and sub-micron scale. Using vapours as lubricants then ensures that the lubricant is evenly and efficiently distributed throughout the device, coating even components that are not directly accessible. The inflow of the vapour lubricant can also be controlled, reducing the amount of excess lubricant present in the system. Studies presenting the effectiveness of this method have been conducted (Ashurst et al. 2003a; Asay et al. 2008), and found to reduce both friction and stiction with only a few monolayers of film thickness, as compared to a dry environment. Studies have also shown prevention of wear (Asay et al. 2007) with an increase in the wear life of up to 4 orders of magnitude with introduction of the vapour. MEMS devices that were stuck after deliberate lubricant depletion could also be recovered upon re-introduction of vapour and continued to run under the same conditions.

Significant research has since been carried out to investigate vapour phase lubrication of MEMS and its feasibility, factoring in geometry of components for replenishment and adapting fluid lubricants for use.

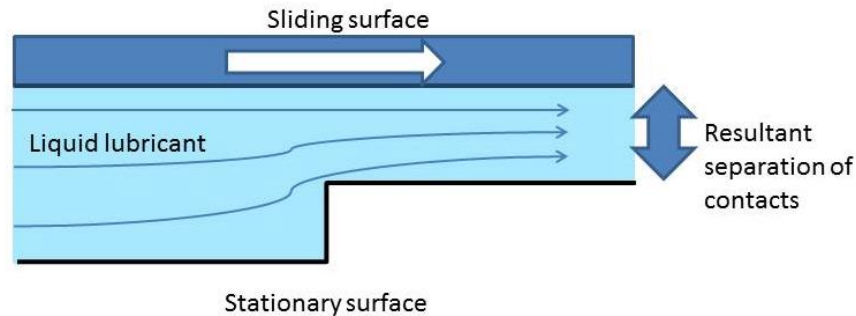
### **2.3.3 Liquid lubrication**

Liquid lubrication, most commonly used in larger machines, provides two types of lubrication; hydrodynamic lubrication resulting from liquid entrainment

(usually at higher speeds) at the contact interface, and boundary lubrication when molecules in the liquid, either of the bulk fluid or of additives, adsorb or react with the surfaces to separate the asperity contacts. Both vapour phase and liquid lubrication are considered self-replenishing as fluid is continuously introduced into the contact, and have shown to prevent wear (Ku et al. 2011) and give low friction (Ku et al. 2012) in a MEMS contact. Liquid lubrication was initially thought to be unsuitable for MEMS due to the high levels of hydrodynamic friction (Mehregany et al. 1992; Keren et al. 1994); however, the liquids used in these early studies were of high viscosity. Later studies with liquids of sufficiently low viscosity show low coefficients of friction at high speeds - below 0.1 for a MEMS thrust pad bearing rotating at 10,000 RPM (Ku et al. 2012). Furthermore, liquid lubrication gives lower friction for the same MEMS contact under certain conditions when compared to lubrication by vapour (Ku et al. 2011). This is not always the case for all conditions since friction in liquid lubricated contact varies strongly with entrainment speed as shown previously in the Stribeck curve (Figure 2-5).

Thin film liquid lubrication, involving both boundary lubrication at low speeds and hydrodynamic lubrication at high speeds has been investigated for high speed sliding MEMS (Ku et al. 2010; Ku et al. 2011; Reddyhoff et al. 2011). Liquid films have been used between the surfaces of MEMS devices and have found to be effective in generating a pressured hydrodynamic film in converging contact conditions. In hydrodynamic lubrication the liquid is conventionally considered to “stick” to the surfaces and this drives the entrainment of fluid into the contact (Figure 2-6). This approach has been shown to prevent wear and give low levels of friction in a MEMS contact (Ku et al. 2011; Ku et al. 2012) and under certain conditions to give lower friction than MEMS surfaces lubricated by the vapour phase method. It should

be noted that this would not be the case in all conditions since liquid lubrication is strongly dependent on the sliding speed between the two surfaces.

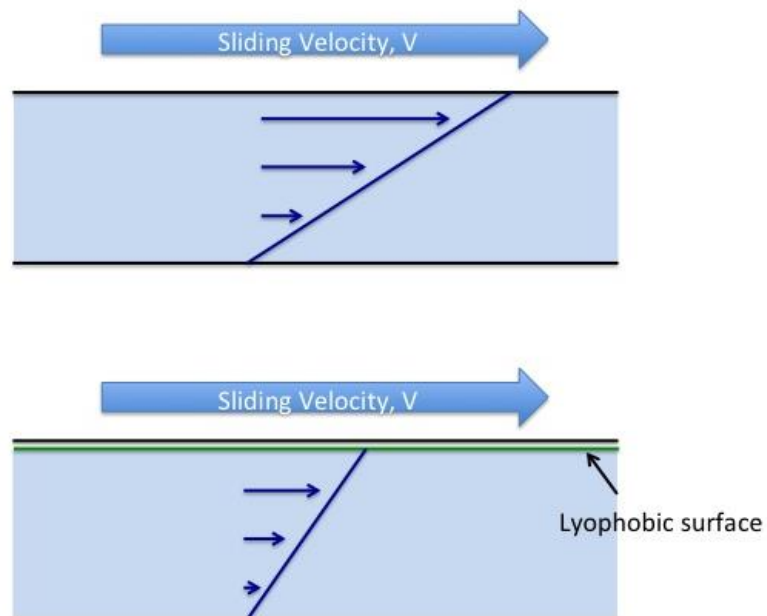


**Figure 2-6: Schematic of a stepped pad bearing with stick of lubricant on the surfaces, resulting in separation of the contacts due to entrainment**

At low speeds, fluid entrainment is not sufficient to separate the contacting surfaces and friction has a level almost independent of speed as the load is being supported by asperity contacts. Boundary friction dominates in this regime and can be alleviated with more viscous fluids or with surface active additives. As speed increases, liquid entrainment starts to separate the two surfaces (the hydrodynamic effect) and friction is decreased – this is known as the mixed regime. At high speeds the entire load is supported by the fluid film, but friction increases with speed as the shear rate increases. At very high speeds, the resulting hydrodynamic friction can become very large. This can potentially be reduced by reducing the surface energies of one of the surfaces enough to allow the liquid to slip against the surface - this phenomenon will be explored in this work. In order for liquid lubrication to be effective in MEMS, the friction in all three of these regimes, boundary, mixed and hydrodynamic, must be controlled. Solid coatings, or vapour deposition, operate only in the boundary lubrication regime, while fluid lubrication (liquid or gaseous) operates in all three – thus, the Stribeck Curve is only relevant when fluids are present.

### 2.3.4 The “Half-Wetted Bearing”

One of the methods of reducing hydrodynamic friction, particularly at high speeds, without changing the viscosity of the liquid, is illustrated in the concept of the “half-wetted bearing” (Spikes 2003a), in which the conventional boundary conditions of no slip at the wall is no longer valid due to partial or even non-wetting of the fluid against the surface. This combines the concepts of surface modification and surface energies with hydrodynamic theory and liquid lubrication. Spikes and co-workers (Spikes 2003a) first investigated this phenomenon by extending Reynolds’ theory to show that loads could be supported with very low friction as a result of a bearing in which the liquid lubricant in contacts was allowed to slip against one surface but not the other. A schematic of the effect of reduction of velocity profile within the liquid film is shown in Figure 2-7.



**Figure 2-7: Velocity profiles of fluid-lubricated gaps with the top surface sliding at a velocity, (top) normal conditions and (bottom) slip conditions. The velocity of the fluid near the wall with slip is reduced.**

By extending the Reynolds Equation to take into account slip at a critical shear stress (taken to be zero at extreme conditions) at one surface, while retaining no-slip conditions at the other surface, hydrodynamic pressure (and therefore the load support under such conditions) is reduced by up to half. This is because when slip occurs on one contact surface it affects both the Poiseuille and Couette shear terms – the Poiseuille shear is doubled while the Couette shear is eliminated. Since the friction resulting from Couette shear is usually much greater than that of the Poiseuille friction, and becomes extremely large in thin film contacts, introducing an element of slip would greatly reduce the overall friction compared to a conventional no-slip bearing. The effect of slip on the critical shear stress is shown in Figure 2-8, illustrating the reduction of critical shear stress for surfaces showing slip across the whole surface as well as regions of partial slip, compared to conditions under which no slip occurs. This effect is especially significant for bearings that have low convergence ratios.

This same principle was further extended to low-load MEMS contacts, where friction could potentially be reduced (Spikes 2003b) and validated experimentally with a low-load tribometer in which hexadecane was made to slip against a smooth lyophobicized sapphire surface (Choo et al. 2007b). Reduced friction from liquid slip was also observed in low load contact where the surfaces were treated with friction modifier additives (Choo et al. 2007a), and a number of other experiments have shown that liquid slip can occur (Choo et al. 2007b). This happens particularly when the surfaces involved are very smooth and the liquid used does not strongly wet the surface. Pit and co-workers used fluorescence recovery after photo-bleaching (FRAP) to show directly the slip of hexadecane against a smooth sapphire surface made lyophobic with a monolayer of OTS (Pit et al. 2000) and further evidence was shown

by Zhu and Granick when reduced hydrodynamic squeeze forces were measured between mica surfaces coated with a lyophobic monolayer and lubricated with tetradecane and water (Zhu et al. 2001).

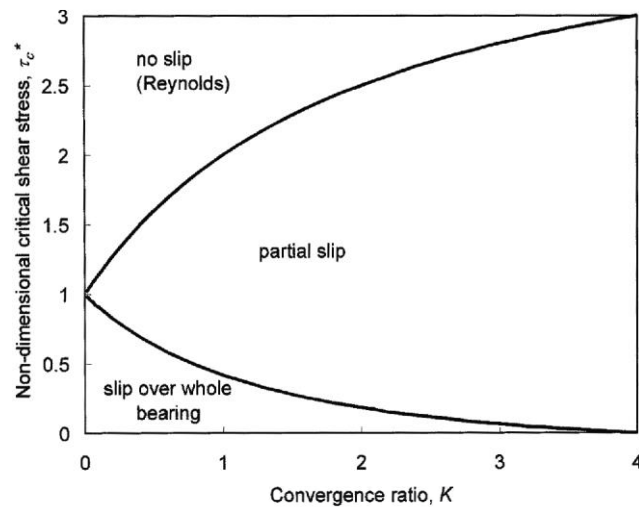
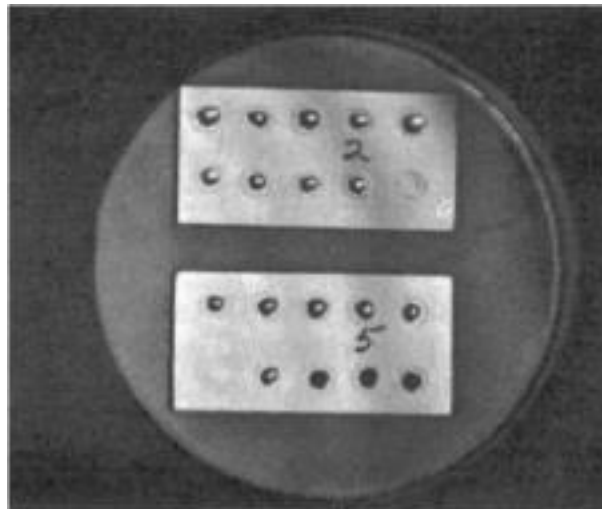


Figure 2-8: Map of occurrence of slip for a fully flooded, infinitely long linear slider bearing (Spikes 2003a). Reprinted with permission.

## 2.4 Liquid Spreading and Starvation

In all lubricated contacts, the possibility of starvation of lubricant is a concern – even at the micro-scale, the lack of a lubricant to prevent direct and excessive contact between two sliding surfaces can cause wear due to insufficiently lubricated contacts (Ku et al. 2011). Most previous studies of the liquid lubrication of MEMS (Jones et al. 1999; Ku et al. 2011; Reddyhoff et al. 2011; Ku et al. 2012) have been conducted with complete submersion of the contact in liquid, which ensures that a complete lubricant film is present at the contact area. In commercial applications, particularly those that involve vapour phase lubrication, hermetic packaging (Potter 2005) is implemented to prevent loss of the lubricant layer and replenishment source. Non-spreading properties of a liquid also prevent excessive evaporation and avoid contamination of the lubricant by reducing the surface area exposed (Cottingham et al. 1964).

Fluorinated polymers have been investigated to prevent spreading, and have been found to contain oils within a designated area (Bennett et al. 1964). In their study, a circle was painted on stainless steel surfaces with the fluorinated compounds using a thin brush (Figure 2-9), and this effectively prevented the spreading of most oils, containing them within the painted area. The only lubricants that were not contained within this painted area were the fluorinated esters, due to the mutual attraction of the two fluorine-containing compounds. The painting method presented however, would be difficult to perform on the micro-scale, particularly on MEMS sidewalls, and thus other methods of application would be needed.



**Figure 2-9: Oil droplets on plates of stainless steel, encircled within a fluorinated coating painted on with a brush (Bennett et al. 1964). Reprinted with permission.**

Non-spreading oils can also be obtained by introducing an additive into the liquid – however, the effect depends greatly upon the combination of oil and the additive used; some additives that cause a particular oil to be non-spreading can also induce rapid spreading in another. Spreading study of various oils with additives on stainless steel has previously been conducted (Cottingham et al. 1964) and categorized into four main classes:

- a) non-spreading liquids,

- b) liquids that initially spread but retract to form many small drops,
- c) liquids that form a substantial contact angle but where droplets form, they skate over the surface without crossing their own paths, and
- d) “catastrophically” spreading liquids which form dendritic patterns on the surface.

The behaviours of the second and third category were attributed to the modification of the surface via additives in the droplet forming a monolayer, thereby changing the critical surface tension and preventing spreading of the liquid over a surface that had been previously spread over by the liquid (i.e. a monolayer had already been formed on the surface). Given the large variety of effects observed, it is clear that introducing additives to create non-spreading oil requires choosing an appropriate additive for the oil and in suitable amounts. For ideal retraction of the droplet, the additive should also be appreciably soluble in the base oil and should adsorb promptly from the leading edge to produce the oleophobic film on the surface. The additive should also not be more volatile than the base oil.

When considering modification of the liquid to prevent spreading, three approaches can be taken: firstly, the liquid can be inherently non-spreading in its pure state, secondly that it can be made non-spreading by addition of carefully selected solutes, and thirdly, the solid surface can be modified by coating it with substances of low surface free energy (Bernett et al. 1964). Some additives which show reduced spreading of refined oils on polished steel, brass, and jewel bearing material are oleic or stearic acid, and olive, castor or lard oil (Bulkley et al. 1933).

Autophobic liquids are a possible candidate in this area, and are characterized by the behaviour of the liquid molecules when it comes in contact with a solid surface – the first molecules of such liquids adsorb on the surface to form a monomolecular



film whose critical surface tension of wetting is less than the surface tension of the liquid itself, preventing it from spreading on its own adsorbed film (Bernett et al. 1964). This description of liquids fits that of the liquids mentioned earlier (Cottingham et al. 1964) and thus these can be categorized as “autophobic”.

Another class of non-spreading liquids are those which have surface tensions so high and adhesional energies so low that it is thermodynamically impossible for the liquid to spread – these liquids differ from autophobic liquids in that they do not leave a film behind them when rolled over a horizontal polished solid surface (Timmons et al. 1964). However, the use of such additives raises issues of its own – they have a limited solubility in oils and only low concentrations of additives can be used so that the resultant contact angle will not be so large as to cause inadequate adhesion between the formed film and the surface.

## **2.5 Obstacles with current methods of lubrication**

For MEMS devices to be viable alternatives to current technology, several key criteria should be fulfilled:

- 1) The devices should be easily produced or replaced,
- 2) They should be as effective (if not more effective) than the current technology,
- 3) Contacting components should exhibit low friction to minimize energy losses and wear, and
- 4) They should be durable and provide long wear life to the components.

Understandably, with a theoretical desired infinite wear life, the first two criteria would diminish in importance.

The current methods of lubrication are not without their own drawbacks or difficulties. Self-Assembled Monolayers (SAMs), though shown to have great potential and widely studied, have their limitations in the formation of the monolayer film and the thickness of the film present on the surface. As SAMs consist of only a single layer of molecules on the surface, which make them viable for MEMS coating given the small clearances, the wear durability of the monolayer is far too short to be of practical use in high sliding velocity MEMS components (Satyanarayana et al. 2005). It had also been noted that although hydrophobic coatings help to reduce the amount of release stiction, in some cases they are found to increase in-use stiction. (Cabuz et al. 2000)

Vapour-phase lubrication requires hermetic packaging (Potter 2005) for the presence of the vapour to act as a self-replenishing lubricant. This increases production cost and limits the practical usage and design of the MEMS devices packaged in such fashion. Replacing such devices would also be inconvenient, although the wear life has been shown to extend by a considerable amount. Practical and commercial applications of such devices are thus uncommon.

Although liquid lubrication shows increasing promise in MEMS lubrication, the conflict between the boundary and hydrodynamic regimes still exists – a liquid of sufficient viscosity to give low boundary friction often causes a large amount of viscous drag at higher speeds leading to high hydrodynamic friction. At the same time, the scale of the lubricant film accentuates the viscous effect; under conventional hydrodynamic lubrication, friction caused by viscous shear increases rapidly with decreasing film thickness – with a thickness in the sub-micrometre scale, these forces are likely to be huge. On the other hand, low viscosity liquids, while reducing hydrodynamic friction, provide less lubrication in the boundary regime and typically

have high vapour pressures, which conflicts with the requirement that sliding contacts should operate for extended periods of time without confinement.

Liquid lubrication for self-replenishment also requires a source of lubricant for replenishment. In cases where the contacts were starved of lubricant over periods of time, particularly during repeated testing, there is an overall increase in the friction measured, especially at high speeds in the hydrodynamic regime. Replenishment of lubricant is a universal problem for all surfaces, even at the macro scale. This issue has been investigated with the use of perfluoropolyether (PFPE) lubricants for magnetic hard disc drives, in which PFPE not only lowers surface energy on the surface but also is known for both mobile and bound phases being present, in which self-replenishment is achieved when both phases are present (Chen et al. 2001; Katano et al. 2003; Sinha et al. 2003).

All methods of lubrication have been tested largely on plane surfaces and sidewall characterization of tribological properties have not been properly examined (Ashurst et al. 2003b). A universal method of lubrication for both plane surfaces and sidewalls, easily implementable into current fabrication practices and applications, would be much desired to drive micro-technology forward.

## **2.6 Lubricants for MEMS Tribology**

### **2.6.1 Perfluoropolyether (PFPE)**

Fluorinated lubricants have received much attention in recent years for use in micro- and nano-tribology because of their low surface free energy, lubricity and chemical inertness. Perfluoropolyethers (PFPEs) have been used commonly in hard disk lubrication, providing low friction and long wear life (Tani et al. 2001; Wang et

al. 2005). PFPE overcoats on other polymers have also been found to improve tribology of polymer coatings (Satyanarayana et al. 2005; Satyanarayana et al. 2006; Kim et al. 2009; Abdul Samad et al. 2010) and have been studied extensively under various conditions.

The remarkable tribological properties of PFPEs in some applications are attributed to the dual phase present within the film – both a mobile phase and bound phase are present on the coated surface. This unique property allows for self-replenishment of the lubricant film. It was also found that a single bound phase of PFPE on surface did little to prolong the wear life and reduce friction (Tani et al. 2001; Eapen et al. 2002). PFPE coatings and overcoats were found to show reduced shear stress and increased water contact angle (implying reduced surface energy), explaining the improvements in wear and friction properties exhibited (Satyanarayana et al. 2006), as well as show a high thermal stability, up to a range of 327 – 477 °C (Lei et al. 2001), which enables them to withstand the heat generated by friction at the sliding interface without degradation of the film. The increased thermal stability along with low friction leads to reduced heating and is doubly beneficial for such a system. In the case of PFPE as an overcoat on Ultra-High Molecular Weight Polyethylene (UHMWPE), Satyanarayana and co-workers also believe that it is possible that the PFPE mobile phase molecules are encased in the valleys on the uneven UHMWPE film overcoat, which explains the extended wear lives on UHMWPE film with a PFPE overcoat, as a ready source of replenishment for the mobile phase is available. Its hydrophobic property reduces adhesion between the counterface and the film, which explains the reduction in polymer transfer on the counterface contact from wear.

Along with the abovementioned factors, PFPE can provide uniform films with thickness in the nanometre range, overall making this fluid a highly suitable candidate for lubricating MEMS components. Their use in MEMS devices have been studied and characterized, and they have been found to exhibit significant durability under MEMS conditions (Liu et al. 2003). Other factors that were found to affect the durability, friction and adhesion of the films include the adsorption of water and the formation of the meniscus, changes during sliding (tribochemistry and third-body generation), viscosity and surface chemistry properties. Eapen and co-workers have also suggested that the common method of dip-coating provides a non-uniform coating on contacting device components (Eapen et al. 2002), implying the need for the development of a new technique of lubrication on MEMS devices that would better suit applications.

Despite the common use of PFPE lubricants in hard disk tribology, as space lubricants, and the unique advantages that it brings, the use of PFPE has been found to produce decomposition products under specific conditions (Helmick et al. 1998; Wei et al. 1998; Nakayama et al. 2006). Fluorinated compounds, though generally inert, can also lead to various undesirable environmental concerns and hazards from the decomposition products of PFPE. The eventual decomposition of PFPE then creates a concern, driving the need for alternative lubricants for the same use. A short description of the physical properties of PFPE is included in Chapter 3.

### **2.6.2 Multiply Alkylated Cyclopentanes (MACs)**

Multiply Alkylated Cyclopentanes (MACs) are synthesized hydrocarbon lubricants commonly used in the aerospace industry, along with fluorinated

compounds such as Z-dol (PFPE). Being developed relatively recently, they are less well-known and have been less studied than PFPE lubricants.

MACs are synthesized hydrocarbons, with molecules that consist of a cyclopentane ring with 2 to 5 alkyl attached chains. They are produced by cracking di-cyclopentadiene to form cyclopentadiene, which then reacts with alcohols in the presence of a strong base (Venier et al. 1991). Because of the relatively high molecular weight they have very low volatility compared to most other hydrocarbon liquids.

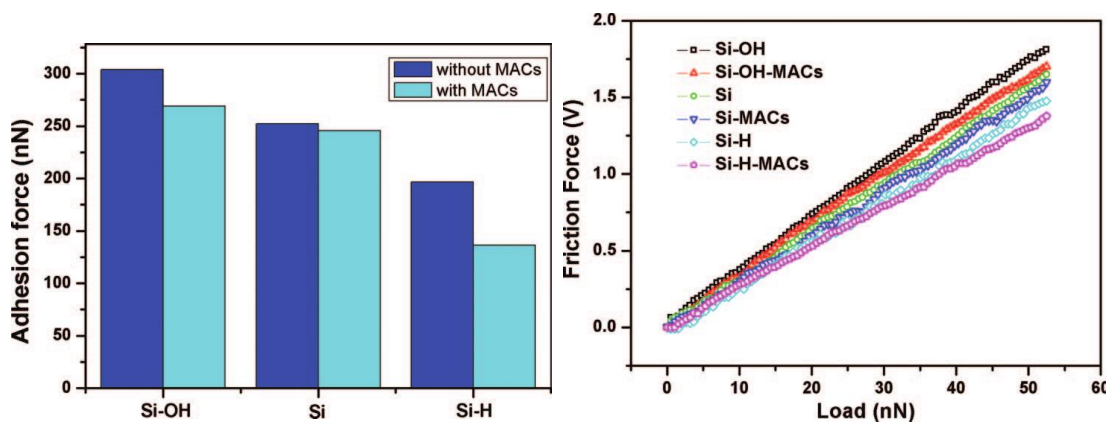
MACs have been tested for friction and wear performances under various conditions such as a four-ball tribometer, and found to give good durability and low wear (Venier et al. 1991; Ohno et al. 2010). The durability and wear properties of MACs have also been investigated as an overcoat on SAMs, similar to previously mentioned studies for PFPE, and found to have self-lubricating ability (Ma et al. 2007). MACs have been used in dual-component lubricant films to show improved durability and load carrying capacity, as well as to greatly reduce the friction upon sliding (Ma et al. 2007; Wang et al. 2011), and have been found to provide lower wear rates compared to some PFPE lubricants under vacuum conditions (Jones et al. 1999), possibly due to the superior chemical stability under those conditions.

Wettability of MAC-coated surfaces have been studied, and it was found that the MAC coating increases the contact angle on the coated surface (Wang et al. 2010a; Wang et al. 2010b). Wang and co-workers have found that the effect is more pronounced for a hydroxylated silicon wafer and hydrogenated silicon wafer than it is for a cleaned silicon wafer (Table 2-1), although all three show an increase in hydrophobicity (Figure 2-10). This was further shown to be the case as the hydrogenated surfaces had adsorbed the most amount of MAC on the surface, with

the other two surfaces not easily wetted. Nano-adhesion forces, characterized with an AFM/FFM using the contact mode, were also found to be most reduced on the hydrogenated surface, and both the reduction in adhesional forces and the hydrophobicity increase were thought to be a result of the topological structure changes of the surface as MACs have no functional groups on the surface. Nano-friction forces measured from the twist of the tip-cantilever assembly and with various external loads were tested, with the hydrogenated silicon showing the least amount of friction and the hydroxylated silicon with the highest friction, similar to the adhesion forces measured.

**Table 2-1: Water Contact Angles on various modified silicon surfaces (Wang et al. 2010a)**

Substrates	Contact Angle without MACs (°)	Contact Angle with MACs (°)
Cleaned Silicon Wafer	46.8	51.8
Hydroxylated Silicon Wafer	2	25.9
Hydrogenated Silicon Wafer (H-Si(100))	74.9	94.1



**Figure 2-10: Nano-friction and nano-adhesion forces measured for treated and untreated silicon surfaces (Wang et al. 2010b). Reprinted with permission.**

In addition to its excellent performance, additives have been investigated for MACs to further reduce the wear rates and improve performance for space applications, using low volatility additives in particular (Peterangelo et al. 2008). The friction and wear properties were tested using a four-ball wear test, as per ASTM D4172 standards, and stainless steel balls. Vacuum four-ball wear tests were conducted to determine the steady wear rates in vacuum, as well as a reciprocating tribometer and a vacuum spiral orbit tribometer (SOT) developed by Pepper and co-workers (Pepper et al. 2003a). SOT tests were also performed to evaluate the performance of a linear perfluoropolyalkylether (PFPAE), a branched perfluoropolyalkylether and a MAC hydrocarbon, with the MAC hydrocarbon showing the longest normalized wear life and lowest friction coefficient (Pepper et al. 2003b). MAC lubricants were shown to be clearly more robust than PFPAE under these conditions despite the statistical scatter in lifetime observed in the SOT. The same setup was used again to compare starvation conditions of PFPE and MAC lubricants, by dipping the specimens in a dilute solution of the lubricant, and the two lubricants were found to exhibit different tribological properties (i.e. friction trends and wear lives) due to different spreading and lubricating mechanisms over the duration of the tests, which will be discussed.

MACs have been compared to PFPE lubricants for thermal stability and decomposition, and found to not react catalytically with aluminium oxide as the fluorine atoms and acetal units which enable Lewis acid attack are absent in MAC molecules. PFPE, on the other hand, is observed to have chain scission at both mid- and end-chain, resulting in faster weight loss and implying that the thermal stability of MACS are superior to that of PFPE lubricants (Chun et al. 2003). Pepper and co-



workers have also concluded that MACs are more resilient to tribo-chemical attack than PFPEs (Pepper et al. 2003b).

It should be noted that the two additives work differently and show different levels of contribution to the improvement of performance (if at all) under different conditions (Peterangelo et al. 2008). This is a strong reminder that tribological properties are largely dependent on the conditions under which they are being tested, as discussed throughout this chapter; whether submerged in lubricant or tested under starved conditions, or even as a thin film or an overcoat.

## **Chapter 3 - Materials and Experimental Methodology**

*In this chapter, a brief summary of the general materials used in the work, the preparation of solutions and films and various other methods are described. Additional information on specific materials, preparation methods, calculations and techniques will be provided in the respective chapters if necessary.*

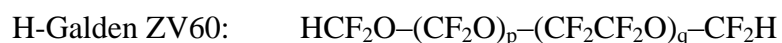
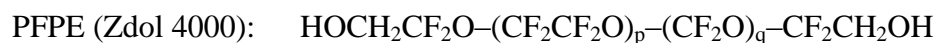
### 3.1 Materials

#### 3.1.1 Silicon

Polished n-type silicon wafers, with approximately 455-575  $\mu\text{m}$  thickness and hardness of 12.4 GPa, were used as the substrates in surface characterization and friction and adhesion measurements. Surfaces were cleaned appropriately prior to coating or tribological testing by ultrasonic rinsing in ethanol for an hour, followed by air plasma cleaning using a Harrick Plasma Cleaner/Sterilizer. The surfaces were exposed to air plasma under vacuum for approximately 5 minutes using an RF power of 30 W, and stored in a desiccator overnight prior to testing.

#### 3.1.2 Perfluoropolyether (PFPE)

PFPE was used at various concentrations in H-Galden ZV60, and both were purchased from Ausimont Inc. The chemical formulae are as follows:



The ratio  $p/q$  was  $2/3$ . The physical properties of PFPE can be found in detail in Table 3-1.

Table 3-1: Physical properties of perfluoropolyether (PFPE) lubricant Fomblin Z-dol 4000

Properties	Units	Description/Value
<b>Functional Group</b>	-	Alcohol (-OH)
<b>Appearance</b>	Visual	Clear liquid
<b>Colour</b>	APHA	Colourless
<b>MW (NMR)</b>	Amu	4000
<b>Difunctional content (NMR)</b>	%	90
<b>C2/C1 ratio (NMR)</b>	-	1
<b>Kinematic viscosity</b>	cSt	100
<b>Density @ 20°C</b>	kg/m <sup>3</sup>	1820
<b>Vapour pressure @ 20°C</b>	Torr	1 x 10 <sup>-8</sup>
<b>Vapour pressure @ 100°C</b>	Torr	1 x 10 <sup>-4</sup>
<b>Refractive index @ 20°C</b>	-	1.296
<b>Surface Tension @ 20°C</b>	mN/m	22
<b>Polydispersity @ 20°C</b>	Mw/Mn	1.15

### 3.1.3 Hexadecane

Hexadecane was used as one of the lubricants or main solvents of lubricants for testing of MEMS over a varying number of speeds, primarily in investigation of hydrodynamic lubrication (Chapter 7) and liquid lubrication for MEMS. Hexadecane was obtained from Sigma-Aldrich Pte Ltd, and was used as obtained, at more than 99% purity.

### 3.1.4 Multiply Alkylated Cyclopentanes (MAC)

MACs were used as both a lubricant and an additive. Details of its use are further elaborated in each chapter. The MAC lubricant used was Nye Synthetic Oil 2001A, obtained from Dulub Pte Ltd, which is a mixture of di- and tri-(2-octylododecyl)-cyclopentane, a saturated hydrocarbon containing no additives. The physical properties of the MAC lubricant are detailed in Table 3-2 and further details are provided by Dube (Dube et al. 2003).

Table 3-2: Physical properties of MAC Lubricant, Nye Synthetic Oil 2001A

Properties	Units	Description/Value
<b>Molecular Formula</b>	-	C <sub>16</sub> H <sub>34</sub>
<b>Molar mass</b>	g/mol	226.44
<b>Appearance</b>	-	Colourless liquid
<b>Density</b>	mg/mL	773

### 3.1.5 Octadecylamine

Octadecylamine (ODA), 97 % purity, obtained from Sigma Aldrich, is a long chain molecule with 18 carbon atoms in its chain. It has been studied as a friction modifier in liquid lubrication with MEMS since ODA adsorbs to form a film on silicon surfaces (Reddyhoff et al. 2011) and has also been found to attach to form a monolayer on mica surfaces (Benítez et al. 2002a; Benítez et al. 2002b).

## **3.2 Surface analysis equipment and techniques**

### **3.2.1 Contact angles**

Contact angles were measured to determine the surface free energies of the Si wafer surfaces, as previously described. This was carried out using a VCA Optima Contact Angle System (AST Product, Inc., USA) with droplets of 0.5  $\mu\text{l}$ . The liquid was dispensed using a syringe and the contact angles between the solid-liquid interfaces were observed and recorded using a microscope. An image was taken using a video-still capture and the contact angle measured using the provided software. Contact angles reported in this work are an average of at least five independent measurements across a minimum of three samples with the same surface conditions. The variation in the contact angles at various locations while measuring is within  $\pm 2^\circ$ , and the error of measurement within  $\pm 1^\circ$ .

### **3.2.2 Surface Profiling**

#### ***3.2.2.1 Optical Profiling***

Optical profiling was performed using a Wkyo NT1100 Optical Profiler obtained from Veeco Instruments Inc., to investigate the roughness and topography of various polished and unpolished surfaces, and to understand the effects of the roughness and topography in lubrication effectiveness. This also assists the study of lubrication mechanisms. The measurements from the optical profiler are made with optical phase-shifting and white-light scanning interferometry, with non-contact static measurements, allowing for surfaces to be scanned prior to testing without affecting the surface properties or lubricant. The vertical measurement range is between 0.1 nm and 1 mm, with a resolution of less than 1  $\text{\AA}$ , and vertical scan speeds of up to 14.4

$\mu\text{m s}^{-1}$ . Profiles were taken with an integrated stroboscopic illuminator and conducted in a class-100 clean booth.

### **3.2.2.2 Ellipsometry**

Ellipsometry was conducted to measure the film thickness of uniform films on Si surfaces, using a Variable Angle Spectroscopic-Ellipsometer (VASE, J. A. Woolam. Co. USA), using wavelengths from 400 nm to 1000 nm at 10 nm intervals. The incident angles used for measurements were  $65^\circ$ ,  $70^\circ$  and  $75^\circ$ . Data analysis for the measurements was done using WVASE Windows Version 3.352 software. Refractive indexes used for the various materials are given in the relevant sections. The ellipsometer uses the refraction of a laser (at a given wavelength) due to the presence of a film on the reflective surface to determine the thickness of the film.

### **3.2.3 Microscopy**

#### **3.2.3.1 Field-Emission Scanning Electron Microscopy**

Surface topography of wear tracks and surfaces both prior to and after friction and wear tests were examined using a Field Emission Scanning Electron Microscope (FESEM) (Hitachi S4300) machine, coupled with an energy dispersive spectrometer (EDS) used to investigate the elements on the surface. EDS was used primarily to observe and map the relative concentration of the elements detected on the surface, particularly those indicative of lubricant present on the surface in question.

### **3.2.3.2 *Optical Microscopy***

Optical microscopy was carried out to observe the surface conditions, wear tracks and film morphologies on the various surfaces tested, and to observe droplet behaviour, shape and profiles.

### **3.2.3.3 *Surface Area and Spreading Measurements***

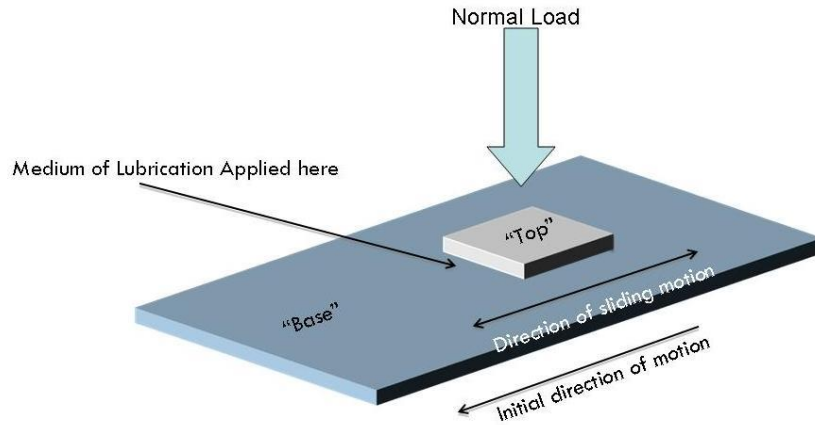
Spreading tests for investigation of spreading of liquids were conducted by placing a 5  $\mu\text{l}$  droplet of test lubricant containing the various additives on a cleaned silicon wafer, and observing their behaviour until a steady state is reached. This behaviour was recorded on video and frames were extracted from the videos for manual outlining of the droplet and calculation of the area of the droplet with a known scale. Surface areas were calculated using image processing and edge identification in MATLAB.

## **3.2.4 Friction and wear tests**

### **3.2.4.1 *Localized Lubrication – “Loc-Lub”***

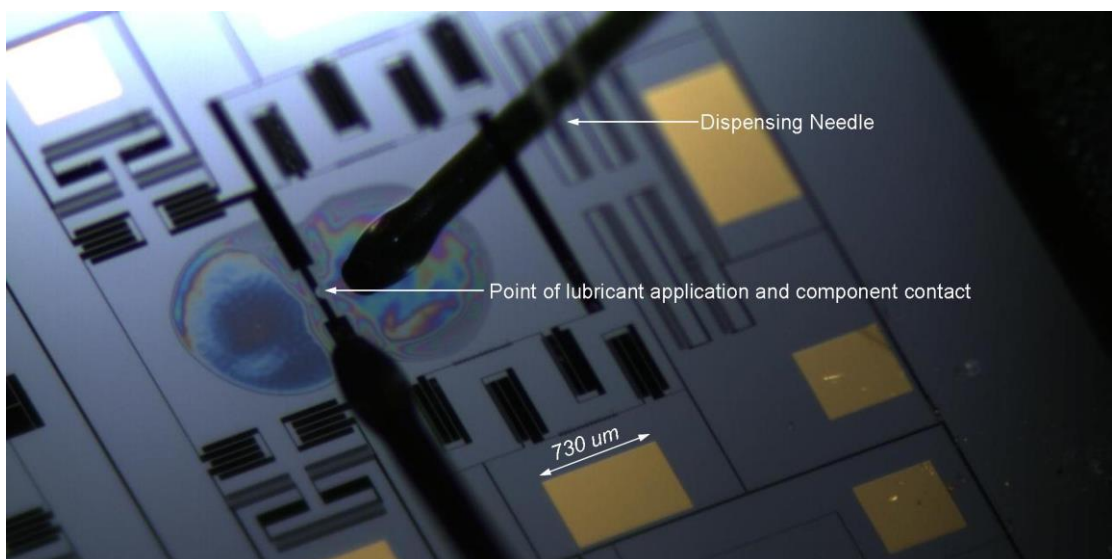
A novel method of lubrication was implemented and tested for effectiveness as part of this work, both for Si wafers on the reciprocating wear tester as well as for the MEMs reciprocating tribometer (Sinha et al. 2010). A schematic of the method of lubrication for reciprocating sliding testing is shown in Figure 3-1.





**Figure 3-1: Schematic of the Loc-Lub setup for reciprocating sliding wear testing**

The “Loc-Lub” setup for Si wafers consists of a needle and syringe coupled with a repeating dispenser to deposit the same amount of lubricant each time. All components were obtained from Hamilton Pte. Ltd. The needle was positioned at the side of the interface between the two silicon wafers, and a set amount of lubricant was dispensed during each experiment, kept consistent within each set and indicated per each section. The lubricant is believed to be pulled between the unloaded specimens’ interface via capillary action depending upon the surface tension of the liquid.



**Figure 3-2: A video still capture of the Loc-Lub method applied to a reciprocating MEMS tribometer. Approximately 0.1  $\mu\text{l}$  of PPF was dispensed onto the tribometer in this case.**

The MEMS device “Loc-Lub” setup consists conceptually of a dispensing needle with a syringe filled with the lubricant – a burst of pressure, controlled by an air pressure regulator, is able to deposit a tiny drop of lubricant on to a surface close to the dispensing needle (Figure 3-2). It is undesirable for a lubricant droplet to suspend from the needle and then contact with the surface, bringing both surfaces into contact with the liquid at the same time, as the devices can be fragile enough for surface tension forces to pull the components out of plane and damage the structure – often breaking it. Hence, the concept is to shoot a droplet of lubricant on a designated location without the needle and the device contacting at any time or the droplet bridging the needle and device. The latter, which is to be avoided, is similar to that of putting a drop of water from a pointed object to a flat surface by bringing the point into contact with the surface – the small scale of MEMS devices means they have very low structural stiffness and the devices would not be able to withstand the viscous and capillary meniscus forces when in contact with the liquid upon pull-off of the point, thereby breaking the device out of plane. The location at which a droplet is deposited can be set by moving the stage on which the MEMS device rests, and ascertaining the location via live video microscopy. If necessary, test runs for the location of the droplet can be carried out on a separate surface or wafer.

This method will be tested for efficiency and application as part of this work in Chapter 4, 5 and 6.

### 3.2.4.2 Reciprocating Wear Tester

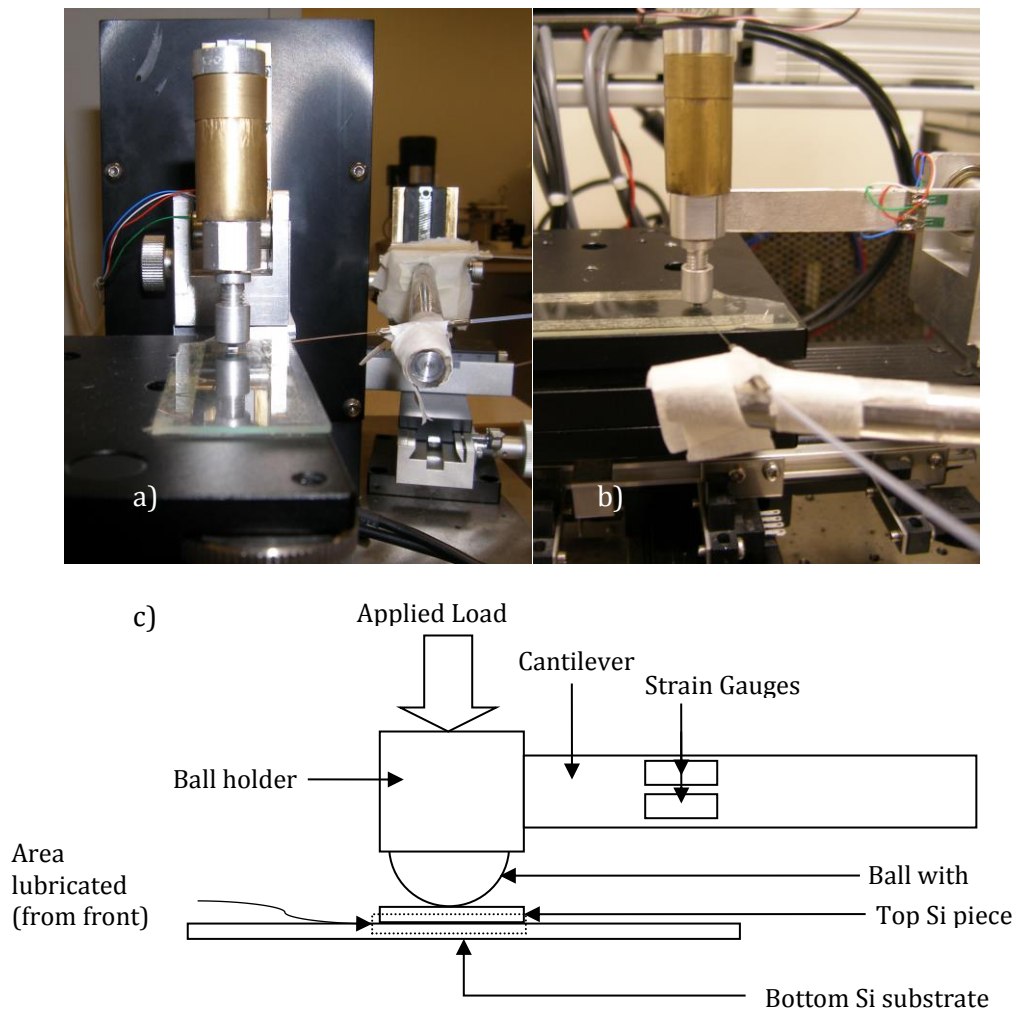


Figure 3-3: Images of Loc-Lub setup for feasibility verification a) from the side, b) from the front and c) a schematic of the reciprocating wear tester

A custom-made reciprocating wear tester was used to investigate linear sliding between two surfaces as a method of verifying the effectiveness of the “Loc-Lub” method for application of lubricant, as well as to compare wear rates and friction coefficient of different lubricants. A schematic of the wear tester is shown in Figure 3-3 along with an image of the tester itself.

The reciprocating wear tester moves the base support in oscillating motion, with linear amplitude of 2 mm. The upper silicon piece, measuring 2 mm by 2 mm, is set into contact on the lower piece, before the silicon ball held on the cantilever is lowered onto the top piece, assuring that the two surfaces are in full contact with each

other and are levelled with each other prior to sliding motion. Calibrated strain gauges attached to the side of the cantilever measure the strain caused by friction between the upper Si wafer and the oscillating lower Si wafer at a sampling frequency of 10 Hz, with the stage oscillating at 2.5 Hz. The strain measurements are then converted into frictional force, and thus coefficient of friction. The deadweight load applied directly above the upper Si wafer is 50 g and is later increased for more severe conditions.

### 3.2.4.3 Reciprocating MEMS Tribometer

A custom MEMS tribometer was designed, which consists of two main components: a sliding component and a contacting component. A schematic of the micro-tribometer is shown in Figure 3-4.

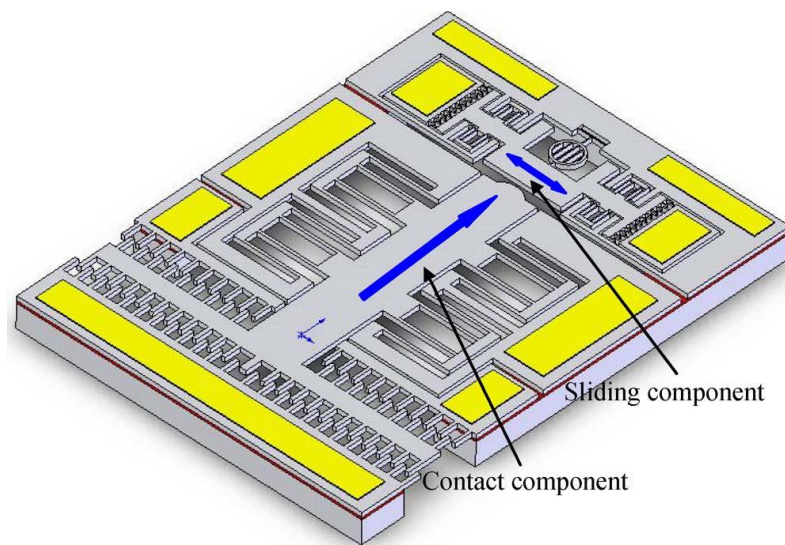


Figure 3-4: Schematic of the reciprocating tribometer (Hongbin et al. 2011)

During the friction test, the contacting component is pressed against the sliding component using an actuating voltage to control the force, thereby affecting the resultant friction. The contact between sidewalls of the two components is controlled from this component. The sliding component is dynamically actuated

during the test to oscillate while in-plane and in contact with the other component, providing the relative motion required for the friction test and to achieve sidewall contact. A novel in-plane displacement detection mechanism is used in this design, based on laser beam scanning for in-plane grating rotation first developed by Zhou and co-workers for high-speed scanning applications (Guangya et al. 2004; Guangya et al. 2006; Yu et al. 2009; Zhou et al. 2009a; Zhou et al. 2009b). In this configuration, a diffraction grating is suspended on two beams (Figure 3-5) with one beam connected to the substrate as an anchor and the other fixed to the sliding component. Rotation of the grating, in-plane as shown by the indicated arrows, occurs upon movement of the sliding structure.

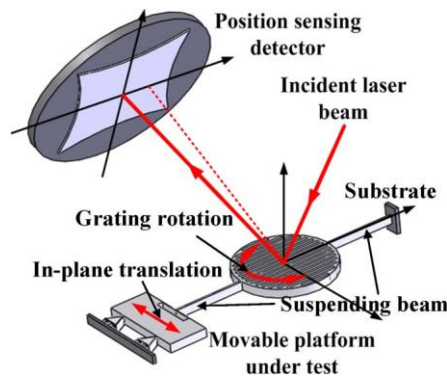


Figure 3-5: Schematic of the displacement sensing mechanism, with rotational grating (Hongbin et al. 2011)

The mechanical deflection of the structure can be summarized by Equation 3.1:

$$EI \frac{d^2y(x)}{dx^2} = Fx - M \quad (3.1)$$

Equation 3-1: Mechanical deflection of MEMS tribometer

where  $y(x)$  is the deflection,  $F$  and  $M$  are the force and moment applied at the tip of the sliding component respectively,  $E$  is the Young's Modulus of the material and  $I$  is the moment of inertia in the displacement direction, where  $I = \frac{hb^3}{12}$  with structural thickness  $h$  and width  $b$ .

The tribometer was first calibrated with known voltages to obtain the displacement and force constants for each test, and then subsequently the normal force and friction force were obtained, allowing for the calculation of coefficient of friction. Further details of the device can be found in the literature referenced above. The device was run using a normal loading voltage of approximately 50 V during wear tests, resulting in a force of about 0.1 mN, and a sliding driving voltage of approximately 40 V with a full sliding distance of approximately 6  $\mu\text{m}$ , at a frequency of 50 Hz. The displacement signal was observed periodically, and devices were considered to have reached their device life when no movement was observed, i.e. the friction became too large for sliding to occur, thereby rendering the device non-functional.

#### ***3.2.4.4 Rotational MEMS Tribometer***

A custom made tribometer (Ku et al. 2010) was used to test the friction and wear properties of high-sliding MEMS under rotational conditions at various speeds. A schematic is given in Figure 3-6. Frictional forces are measured as the torque induced on the lower specimen by bringing the upper specimen into contact (loaded) and rotated at varying or a constant desired speed. The upper specimen is mounted onto a high speed DC motor, whose vertical position is controlled accurately using a computer-controlled z-stage. A laser is used to detect the torque induced by friction due to rubbing or viscous drag between the two specimens.

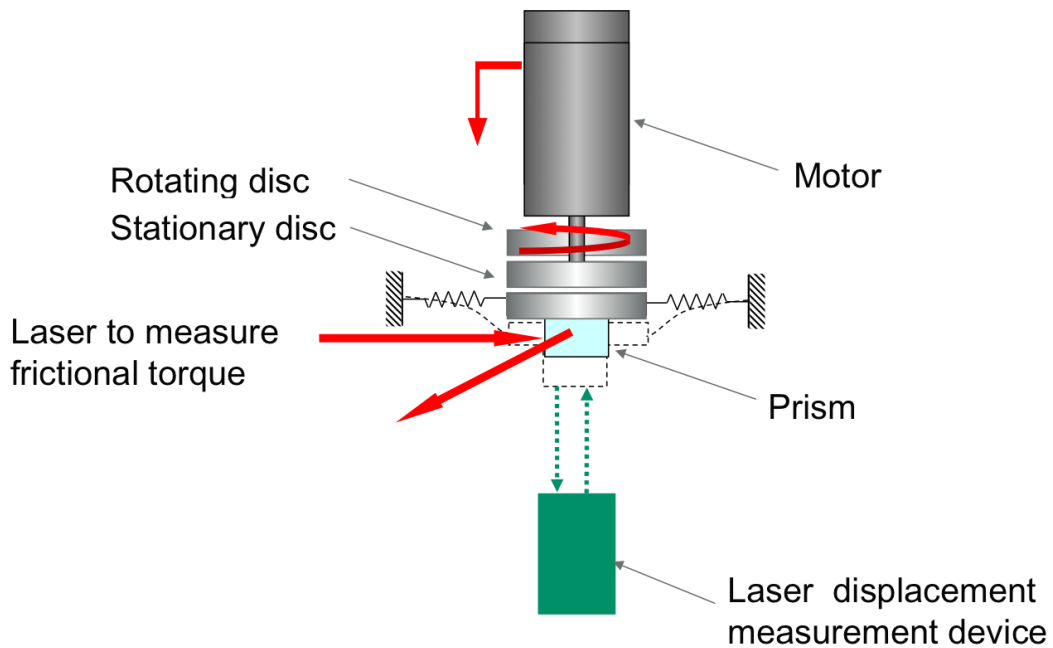


Figure 3-6: Closeup schematic of tribometer showing springs and loading

Prior to each test, a drop of lubricant was placed on the lower specimen - the axes of the disc specimens were aligned using two video cameras and loaded against each other. The required normal force was adjusted by changing the vertical position of the upper specimen and motor, utilizing the spring force of the supporting platform. Once loaded, tests can be conducted at a constant speed for a fixed duration for wear tests, or with stepwise increasing speeds up to a limit for measuring friction behaviour over a range of speeds. Frictional torque and normal load was determined by multiplying the relevant platform stiffness by their respective displacement. Data acquisition and motor control were automated using LabVIEW software, with a screenshot shown in Figure 3-7.

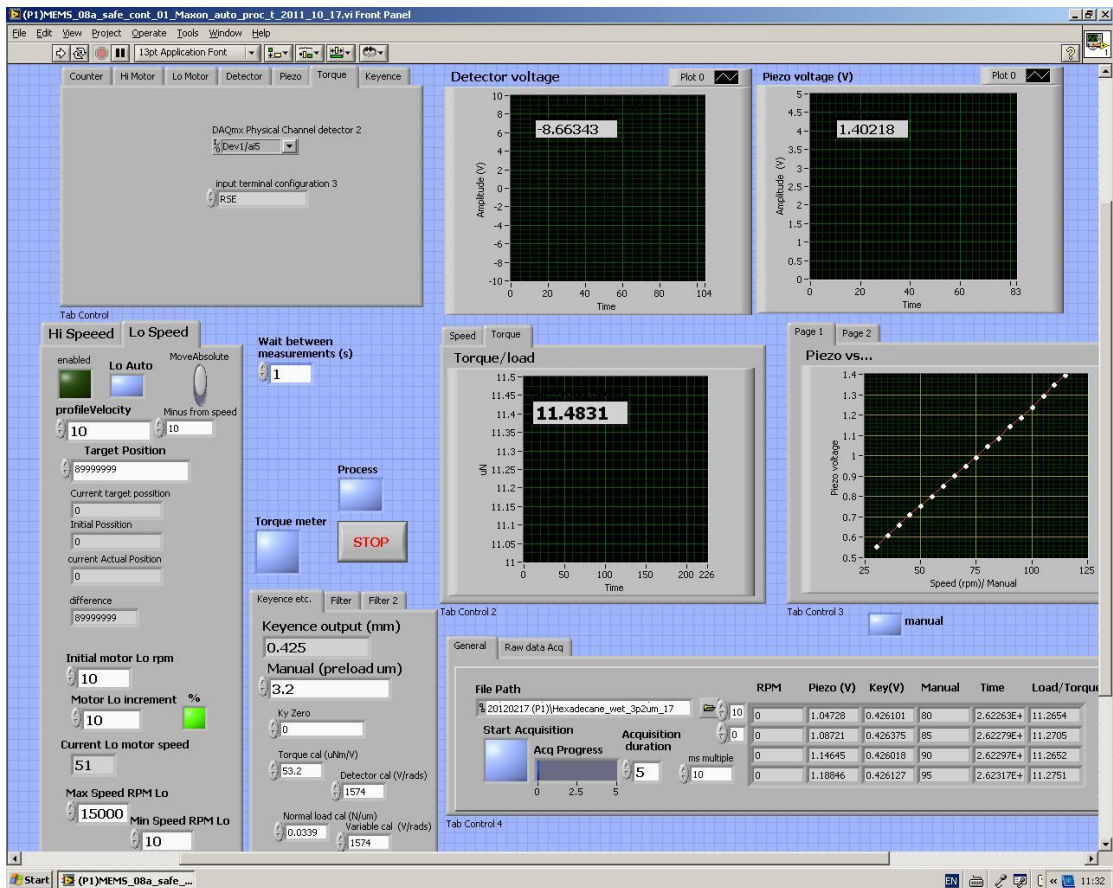


Figure 3-7: Screenshot of LabView VI used in motor control and data acquisition

Tests were run against a lower specimen surface – a patterned MEMS disc with dimensions shown in Figure 3-8, with patterns similar to that of a thrust pad bearing with a step height of  $50\ \mu\text{m}$ . These were fabricated from silicon wafers with a combination of photolithography and through-wafer Deep Reactive Ion Etching (DRIE).

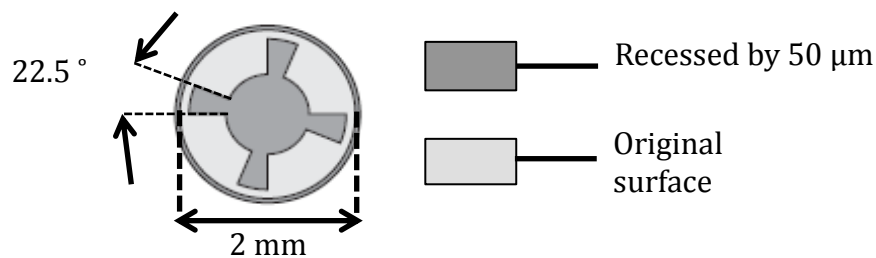


Figure 3-8: Dimensions of etched stepped pad bearing used in experiments



This equipment was developed by Ku and co-workers (Ku et al. 2010), and has been used in their work to study and quantify lubrication of high-sliding MEMS contacts (Ku et al. 2011; Reddyhoff et al. 2011; Ku et al. 2012). A photograph of the full equipment set-up is shown in Figure 3-9.

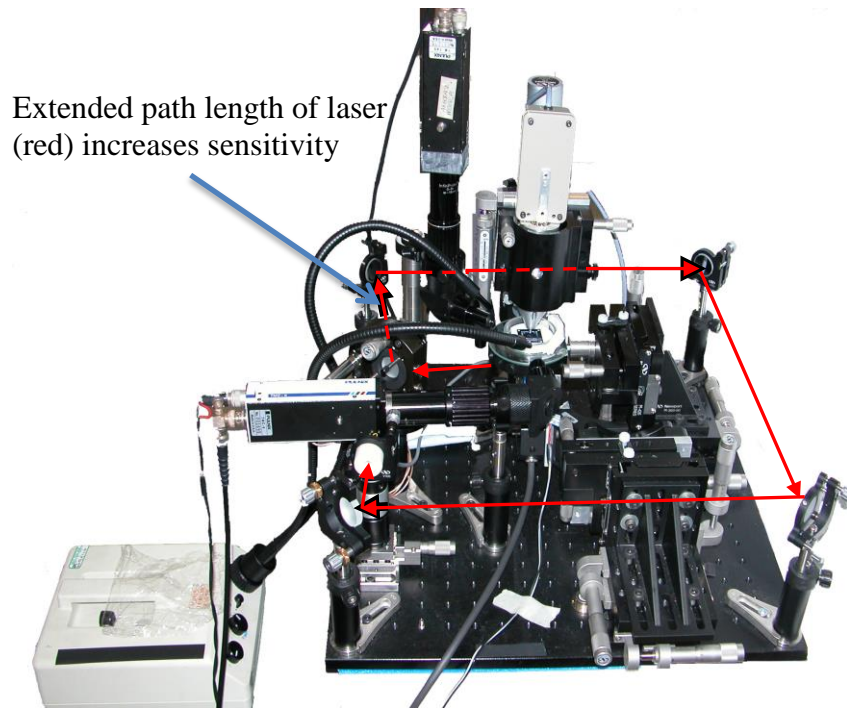
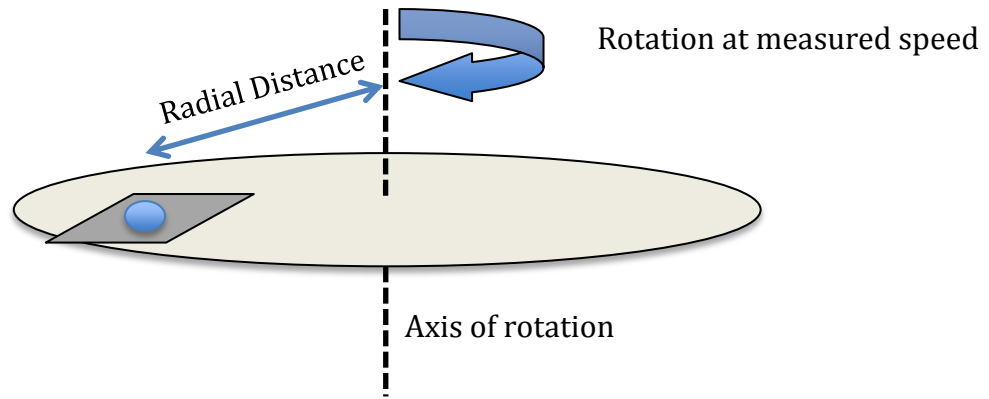


Figure 3-9: Picture of the rotating MEMS Tribometer, with the laser path indicated with red arrows

#### 3.2.4.5 Spin Tests

Spin tests were conducted on a spinning plate (Figure 3-10) to determine the force required to move the droplet from its original applied position on a silicon wafer, thereby simulating starvation of lubricant at a point due to gravity- or other force-induced flow.



**Figure 3-10: Schematic for spin tests conducted on a spinning disc, with a silicon specimen and a drop of lubrication placed at the tested distance**

Radial distances of 40 mm and 20 mm were used on this spinning plate, to provide radial forces. The silicon samples were stuck the designated distance from the axis of rotation, approximately at the centre of the wafer. The rotating plate was then spun at increasing speed and droplet movement observed. When the droplet was seen to occupy almost a completely different area on the wafer, the speed at which this occurred was recorded and the centrifugal force on the droplet at that instant was calculated using the following formula:

$$F = mr\omega^2 \quad (3-2)$$

**Equation 3-2: Formula for centripetal force exerted on liquid droplet under spin tests**

where  $m$  is the mass of the droplet,  $r$  the distance from the axis of rotation, and  $\omega$  the angular velocity. This force, called the “throw-off force” is then characteristic of the force required to cause the liquid drop to move or spread from its original position, and therefore indicative of the ability of various investigated surface modifications to contain liquid. Each type of surface was tested at least 5 times with consistent results, and the average taken. Tests were conducted with two liquids; water and hexadecane, both of which have been proposed as liquid lubricants in MEMS (Ku et al. 2011; Ku et al. 2012).

## **Chapter 4 - Localized Lubrication (“Loc-Lub”) – A Novel**

### **Method**

*This chapter presents a novel method of lubrication of MEMS devices that is designed to avoid the problems of flooding of lubricant over an entire MEMS surface, and to overcome the difficulty of lubricating MEMS sidewalls (due to their small scale and inaccessibility). Experimental results, typical wear and friction data and analysis are presented to verify the effectiveness of the method.*

## 4.1 Introduction and Objective

MEMS sidewalls have been known to exhibit large amounts of stiction and friction, for example in micro-gears. The small size and cross sectional area as compared to plane surfaces make lubricating the sidewall surfaces more challenging as there is a smaller surface area for lubricant containment and it is more difficult to access the sidewalls after fabrication of the devices. Furthermore, the sidewalls and plane surfaces have different surface characteristics due to the different exposure to the environments and fabrication processes. Combined with the small size of the gaps, which can be as small as 10  $\mu\text{m}$ , both characterizing and lubricating sidewalls have proved a challenge. At the same time, it is undesirable for coatings or lubricant to spill over or form a layer over the entire surface of the MEMS device as certain components require unmodified surfaces to function optimally, such as electric pads for actuation. In order to circumvent this problem, a method of applying the lubricant to a very small area without affecting the rest of the device and yet remain effective at the contact and sliding points was needed.

A novel method of lubricating sidewalls – “Localized Lubrication” or “Loc-Lub” – was invented, and first tested on silicon wafers at the macro scale. The friction and wear life was tested using various methods, viz. dry, dip-coated, vapour phase and “Loc-Lub” method, to ascertain that the novel method was effective. It was also subsequently investigated in an actual MEMS tribometer (Chapter 6).

## 4.2 Materials and Methodology

Si wafers were used in macro scale tests on a custom-made reciprocating wear tester to investigate the effectiveness of the Loc-Lub method in principle, compared to various other common methods of lubrication for Si surfaces. The “Loc-Lub”

application method used a syringe to apply a fixed amount of PFPE lubricant at the interface between the two Si wafers as detailed in Chapter 3. Both the polished (smooth) and unpolished (rough) surfaces of the Si wafer were used and the roughness measured.

The novel method was compared to Si wafers lubricated via dip-coating in a solution, and Si with PFPE on the surface via a vapour deposition method in which the wafer was functionalized with air plasma before being inverted over a solution of PFPE in a vacuum chamber. Dip coated was performed by vertically lowering the wafer into a solution, and then vertically lifting it out of the solution at the same speed, utilizing a dip-coating machine for this purpose (Myo et al. 2008). All three surfaces were analysed for the presence of PFPE before and after testing as part of the comparison of the techniques.

All concentrations of PFPE used in this section were of 4 wt% in H-Galden unless otherwise indicated. The surfaces were considered to have failed when the average coefficient of friction exceeded 0.3, when the frictional measurements fluctuate greatly, or when visible wear debris was observed on the surface, whichever happened first. For samples that achieved a stable and sustained coefficient of friction without failing, the frictional values were also recorded prior to the gradual increase of friction leading to failure.

Other experimental details are elaborated in Chapter 3.

### 4.3 Experimental Results

#### 4.3.1 Water contact angle measurements

**Table 4-1: Water contact angles for various Si surfaces. All surfaces were lubricated with 4.0wt% PFPE in H-Galden solvent.**

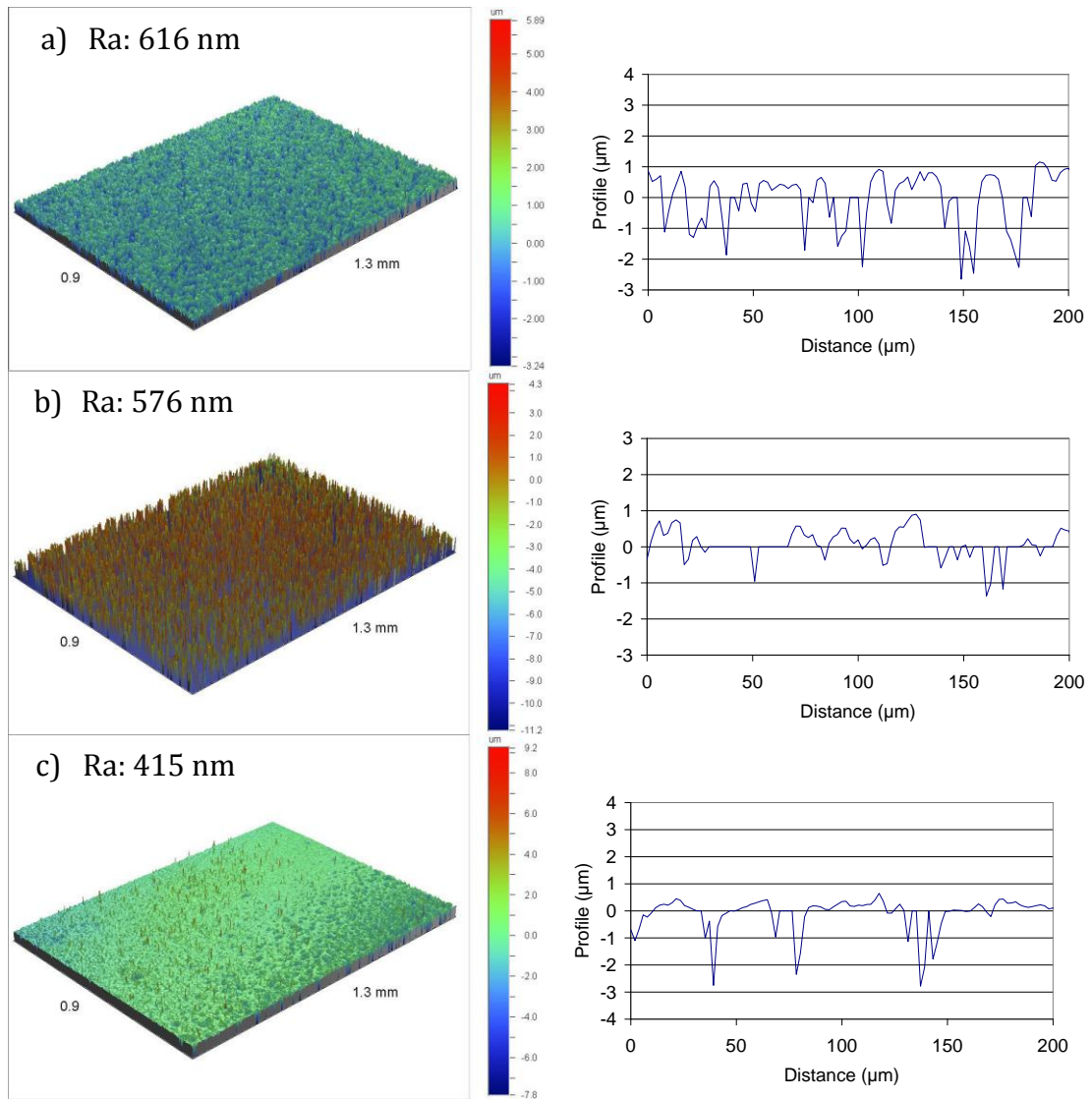
<b>Surface &amp; Method of Lubrication</b>	<b>Water contact angle (°)</b>
Polished Si (uncoated)	5.5
Unpolished Si (uncoated)	5.7
Polished Si, Loc-Lub	55.0
Unpolished Si, Loc-Lub	38.8
Polished Si, Vapour deposition	25.2
Polished Si, Dip coated	38.5
Unpolished Si, Dip coated	30.4

Water contact angle measurements (Table 4-1) were taken to observe the differences in surface conditions between specimens with different surface roughness and different lubrication application methods. The changes in water contact angle indicate that the Si surfaces have successfully been modified – this is especially evident in samples that were dip-coated and under “Loc-Lub”. Uncoated samples and samples lubricated showed little change in the contact angles (and therefore surface energy). Vapour deposited samples showed an increase in the contact angle lower than that induced by dip-coating and “Loc-Lub”, possibly due to the low density of PFPE molecules bonded to the surface via the vapour deposition process – this is later investigated in the EDS mapping analysis for the surface conditions. As PFPE is known to induce a semi-hydrophobic property on the surface, a higher density of PFPE molecules on the surface would lead to a higher water contact angle measured.

Dip coated specimens were observed to have a high variation in the contact angles recorded, compared to the other methods of lubrication. It was also observed that a dewetting effect occurred on polished surfaces for dip-coating and “Loc-Lub” processes, in which the lubricant solution was not evenly spread over the surface, and dewetting marks and droplets could be seen. These uneven spreading and dewetting marks could be due to the high concentration used – 4.0 wt% as compared to 0.2 wt% as sometimes used in the lubrication of magnetic hard disks. The same dewetting marks were not observed on unpolished surfaces probably due to lower visibility on the roughness of the surfaces. The effects on both polished and unpolished surfaces, and the conglomeration of PFPE droplets or the dewetting will be discussed shortly as effects of texturing.

### **4.3.2 Optical Profiling and Ellipsometry**

The topography of the surfaces before and after lubrication gives a broader perspective of the surfaces prior to wear testing, and also provides insight into the lubrication mechanisms, as will be later discussed.



**Figure 4-1: Optical profile images of a) bare unpolished silicon, b) dip-coated unpolished silicon and c) unpolished silicon with localized lubrication, with their respective line profiles taken across the centre of the scan. Roughness values ( $R_a$ ) are given beside each profile image.**

Polished surfaces were found to have an increase in roughness due to the dewetting effect – this provided positive evidence that lubricant was present on the surface in sufficient amounts to form droplets. For unpolished surfaces, the  $R_a$  roughness prior to lubrication was 616 nm, and after lubrication via dip-coating and “Loc-Lub” were 576 nm and 414 nm respectively. The reduction in the surface roughness is due to the filling up of the lower portions, or the “valleys”, of the asperities with the lubricant. This phenomenon also contributes to the improved wear

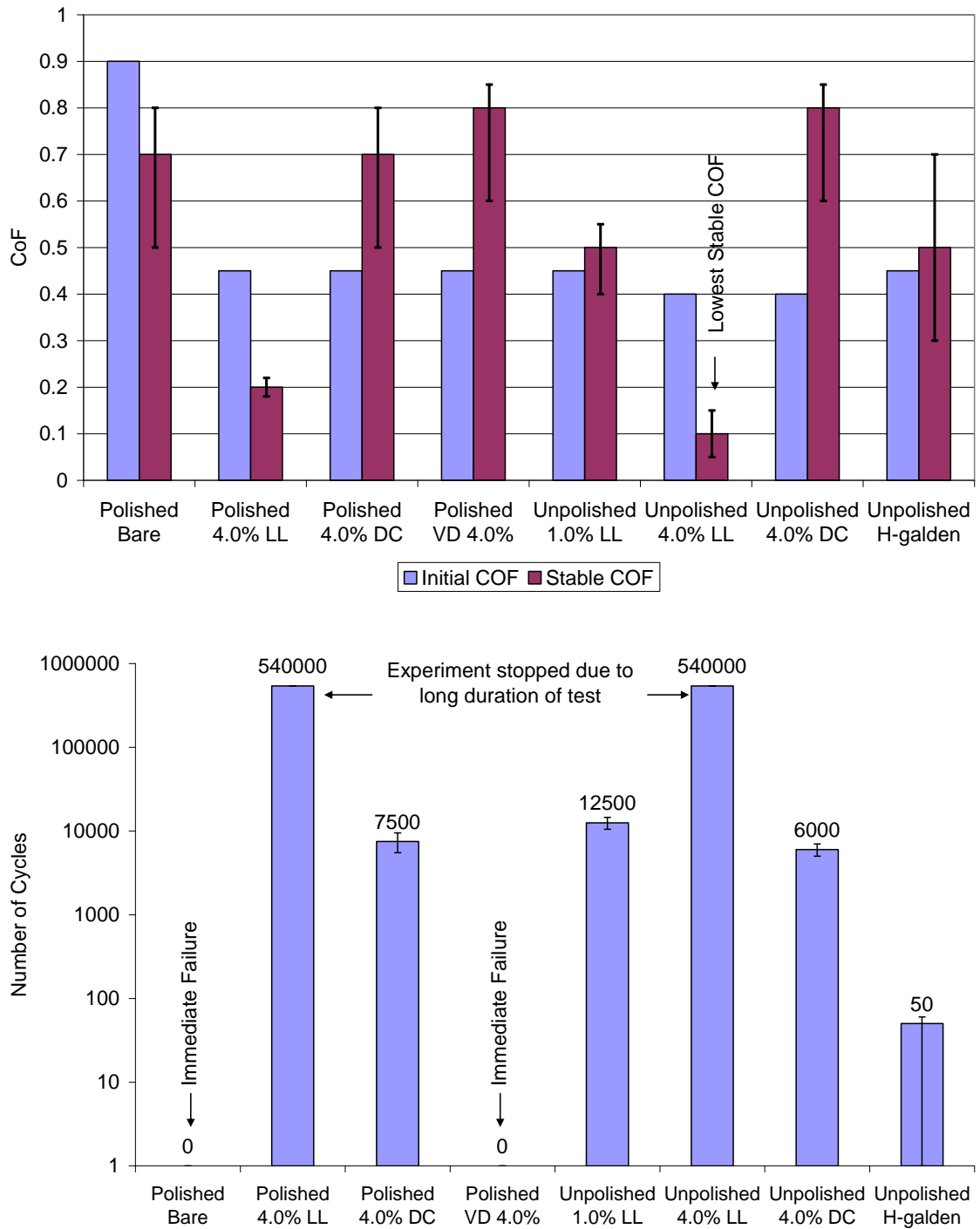


life and friction properties. The presence of the lubricant in excess amounts in the “valleys” is also later found to contribute to the greatly improved tribological properties, extending the wear life by several orders of magnitude. The optical profiles in 3D plane and 2D line graphs for the various surfaces are shown in Figure 4-1.

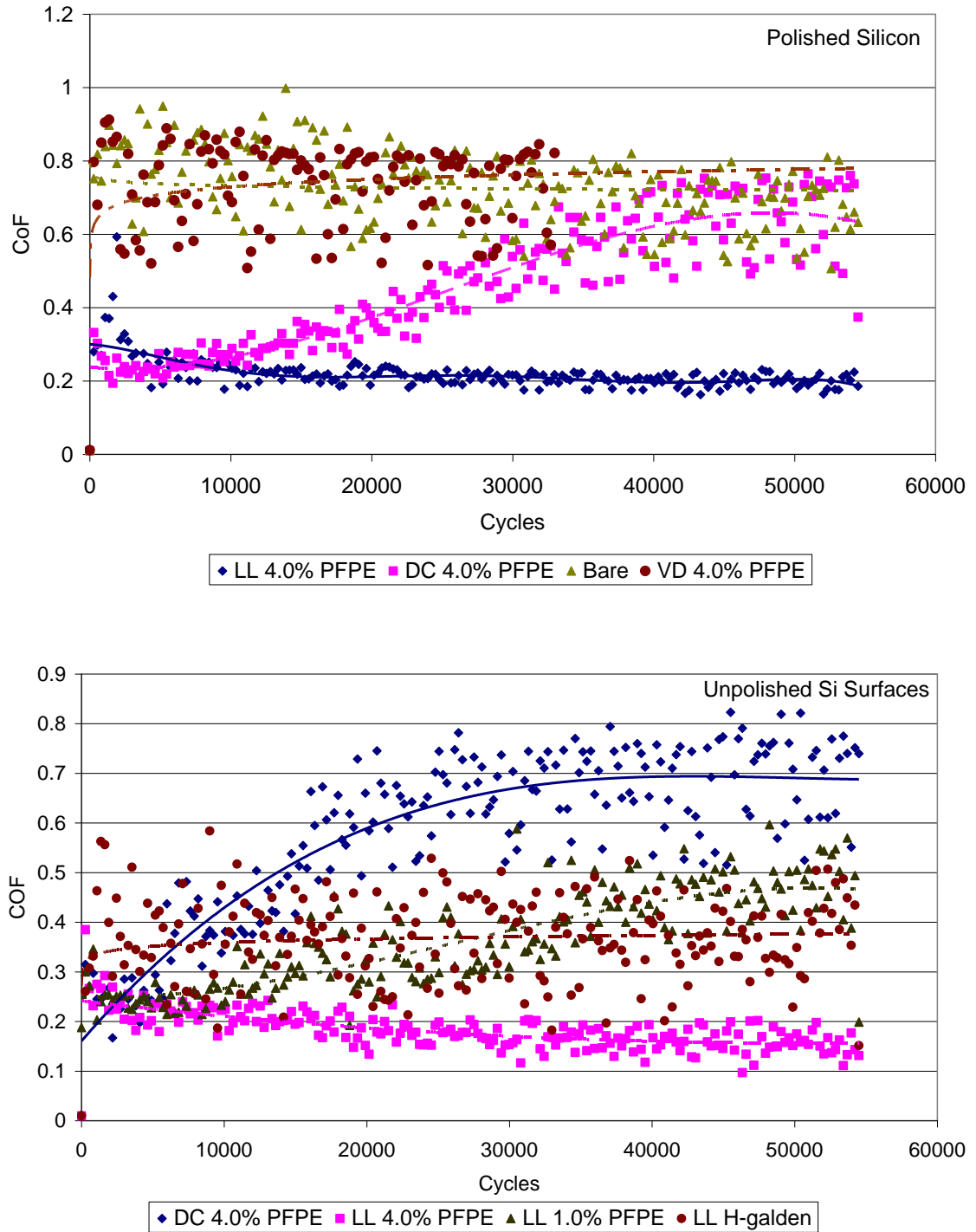
The PFPE present in these valleys provide self-replenishment during the sliding of surfaces, improving the tribological properties (Tani et al. 2001). These improvements are also investigated and verified in the reciprocating wear tests, optical analysis and surface chemical analysis using EDS.

Ellipsometry, which requires a highly reflective surface, was only conducted on polished surfaces due to this experimental constraint. The thicknesses of the lubricant films from the different methods of lubrication were measured, showing an average film thickness of 4.07 nm for “Loc-Lub” lubricated specimens, 2.40 nm for dip-coated specimens, and 0.15 nm for vapour-deposition lubricated specimens. The thickness and amount of lubricant present at the sliding interface also plays a strong role in the durability and the coefficient of friction observed which will be realized in the later sections.

### 4.3.3 Friction and Wear Life



**Figure 4-2: Summary of results from Reciprocating Sliding Wear (R.S.W.) and Ball-On-Disc Tests, showing the initial and stable coefficient of friction (top) and wear lives of samples (bottom). Large fluctuations were noted in the CoF (even before failure) for all samples except in the case of 4.0% LL. (DC = Dip Coating, LL = “Loc-Lub”, VD = Vapour Deposition)**



**Figure 4-3: CoF data, taken over the duration of the test, with respect to the number of reciprocation cycles for different lubrication methods and PFPE concentrations for both a) polished and b) unpolished Si surfaces. (DC = Dip Coating, LL = “Loc-Lub”, VD = Vapour Deposition)**

A summary of the wear life, initial and stable coefficient of friction, as well as the friction versus cycles trends of the surfaces lubricated with different methods are

shown in Figure 4-2 and 4-3. Initial tests with 1.0 wt% PFPE were carried out but the concentration was later increased to accentuate the differences between the methods investigated and to further improve the tribological properties. With the increased concentration, the stable measured coefficient of friction between two polished Si surfaces lubricated via “Loc-Lub” was 0.2, and lasted beyond both the standard test length of 6 hours (54,000 cycles) and extended test length of 60 hours (540,000 cycles). Less visible wear debris along the edges was observed and the surface was less scratched, if at all. Both polished and unpolished Si surfaces showed a great improvement in the friction and wear properties. The initial coefficient of friction for both lubricated surfaces was slightly higher at 0.45, but reduced quickly before any scratching or wear of the Si surface could occur. Once the surfaces reached a steady state, there was sufficient lubrication to prevent wear from occurring, and to keep friction at low levels. Due to the very thin films in vapour deposited samples, the wear life was found to be very low and very high friction was exhibited, akin to that of uncoated samples. This method was therefore not investigated beyond the standard 6-hour wear test.

For unpolished Si surfaces tested and lubricated under the same conditions with “Loc-Lub”, the steady coefficient of friction was 0.1, lower than that of polished surfaces, with the initial coefficient of friction only slightly lower at 0.4, compared to 0.45. This implies that the lubricant initially is not able to cover the entire area of the contacting surfaces and hence the high initial friction is caused by the bare silicon surfaces rubbing against each other, as will later be supported by EDS mapping scans. Similar to the polished surfaces, the high initial coefficient of friction dropped rapidly from the start of the test, avoiding any wear or debris, thus also preventing premature failure.

Both polished and unpolished Si surfaces lubricated under “Loc-Lub” with 4.0 wt% PFPE lasted beyond 540,000 cycles (60 hours) of reciprocating sliding wear tests, with unpolished surfaces showing a significantly lower stable coefficient of friction. The reduced friction in the case of textured samples is due to the presence of the asperities, which help to dissipate the capillary forces involved when lubricating the interfaces. As the film is broken up into smaller regions in a textured surface, the capillary forces are reduced due to the discontinuity of the lubricant. This adhesion was observed in separating the polished Si specimens after completing an extended test – in some cases the glue between the holding ball and upper specimen broke under the adhesion force during attempts to separate the specimens. The same adhesion was not observed in unpolished surfaces for the reasons stated above. At the same time, the excess lubricant stored in the “valleys” of the asperities readily provides a source of self-replenishment of the lubricant mobile phase when the original mobile phase between the two surfaces has been depleted due to the reciprocating sliding action, allowing for lower coefficient of friction at longer durations.

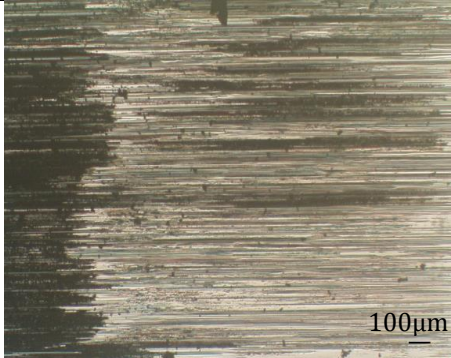
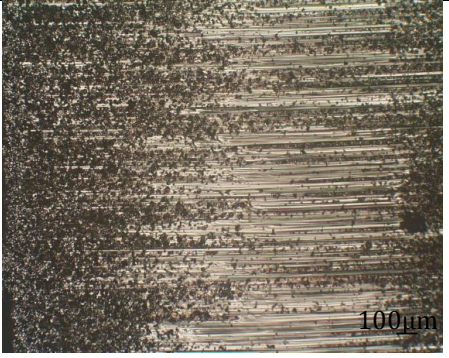

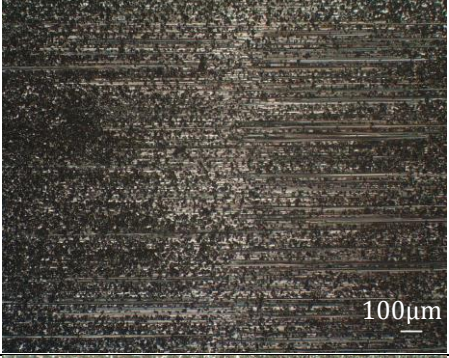

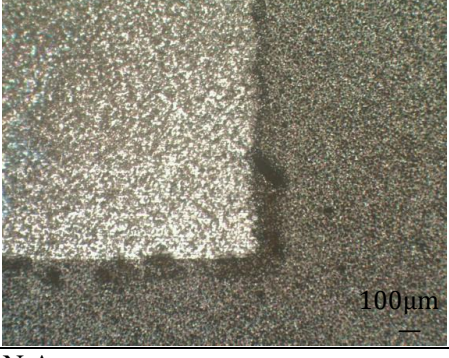
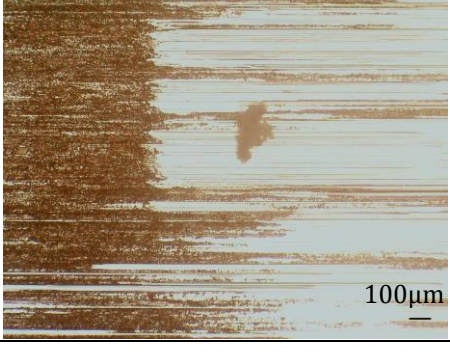
The same wear tests were conducted with only H-Galden solvent as the lubricant to eliminate the solvent effect and ensure that the PFPE component is what affects the surface. Figure 4-2 and 4-3 show that the wear life and friction properties were not affected significantly by the presence of H-Galden, and therefore the improved tribological properties were because of the presence of PFPE in the solution.

A comparison of the three methods of lubrication at the same concentration show that the “Loc-Lub” method provides the best tribological properties, showing the best combination of lowest stable coefficient of friction, the longest wear life,

followed by the dip-coated specimens. There was little observable difference between the wear lives of the vapour-deposited samples and the uncoated Si samples. It is interesting to note that with PFPE, the rough Si surfaces have a lower amount of friction and a longer wear life – this phenomenon will be further investigated in later sections in this chapter.

### 4.3.4 Surface analysis and film morphology

Table 4-2: Optical images for the wear tracks of different surfaces under different lubrication methods, after 6 hours of R.S.W test. All lubricant concentrations were held at 4.0 wt%

<i>Method</i>	<i>Polished Si</i>	<i>Unpolished Si</i>
Bare Si		
Dip Coated		
“Loc-Lub”		
Vapour Deposition		N.A.

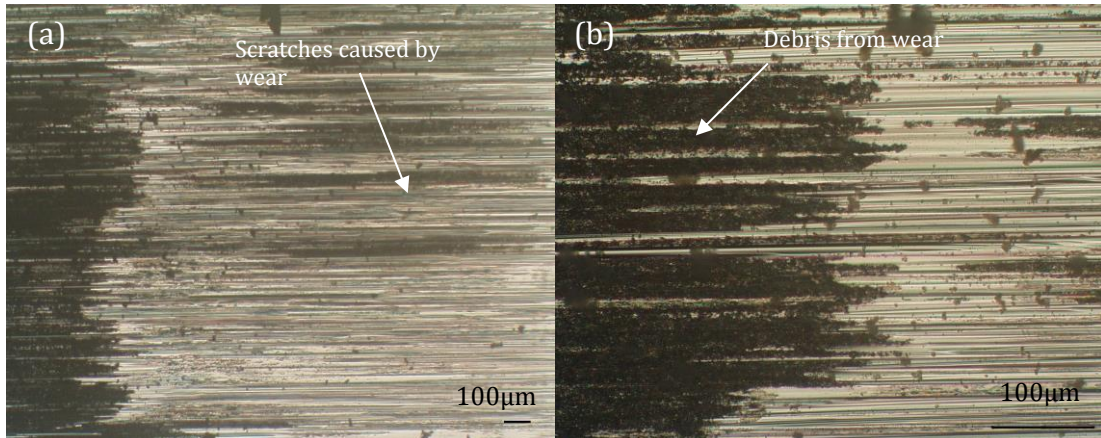


Figure 4-4: Optical images at (a) lower magnification (50x) and (b) higher magnification (200x) for bare polished silicon. Extensive wear scratches and debris can be seen on the surface.

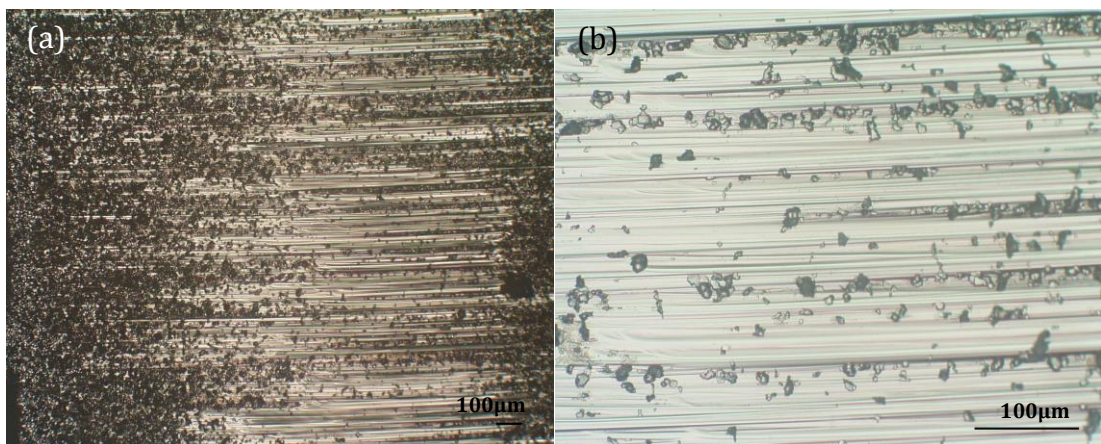


Figure 4-5: Optical Images for unpolished bare Si at (a) lower magnification (50x) and (b) higher magnification (200x). Excessive scratching and wear on surface can be observed on the wear track.

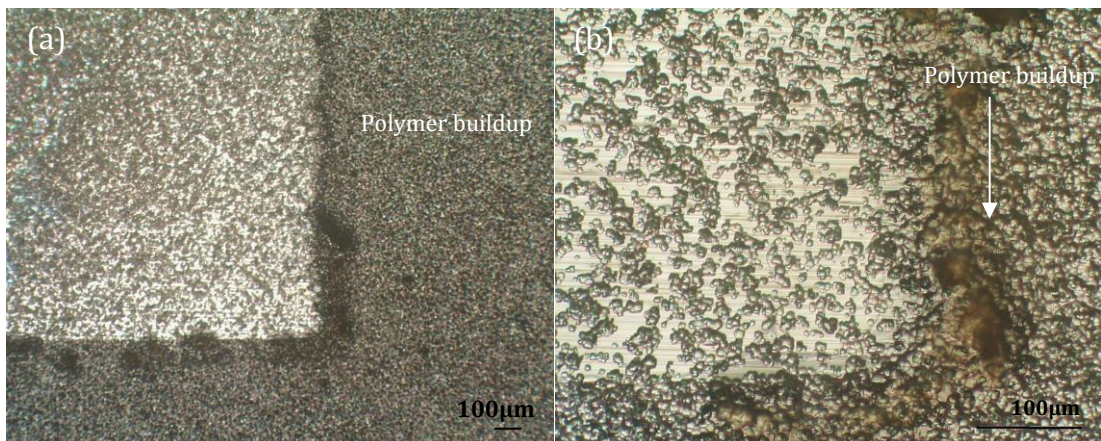
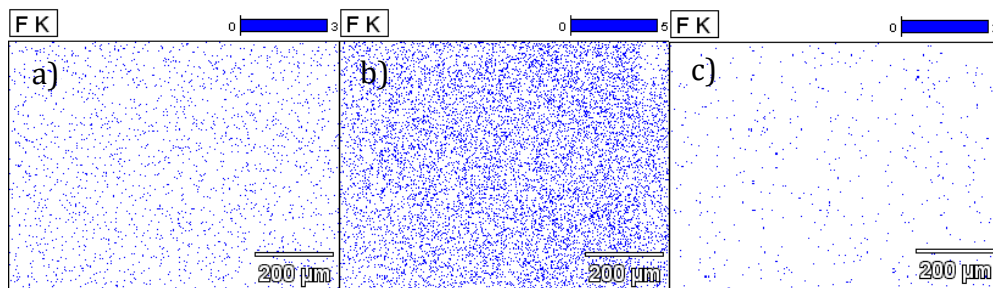


Figure 4-6: Optical images for unpolished Si LL 4.0% at (a) lower magnification (50x) and (b) higher magnification (200x). There was no obvious scratching except some polymer build-up along the edges of the wear track.



Optical microscopy (Table 4-2) showed a reduction of wear under both the dip-coated and “Loc-Lub” lubricated conditions as compared to uncoated Si and Si under vapour deposition. No surface wear was observed on “Loc-Lub” specimens for up to 60 hours, whereas dip-coated specimens had no wear initially but started to wear as the test continued, eventually being extremely worn as the lubricant film failed. Presence of the lubricant could be seen on polished surfaces in marks similar to that of an oil diffraction coating, primarily on the perimeter of the wear track for samples under “Loc-Lub” – this confirms that the lubricant has been partially swept to the perimeter during the sliding wear test. Notable differences between the amounts of wear debris for different methods of lubrication were observed in tandem with the improvement of the tribological properties investigated earlier in the wear tests (Figure 4-4, 4-5 and 4-6). Scratching on the surface was most severe in unlubricated surfaces and vapour deposited surfaces, in which the wear and scratches were clearly visible even by the naked eye. No noticeable difference could be observed between these two surfaces, indicating that the film formed by vapour deposition is insufficient to provide any form of protection against wear on sliding.

Dip coated specimens experienced a small amount of scratching, while the “Loc-Lub” specimens had no observable scratches even under optical microscopy. The same trend was observed for the unpolished surfaces, although a slight “polishing effect” was observed under “Loc-Lub” lubrication. The effect of the removal of asperities did not increase the friction, and even seems to have contributed to improving the tribological properties.



**Figure 4-7: EDS element maps of fluorine (F) for unpolished Si samples lubricated with 4.0 wt% PFPE under a) dip-coating, b) localized lubrication, and c) vapour deposition.**

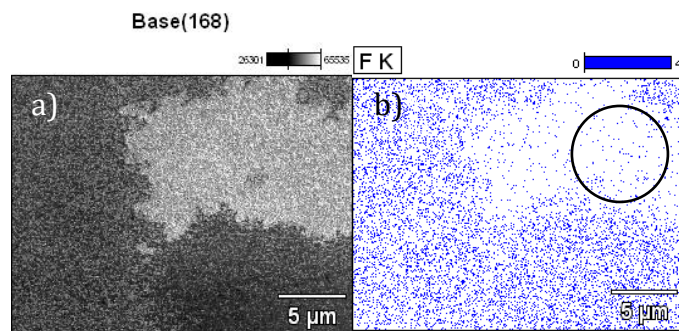
The different methods of lubrication were found to produce different distributions of the lubricant film across the surface. EDS analysis was used to detect fluorine, which is representative of the PFPE lubricant solution – the EDS element maps are shown in Figure 4-7 and provide information on the correlation between the method, the distribution of the lubricant and the tribological properties under the test conditions.

The highest density observed on the Si surface was for “Loc-Lub” specimens, followed by dip-coated specimens, and then finally vapour deposited specimens and uncoated specimens. The distribution density of the lubricant film prior to sliding is directly correlated to the tribological properties.

The amount of lubricant as well as the distribution density is due to the difference between the methods and their respective lubricating or bonding mechanism. Vapour deposition relies on a functionalized surface to allow the vapour molecules of the lubricant to bond onto the surface, creating a molecularly thin film on the surface – the vapour deposition method was specifically designed to control the thickness of the films to a molecular thickness. Dip coating relies on the surface tension of the substrate with the liquid and its wetting by the liquid – again, only a thin film is formed as the bulk of the molecules that remain on the surface are in

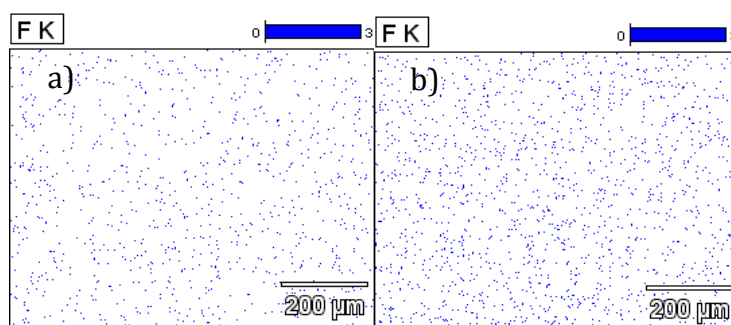
contact with the substrate. “Loose” molecules on top of this first layer are also present when they are entangled among the molecules attached to the substrate surface, or when the surface tension or viscosity of the liquid is sufficiently high to bring about a thicker layer. In the case of PFPE, with a concentration of only 4 wt% in H-Galden, the viscosity is maintained at a very low value, particularly since the H-Galden solvent evaporates rapidly in exposure to air. Dip-coating has also been recognized as a method in which the thickness of the film is controlled within sub-nanometre to nanometre thickness (Buttafava et al. 1985; Streator et al. 1991; Gao et al. 1995). The Loc-Lub method, however, does not rely on any of these surface factors, and simply utilizes mechanical means to dispense a fixed amount of lubricant at the desired location, thereby allowing for a greater amount at the desired location. However, due to the nature of the method, surfaces and the surrounding areas are not damaged, and only the immediate perimeter of the location is affected due to slight spreading of the lubricant solution – this helps to achieve the objectives of the method: to provide superior wear protection than other methods particularly in the case of inaccessible sidewalls and small gaps, and to locally apply lubricant at the required point without affecting other portions of the device or surface.

Another factor that contributes to the good lubricity of the specimens is the bonding mechanism – PFPE is known for its dual mobile/bound layer property which aids self-replenishment (Tani et al. 2001). Due to the nature of the vapour-deposition method, only the PFPE bound phase is present on the surface, which has been noted and shown in this work to give poor tribological properties (Tani et al. 2001; Eapen et al. 2002).



**Figure 4-8: a) FESEM image and b) EDS mapping for the presence of fluorine (F), which is representative of PFPE lubricant. The centre of the contact area between the two specimens (circled), upon application, is initially not fully lubricated immediately after lubrication.**

EDS conducted across various locations on the surface of “Loc-Lub” specimens prior to wear testing showed that certain locations were not as lubricated as others, mainly in the centre of the contact interface (Figure 4-8). It was concluded that the capillary action was insufficient to spread the lubricant across the entire contact area, leaving a section of the contact area of about  $\leq 15 \mu\text{m}$  in diameter not completely lubricated. Compared to the overall surface area of  $4 \text{ mm}^2$ , this area is negligible and the method is still deemed suitable for application on MEMS devices as the capillary action will cover micro-contacts easily.



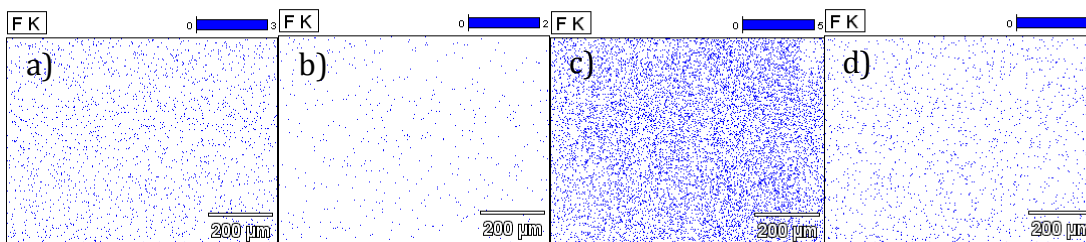
**Figure 4-9: EDS mapping of element fluorine (F) for (a) area near wear track that has an overflow of lubricant, (b) area in the centre of the wear track, both after 540,000 cycles**

The distribution densities of PFPE (Figure 4-9) were compared across three different locations on a “Loc-Lub” sample, the middle of the contact between the

samples (as mentioned above), at lubricated areas around the contact area, and a location further away from the contact area or lubricated area. The highest density was found at lubricated areas around the contact area, followed by the area in the middle of the contact area, and finally negligible traces of lubricant at locations further away from the applied area. This profiling of lubricant distribution density explains the initial relatively high coefficient of friction for “Loc-Lub” samples, as there is a small section in the contact area that remains unlubricated, contributing to initial dry sliding. However, upon further sliding the mobile phase of the lubricant slides into the lesser-lubricated areas, providing a more uniform film and reducing the friction prior to the onset of premature wear. It was also noted that if the lubricant was applied and the setup left to rest for a short period, the lubricant is then allowed to spread across the interface and the entire area of the contact, including the middle. The density profile would then become the same as that in Figure 4-7(b) as opposed to Figure 4-8.

**Table 4-3: Levels of Element F detected from EDS scans in Figure 4-10**

<u>Surface Condition</u>	<u>Normalised Wt% of F</u>	<u>Atom% of F</u>
Dip-coated (4 wt% PFPE), Untested	9.53	11.36
Dip-Coated (4 wt% PFPE), Tested for 6 hrs	1.17	1.39
“Loc-Lub” (4 wt% PFPE), Untested	38.37	36.07
“Loc-Lub” (4 wt% PFPE), Tested for 6 hrs	28.90	28.51



**Figure 4-10: EDS fluorine mapping for wear tracks of unpolished dip-coated Si samples (a) before and (b) after a 6 hour wear test; and samples undergone localized lubrication (c) before and (d) after a 6 hour wear test. The amount of fluorine is higher for the “Loc-Lub”**

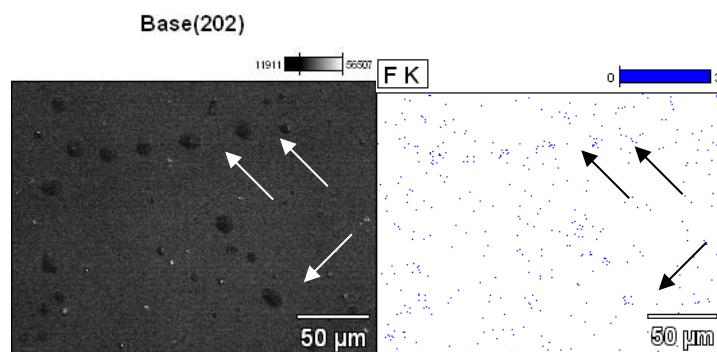
Dip-coated samples showed a much lower level of PFPE presence upon EDS mapping (Table 4-3 and Figure 4-10). However, the EDS mapping done on “Loc-Lub” specimens after the wear test indicates a high level of PFPE still present on the surface after 54,000 cycles – this confirms that the lubricant is still present in sufficient amounts and protects the surfaces in contact during the sliding motion, resulting in low coefficient of friction and low wear as observed throughout the test. The highest distribution across the surface, after the wear tests, were detected on the wear track surface, due to the sliding-assisted spreading of the lubricant and direct application to that area prior to the wear test. The retention of the high density is partly due to the self-replenishing properties of the PFPE lubricant, and partly due to the presence of the lubricant in excess in the “valleys” of the rough surface which remained even when the top layer of lubricant was removed.

In comparison, the dip coated samples showed a much lower density of lubricant after the wear test, as compared in Figure 4-10 and Table 4-3. It should be noted that the initial amount of PFPE on the dip coated surface was already much lower than that of the “Loc-Lub” surface – it is therefore expected that the self-replenishment mechanism would not be as concentrated or as effective as that of “Loc-Lub”. As mentioned earlier, the reservoirs of mobile phase PFPE stored in the

valleys of the asperities on textured surfaces also provide ready sources to draw upon for the self-replenishment process, thus preventing wear. This is evidenced from the sustained presence of PFPE under the “Loc-Lub” method after wear testing for 54,000 cycles, but a considerable drop in the dip coated samples, which is insufficient to prevent further wear. In the case of “Loc-Lub” specimens, the lowered level of PFPE after the wear test is still sufficient for it to last 540,000 cycles.

#### 4.3.4.1 *Effects of texture on the tribological properties upon PFPE lubrication*

The differences in friction and adhesion forces are clearly visible from the experimental wear test results: unpolished silicon under “Loc-Lub” 4wt% PFPE gives the lowest coefficient of friction and the longest wear life. Adhesion between the surfaces when separating after lubrication and wear testing is only observed in the polished surfaces and not in unpolished surfaces, implying that the rough texture affects the adhesion properties of the lubricated surfaces. Effects of texturing to modify the surface properties have previously been investigated (Talke 2000; Tan et al. 2006; Krupka et al. 2009; Marchetto et al. 2010; Singh et al. 2011; Tay et al. 2011) and are also thought to reduce the stiction, friction and wear in MEMS devices.



**Figure 4-11: a) SEM and b) EDS mapping for fluorine (F) of polished dip-coated Si surface. Droplets of PFPE, after the solvent has evaporated, were detected on the surface and are indicated by arrows on both images**

The conglomeration of PFPE lubricant on polished dip-coated surfaces previously noted, leaving dewetting marks and micro-droplets on the polished surfaces, (Figure 4-11) leads to a non-uniform distribution of PFPE. The extremely low roughness of the surface would contribute to the agglomeration of the high concentration of PFPE solution as the solvent evaporates – this is avoided in the case of unpolished surfaces as the lubricant solution sinks into the valleys between the asperities, allowing for a more uniform distribution on the topmost surface layer. This is also shown in the optical profiling, where the roughness of the surface is reduced upon lubrication – however, due to the transparency of the lubrication solution, only a small relative reduction was detected.

It is therefore proposed in this work that texturing not only provides a lower real contact area, thereby reducing stiction, but also physically acts as a temporary reservoir or storage for mobile phases of lubricant, allowing for easy access during instances of depletion and assisting the replenishment process. Eapen and co-workers have shown that PFPE lubrication exhibit good friction and wear characteristics when both the bonded and mobile layer are present, and no remarkable improvement when only bonded or only mobile layer is present (Eapen et al. 2002). EDS scans on both unpolished and polished surfaces also reveal that a greater amount of PFPE was detected on unpolished surfaces having been tested for 54,000 cycles, implying that the texturing indeed allows for more effective replenishment and therefore lead to improved lubrication of the surfaces compared to the polished surfaces under the same conditions.

The unpolished surface also prevents excessive sweeping of the lubricant to the edges of the wear track by giving the lubricant enclaves in which to reside, allowing for an extended wear life. This also prevents the surface tension forces



between the sliding surface and the liquid to draw out too much liquid at one shot. The absence of these enclaves on the polished smooth surfaces allow the sliding motion to sweep away the lubricant, resulting in a decreased amount of lubricant detected on the surface and observed as a build-up around the perimeter of the wear track. This removes the mobile layer of PFPE and greatly decreases the wear and friction prevention properties.

This same effect is also present in the “polishing effect” observed in the rough surfaces upon sliding. Although asperities have been removed during the wear test, the stable coefficient of friction remains low – this is attributed to the release of excess lubricant, which prevented third-body abrasion from taking place, effectively increasing the thickness of the film or amount of lubricant when required. As a result of the combination of effects discussed above, the unpolished surfaces exhibit better tribological properties. It is thought that the same effects can be translated to relatively rough surfaces on MEMS devices at the smaller scale as well.

#### **4.4 Conclusion**

By comparing various methods of lubrication, the “Loc-Lub” method has been proven to be effective in reducing friction and wear against reciprocating sliding surfaces, both polished and unpolished. The friction and wear properties were shown to be the best among the three compared methods of lubrication. Local application of lubricant to the desired point has not only been shown to prevent wear and lower friction, but leave the rest of the surface untouched – this can be adapted for application on MEMS devices in which the bulk surface of the MEMS device must remain unmodified for functionality, and will be particularly useful for lubricating the small gaps in sidewalls which are difficult to access. This system has been

implemented in actual MEMS devices for further study on the effectiveness of reduction of friction and wear of sidewalls under “Loc-Lub”.

Among the three methods compared, vapour deposition showed no evidence of self-replenishment and had the worst friction and wear properties, due to the complete absence of the mobile layer. Dip coated specimens showed signs of self-replenishment, but insufficient to prevent wear over extended test lengths. The lubricant films eventually failed and caused the surface to exhibit high levels of friction. Although reciprocating sliding wear is thought to assist self-replenishment of lubricant due to the oscillatory motion, only “Loc-Lub” specimens show evidence of self-replenishment in sufficient amounts to last an extended test at the lowest observed friction of the three samples.

Rough unpolished surfaces showed better tribological properties due to the availability of excess mobile phase PFPE, both in the valleys of the asperities as well as the surrounding around of the wear track. Unpolished surfaces also exhibited little adhesion when the samples were separated due to the alleviation of the surface tension forces between the lubricated surfaces caused by the texturing. Textured surfaces tend to provide discontinuity in the liquid film between the surfaces and hence are easily fractured when the surfaces are pulled apart.

## **Chapter 5 - Comparison of MAC and PFPE Lubricants under “Loc-Lub”**

*The type of lubricant used varies from material to material, often due to compatibility as well as performance issues. Different lubricants exhibit different results under the same conditions. This chapter compares the tribological performance of a MAC and PFPE lubricant under “Loc-Lub”, and also ensures that the technique can be performed using various types of lubricant solution without detrimental effect. MAC was found to exhibit lower wear rates and higher wear prevention, even at higher loads, when compared to PFPE, and this was largely attributed to its cohesive behaviour within the contacts.*

## **5.1 Introduction and Objective**

The “Loc-Lub” method has been successfully proved in the previous chapter to work with a known perfluoropolyether (PFPE) lubricant, Z-dol 4000, and found to reduce the wear life by several orders of magnitude and to lower friction considerably. Another kind of lubricant is used with the same comparison techniques in this chapter - the purpose in this study is twofold: firstly, to ascertain the versatility of the “Loc-Lub” technique in using various lubricants, and secondly to compare the performance of a multiply-alkylated cyclopentane (MAC) lubricant against that of a PFPE lubricant, for use on MEMS devices.

## **5.2 Materials and methodology**

The same reciprocating sliding wear tester as introduced in Chapter 4 was used, with PFPE and MAC as the lubricants, and with silicon wafers as the substrates. Both lubricant solutions were kept at 4.0 wt% for consistency. Surfaces were considered to have failed when any of the following occurred: the measured coefficient of friction went above 0.3, the coefficient of friction experienced large fluctuations, or the surfaces had visible wear and debris pileup.

## **5.3 Experimental results**

### **5.3.1 Contact Angle Measurements**

Water contact angles were taken on surfaces coated with various lubricants and methods, as summarized in Table 5-1. Bare Si after cleaning in air plasma showed water contact angles of  $5.5^\circ$  for polished surface and  $5.7^\circ$  for unpolished

surfaces, while the water contact angles for PFPE shown are the same as those presented in the previous chapter.

**Table 5-1: Water contact angles for silicon surface lubricated with various methods and lubricants**

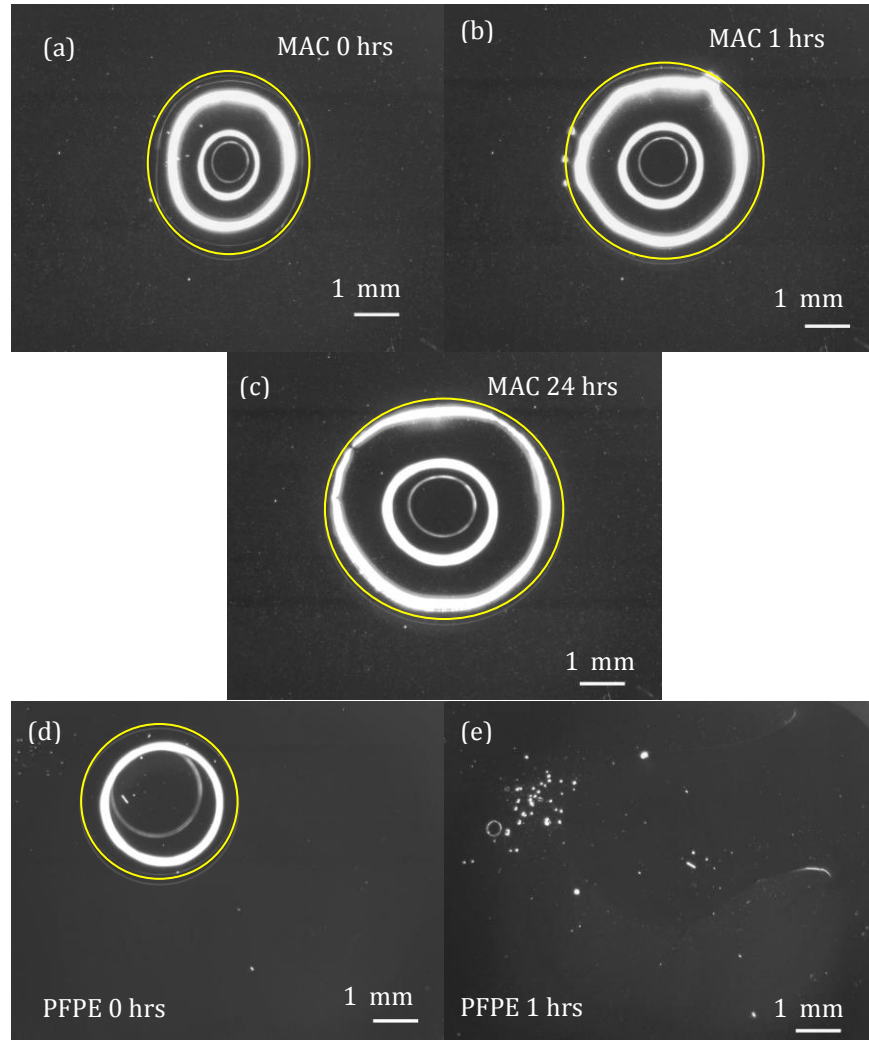
<b>Water contact angles (°) / Surface Conditions</b>	<b>MAC lubricant</b>	<b>PFPE lubricant</b>
<b>Polished, Dip-coated</b>	46.3	38.5
<b>Unpolished, Dip-coated</b>	56.0	30.4
<b>Polished, Loc-Lub</b>	-	55.0
<b>Unpolished, Loc-Lub</b>	-	38.8

The contact angle measurements for samples lubricated with MAC via the “Loc-Lub” method could not be carried out as the lubricant remained as a cohesive droplet on the Si surface, making it impossible to deposit a water droplet on top of it. As a result, the main points of comparison are that of the dip-coated samples and it was observed that the water contact angles taken on MAC lubricant were generally higher than that of PFPE samples, implying a surface with lower surface energy when using MAC lubricant.

### **5.3.2 Spreading of lubricant**

The cohesiveness of the MAC lubricant mentioned prompted an investigation into the behaviour of MAC lubricant when a small amount (approximately 0.1  $\mu\text{L}$ ) was deposited on a clean Si surface via the Loc-Lub method. The spreading of both lubricants were noted to be very different, with PFPE spreading rapidly upon application, forming a film with no discernible shape on the surface after 1 hour, but

with MAC remaining as an approximately circular droplet even after 24 hours (Figure 5-1)



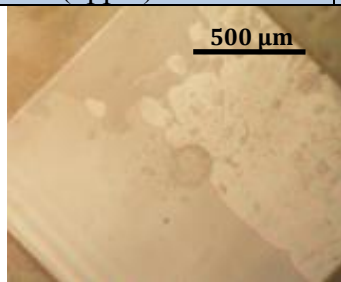
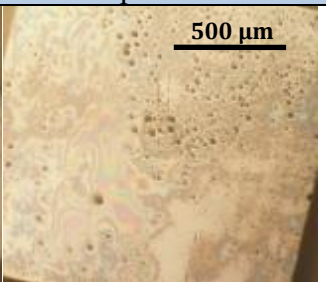
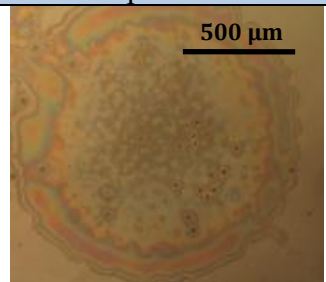
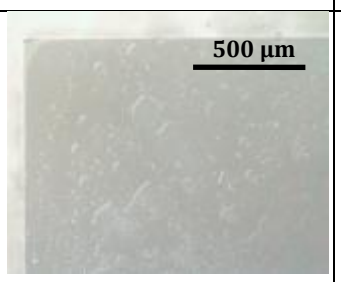
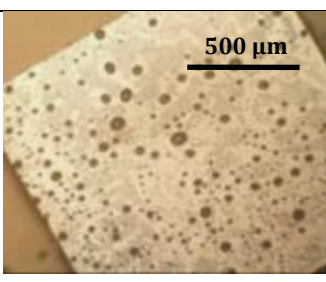
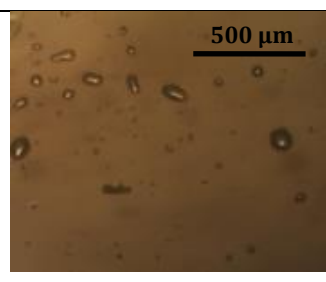
**Figure 5-1: Spreading of MAC and PFPE lubricant with droplets outlined, showing the spreading of MAC lubricant a) upon dispense, b) 1 hour after dispense, c) 24 hours after dispense and PFPE lubricant d) upon dispense and e) 1 hour after dispense with no discernible shape, on cleaned Si surfaces. Approximately 100 nL of each solution was dispensed on the surface using the “Loc-Lub” method.**

Spreading of MAC is thus observed to be very limited, and usually reaches a stable state with no further change after the first 6 hours. These observations it can be suggest that PFPE, with its much higher propensity and rate of spreading, may provide very good self-replenishing properties, but its mobile layer may also be more easily spread or swept away from the interface, effectively losing lubricity.

The cohesiveness of MAC lubricant to itself can be attributed to the higher surface tension of the liquid – approximately 32 dynes/cm for neat Nye Synthetic Oil 2001A, compared to 23 dynes/cm for neat Fomblin Z-dol 4000. This would imply that MAC lubricant is less likely to break apart into smaller droplets or spread, and therefore be less easily removed from the contacting interface.

Spreading of lubricants was also investigated by performing Loc-Lub between a smaller silicon wafer (the upper piece used in wear tests) and a glass slide cleaned in the same manner as the normal, larger silicon counterface; this allows for observation of spreading while the surfaces are in contact, and upon removal of contact. The optical images are summarized in Table 5-2.

**Table 5-2: Spreading of lubricants during and after contact when applied with the “Loc-Lub” method, using a glass slide as the larger counterface and a diced silicon wafer as the smaller counterface. The surfaces were cleaned in the same manner to mimic the actual performance and behaviour with two silicon surfaces as close as possible**

	During contact between Si (lower) and glass (upper) surfaces	Si surface (lower) after prior contact and separation	Glass surface (upper) after prior contact and separation
4 wt% PFPE			
4 wt% MAC			

The application of both lubricant solutions with the aforementioned substrates revealed great differences between the behaviours of the two lubricants at the interface and upon surface separation. PFPE formed a thin, continuous film upon

application while the two surfaces were in contact with no load applied. This visible spread of lubricant on the surface only changed slightly when the two surfaces were separated and the movement could be attributed to the meniscus and surface tension effects of the liquid. MAC lubricant, however, remained in distinctly discrete droplets – merely flattening under contact, and once normal contact was removed, not wetting either surface uniformly, as opposed to forming a film over the entire area.

The differences of the spreading behaviour are believed to cause different lubricating mechanisms – the lack of spreading of MAC lubricant will reduce the propensity for depletion upon sliding, as the lubricant cohesiveness prevents excessive sweeping of lubricant and depletion at the sliding contact. This in turn reduces the critical need for self-replenishment, but also implies that self-replenishment will not be present to the same extent as PFPE should it be required. In contrast, PFPE with its dual-layer lubrication mechanism spreads easily and its self-replenishing effects are well investigated – however, the ease of spreading would also imply that the lubricant will be more easily swept aside and expose the surface more readily as a thinner layer is formed. The tribological implications of these differences in the lubricants’ final performance depend heavily on the test conditions, and will be further investigated when compared in the wear tests and film morphology.



### 5.3.3 Reciprocating Wear Tests

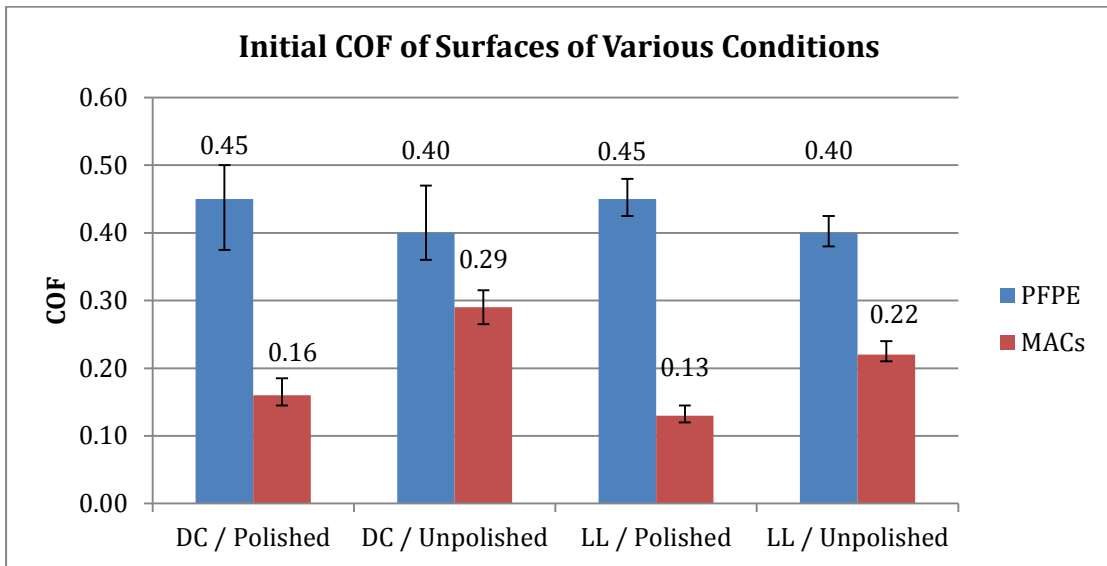


Figure 5-2: Initial coefficient of friction for various lubricated Si surfaces under dip-coating (DC) and "Loc-Lub" (LL), conducted with the reciprocating wear test machine at a speed of  $5 \text{ mm s}^{-1}$  and 50 g load

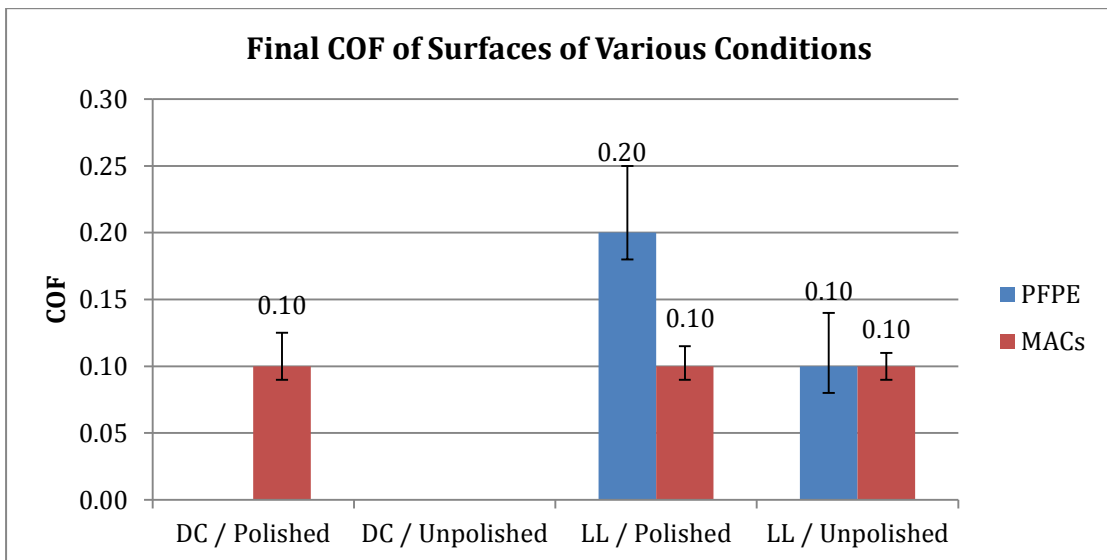


Figure 5-3: Final coefficient of friction for samples that did not fail after 54,000 cycles (6 hour wear test), under dip-coating (DC) and "Loc-Lub" (LL) at a reciprocating speed of  $5 \text{ mm s}^{-1}$  and 50 g load

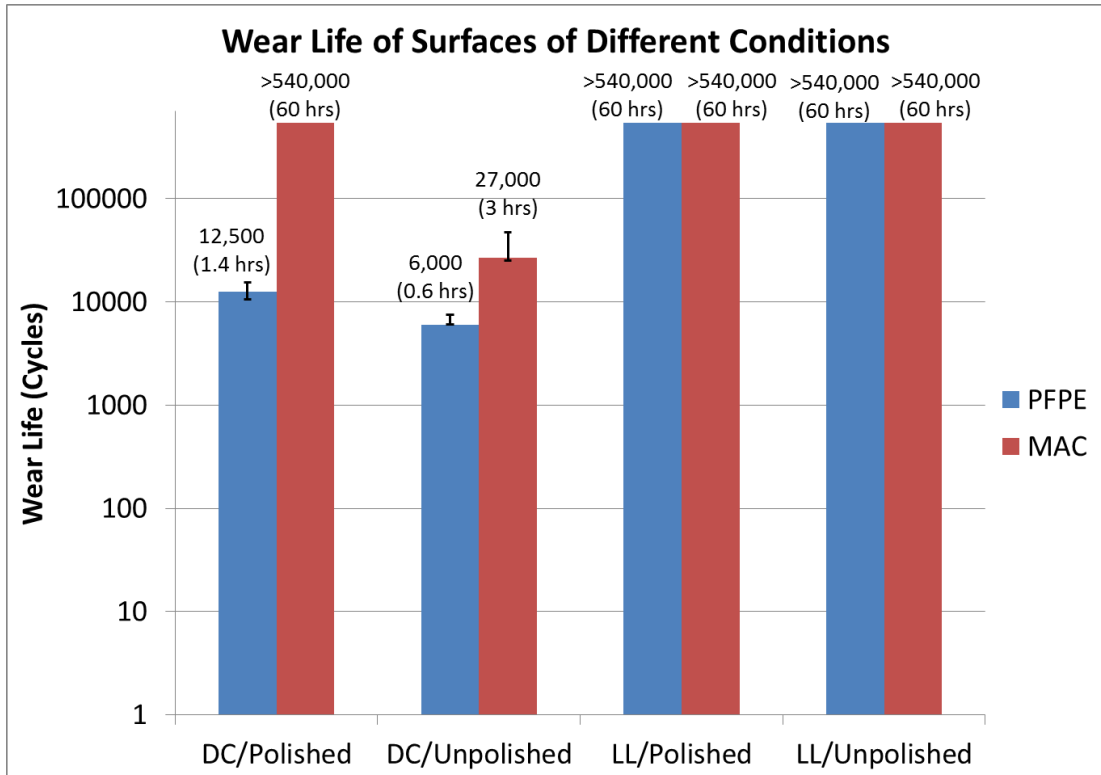


Figure 5-4: Wear lives (vertical log scale) of various Si samples lubricated via dip-coating (DC) and “Loc-Lub” method (LL), at a reciprocating speed of  $5 \text{ mm s}^{-1}$  and 50 g load

The initial coefficients of friction, final coefficients of friction for samples that did not fail during the 6-hour (54,000 cycles) tests and the wear lives of all samples are presented in Figure 5-2, 5-3 and 5-4, respectively. Surfaces that did not fail after the first 54,000 cycles were further tested to 540,000 cycles for comparison and are labelled appropriately in Figure 5-4. The final coefficient of friction for dip-coated PFPE polished Si surfaces and dip-coated unpolished surfaces for both MAC and PFPE lubricants could not be determined as a stable coefficient of friction could not be measured; the measured friction coefficient either had a continual increase or experienced great fluctuations - they were therefore considered to have failed. The overall view in Figure 5-4 shows a general improvement of wear life when using MAC lubricant, and all measured coefficients of friction were lower when tested with MAC lubricant as compared to PFPE lubricant.

When observing the raw test data at the start of the test, akin to the initial coefficient of friction presented in Figure 5-2, the samples that were lubricated with MAC lubricant did not have a discernible running-in time, while the samples with PFPE experienced a significant amount of time at a higher level of friction before stabilizing at a lower level.

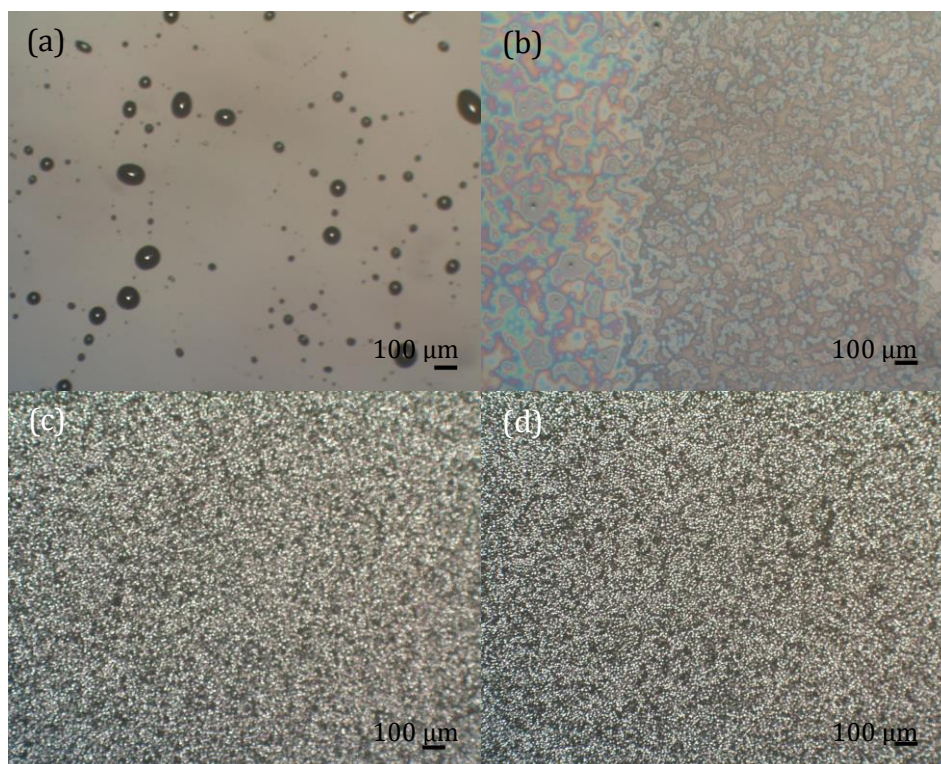
Wear tests were then conducted with the same parameters, but at higher loads of 70 and 100 g, for more extreme conditions to compare the properties of MAC and PFPE lubricated surfaces. The results are summarized in Table 5-3.

**Table 5-3: Initial and final coefficients of friction for wear tests conducted at higher loads and with various lubricants under Loc-Lub. Final COF was taken after 540,000 cycles**

<b>Lubricant</b>	<b>Load (g)</b>	<b>Initial COF</b>	<b>Final COF</b>
<b>PFPE 0.4 wt%</b>	70	0.195	0.10
<b>PFPE 4 wt%</b>	70	0.147	0.075
<b>PFPE 4 wt%</b>	100	0.125	0.073
<b>MAC 0.4 wt%</b>	70	0.19	0.11
<b>MAC 4 wt%</b>	70	0.23	0.09
<b>MAC 4 wt%</b>	100	0.155	0.075

As both PFPE and MAC lubricants showed low friction coefficient at higher loads, even after 540,000 cycles, surface analysis via microscopy was carried out to investigate the conditions of the surfaces and to compare the two.

### 5.3.4 Optical Microscopy



**Figure 5-5: Silicon surfaces lubricated via dip-coating before wear test; a) Polished Si dip-coated with MAC, b) Polished Si dip-coated with PFPE, c) Unpolished Si dip-coated with MAC, and d) Unpolished Si dip-coated with PFPE. Due to the roughness of the unpolished surfaces, no discernible differences could be observed.**

Observations for dip-coated specimens prior to wear testing once again showed the propensity for MAC to dewet the surface and form a discontinuous film with many micro-droplets, as compared to PFPE, which formed a uniform film over the silicon surface (Figure 5-5).

Figure 5-6: Optical images of Si samples dip-coated with MAC and PFPE lubricant at 4.0 wt% after 6 hours (54,000) cycles of reciprocating sliding wear, at a reciprocating speed of  $5\text{mm s}^{-1}$  and 50 g load

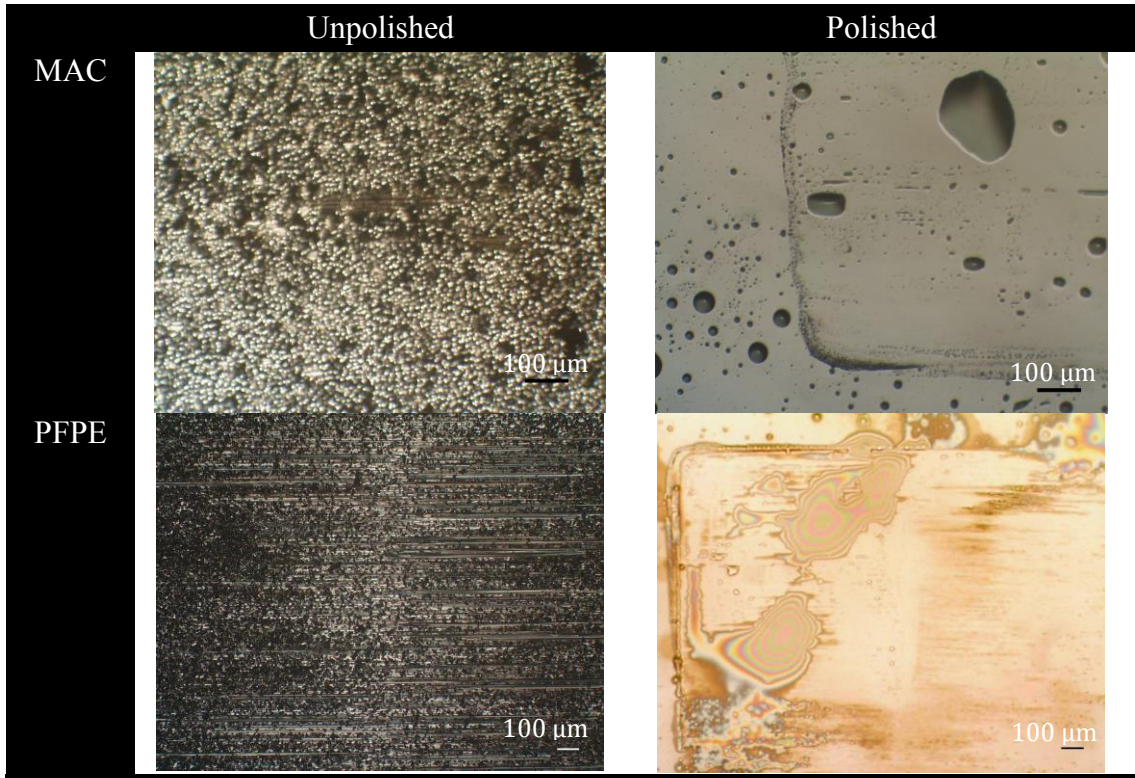
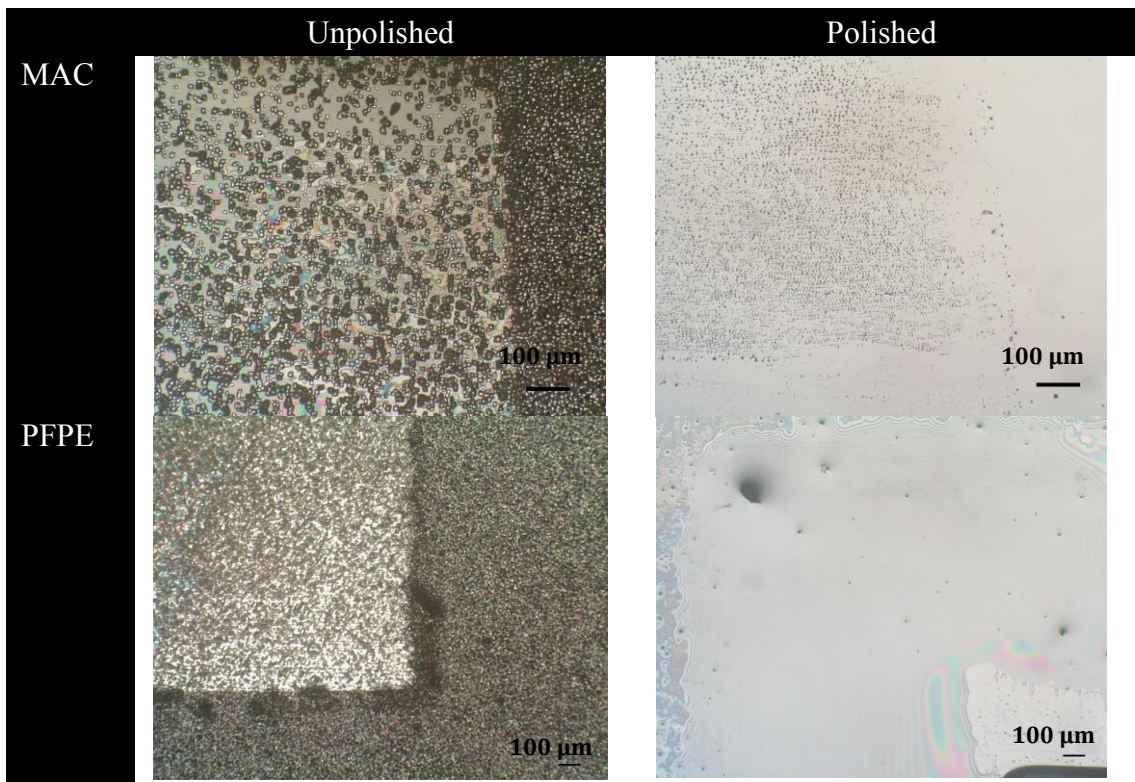


Figure 5-7: Optical images of silicon surfaces lubricated with “Loc-Lub” method with MAC and PFPE lubricant at 4.0 wt%, after 60 hours (540,000) cycles of wear tests, at a reciprocating speed of  $5\text{mm s}^{-1}$  and 50 g load



Optical microscopy conducted on all tested surfaces (Figure 5-6 and 5-7) showed no scratches on polished silicon surfaces for both techniques and both lubricants tested, indicating that no visible wear has taken place on the contact surface; this is in agreement to the results shown in Figure 5-3, with low coefficient of friction observed beyond the duration of the test. Scratches were evident on unpolished dip-coated samples using MAC lubricant, and a polishing effect for samples under “Loc-Lub” with MAC lubricant, akin to those observed for PFPE - this was observed in this study as well as in Chapter 4. No evident scratches were present on any of the surfaces lubricated by “Loc-Lub”, regardless of the lubricant used.

**Table 5-4: Optical images of wear track on polished silicon surfaces for various concentrations and types of lubricants and loads, after 540,000 cycles (60 hours) of reciprocating wear tests at  $5 \text{ mm s}^{-1}$**

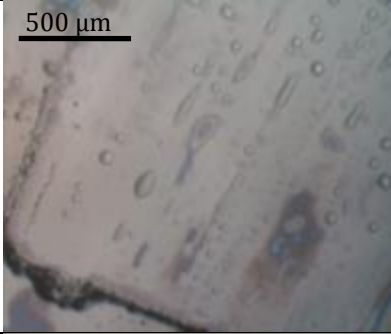
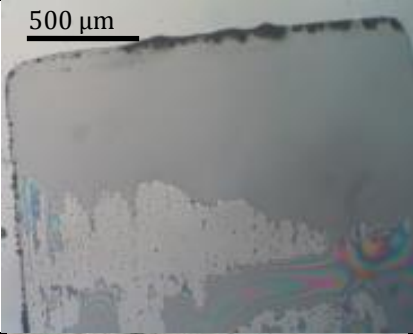
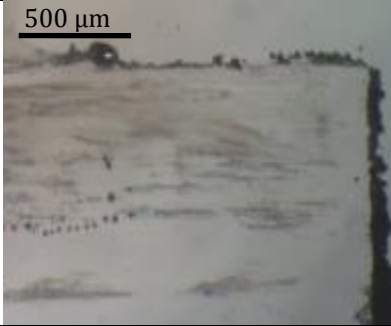
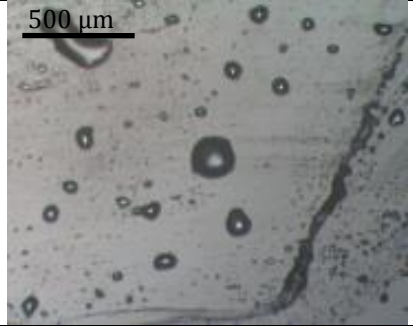

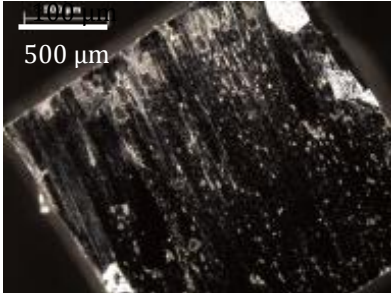
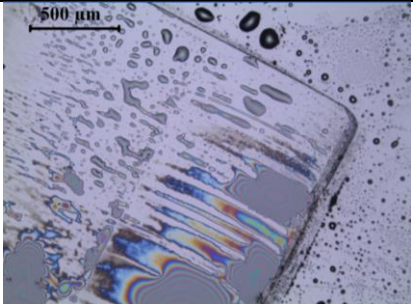
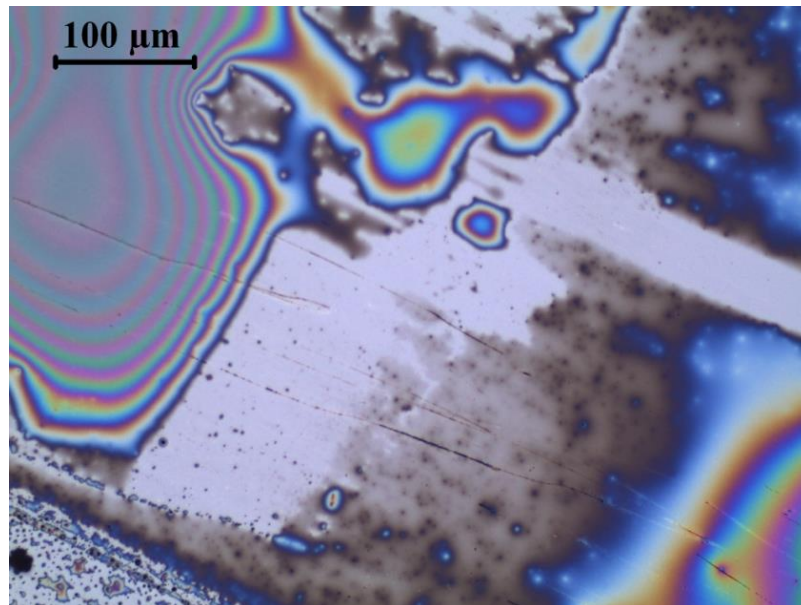
Conc. (wt%)	Load	PFPE lubricant	MAC lubricant
4%	70g		
4%	100g		
0.4%	70g	 	

Table 5-4 Table 5-4 presents a summary of the optical images of surfaces after wear tests had been conducted at higher loads (70 and 100 g), revealing a significant amount of build-up around the wear track perimeter for PFPE lubricated surfaces. A test conducted at a lower lubricant concentration in solution (0.4 wt%) for both lubricants resulted in wear on both the top and bottom surfaces for PFPE lubricated specimens, but only polymer build-up on MAC lubricated specimens at lower magnifications. Wear scars were observed, but required much higher magnifications to appear visible (Figure 5-8).



**Figure 5-8: Optical image of wear track on polished silicon surface tested at 70g load and lubricated via “Loc-Lub” with 0.4 wt% MAC, after 540,000 cycles of wear test at 5 mm s<sup>-1</sup>**



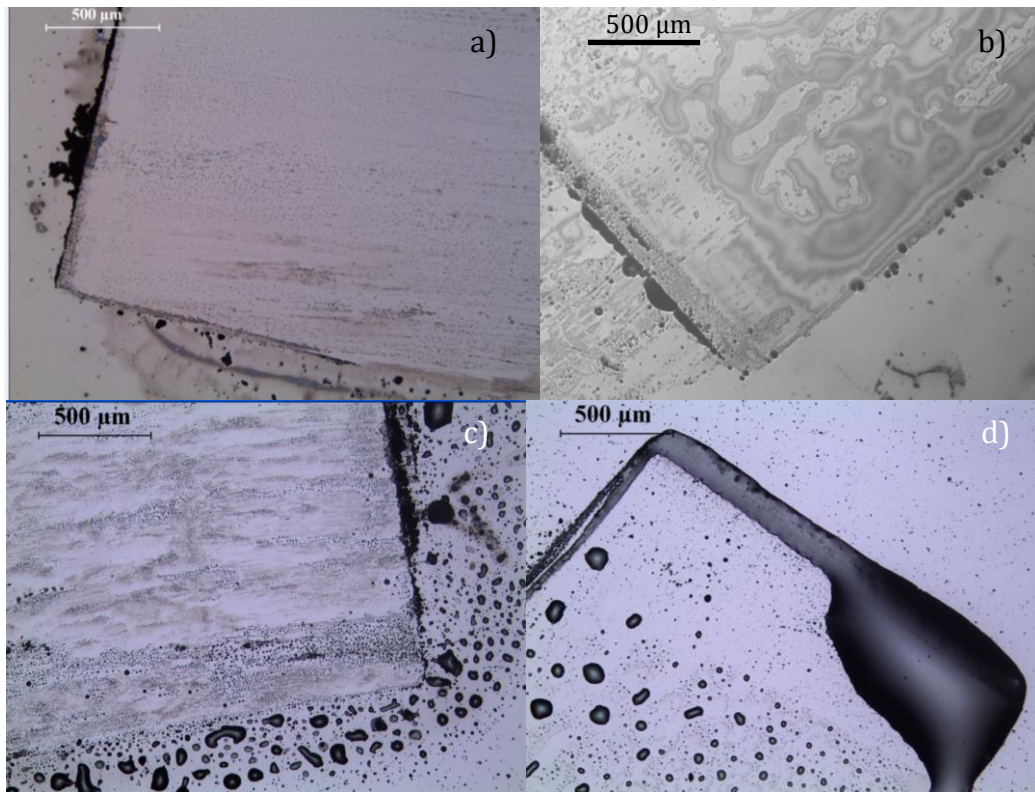


Figure 5-9: Optical images of wear tracks for polished silicon surfaces after testing for 54,000 cycles at  $5 \text{ mm s}^{-1}$  and 70 g load for a) 0.4 wt% PFPE, b) 4 wt% PFPE, c) 0.4 wt% MAC and d) 4 wt% MAC

Wear scars were also examined for wear tracks on polished silicon surfaces after 54,000 cycles at 70 g, with two different concentrations of each lubricant (Figure 5-9). Lower levels of wear were observed and expected with high concentrations of lubricant, and less debris from the silicon surface was observed when comparing surfaces lubricated with 4 wt% MAC lubricant to PFPE lubricant at the same concentration. The visible lack of wear and the differences between the resulting surfaces suggests strongly that MAC lubricant is more effective at preventing wear.

The optical images taken after the tests show the same cohesive behaviour for MAC and uniform spreading for PFPE lubricant as presented earlier in Figure 5-1, Figure 5-5 and Table 5-2. This cohesive behaviour of MAC lubricant has thus far shown to be beneficial for maintaining a lubricant layer between the two flat surfaces, reducing the need for self-replenishment. The cohesiveness is also thought to

successfully prevent direct contact between the surfaces, in particular the smooth polished surfaces.

### 5.3.5 FESEM and EDS analysis

FESEM imaging along with EDS mapping of the surfaces revealed a detectable weight percentage of either lubricant on the surfaces – for MAC, the characteristic element is carbon, while for PFPE it is fluorine. As the lubricant compounds are of different molecular weight and are present in their respective compounds in the lubricant in differing amounts, the relative contents and numerical values of the element cannot be used as a comparison of the amount of lubricant. However, the density at which the element appears in the image mapping can be used as a comparative analysis of the extent of the presence of each lubricant and the position on the surface. The relative reduction in the individual weight percentages can also be used as an indicator of the amount of lubricant removed from the mapped area.

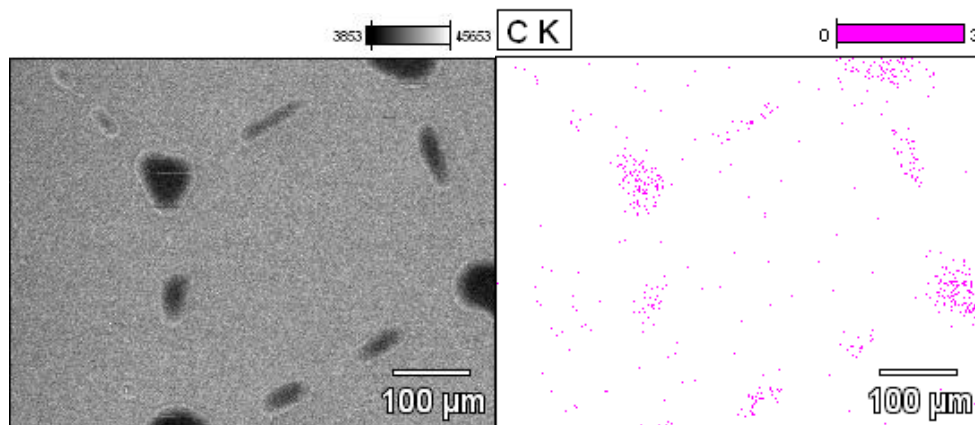
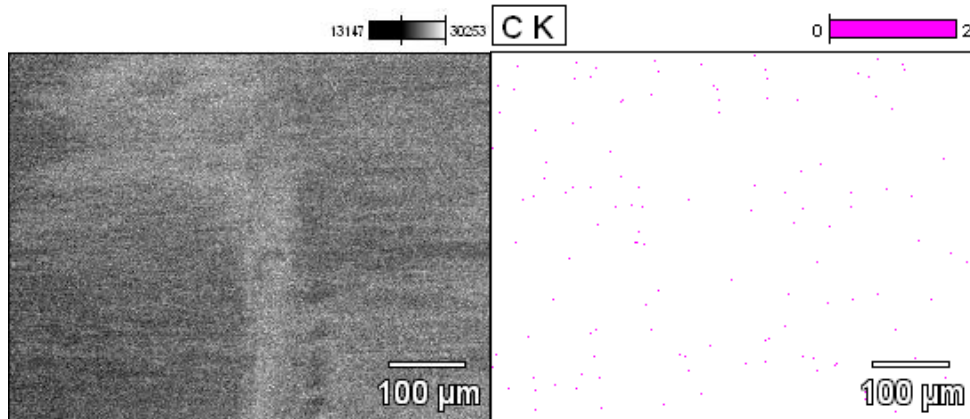


Figure 5-10: FESEM (left) and EDS mapping (right) for element C on silicon surfaces dip-coated with MAC lubricant (4 wt%), untested, and taken at 200x magnification



**Figure 5-11: FESEM (left) and EDS mapping (right) for element C on silicon surfaces dip-coated with MAC lubricant, after 540,000 cycles (60 hours) of reciprocating wear tests at  $5 \text{ mm s}^{-1}$  and 50 g load, taken at 200x magnification**

MAC lubricant was once again noted to form mist-like micro-droplets on the silicon surface (Figure 5-10). This was evident on both the upper and lower silicon piece, and the EDS mapping clearly shows its tendency to conglomerate and form droplets even when coated on a surface with high surface energies such as silicon. Even though only a sparse distribution of MAC lubricant was mapped prior to tests (Figure 5-10), the layer appears to have sufficiently lubricated the surfaces, as shown by the low levels of friction and reduced wear presented in Figure 5-1, 5-3 and 5-4. The small droplets are believed to eventually aggregate during the wear tests due to the sliding motion before spreading over the surface as shown in Figure 5-11.

#### 5.4 Discussion

A general comparison between PFPE and MAC lubricant friction and wear performance, combined with surface characterization, shows that the MAC lubricant exhibits better wear prevention and lower friction for the flat-on-flat geometry studied. Compared to PFPE lubricants investigated in Chapter 4, MAC has also been shown to provide longer-lasting lubrication on polished silicon, with the prolonged

presence of the film. These improved tribological properties observed are due to a number of differences between the lubricants behaviour. PFPE is known to form an extremely thin lubricant film, which makes it highly suited for application such as the lubrication of magnetic disk drives, where contacting surfaces move very close to each other (Sinha et al. 2003; Li et al. 2011). MAC, on the other hand, has been discovered to de-wet silicon surfaces, which, combined with its high mobility, enables it to replenish itself in depleted areas within the contact by capillary movement along with the contact (Ma et al. 2007). MAC therefore shares the same self-replenishing property as PFPE, but without the loss to the contact zone.

However, as PFPE only forms a very thin layer on the surface it is applied to, the availability of the lubricant for self-replenishment over a longer period of time is lessened compared to that of MAC, possibly also due to the spreading of the lubricant outside the wear track. Since MAC droplets have a tendency to stay intact and cohesive instead of spreading thinly on the surface (due to the de-wetting effect), they create a persistent and comparatively thicker film between the two sliding surfaces. This decreases the chances of direct contact and reduces asperity interlocking, and avoids depletion due to increasing contact area, which is in contrast to PFPE behaviour.

The absence of running-in friction or a high initial coefficient of friction for MAC lubricant under these conditions suggest that the MAC lubricant may show a better performance in lubricating MEMS devices under reciprocating sliding. This is exceptionally important as a high initial coefficient of friction at the start of the movement of the component may provide enough force to damage or wear the component from the start. In addition to low initial coefficient of friction, low friction

was observed throughout the duration of the test – even after 540,000 cycles, minimal wear could be detected on the surfaces.

FESEM and EDS imaging as well as optical microscopy revealed that the surfaces lubricated with MAC lubricant were not evenly coated, even prior to testing, and individual droplets of MAC lubricant were discernible either under high magnification or EDS mapping of the lubricated surface. At the same time, the low volatility and spreading of MAC lubricant would imply the presence of a continuous liquid film between the surfaces when sliding occurs, effectively reducing boundary friction on contacts. The resistance of the liquid film to flow away from the contacting surfaces when the surfaces slide across each other ensures that lubricant is not easily swept aside or depleted at the contact – this is a combination of both the capillary forces as well as the cohesiveness of the lubricant itself. This behaviour was also confirmed with investigation of the spreading of the two lubricants over time.

Examination of the wear tracks using EDS showed that the lubricant presence was still detectable after 540,000 cycles of sliding tests, showing that a persistent film does indeed exist between the surfaces during sliding. The effect of the cohesiveness and lubricity of MAC lubricant, if present to a sufficient extent, may make it possible to eliminate the need for self-replenishing altogether.

It was believed that the major factor responsible for the lubricants’ differences in performance was the volume of the lubricant at the contacting interfaces (i.e. on the wear track), especially when comparing the two dip-coated specimens. The thickness of the lubricant layer on the Si surface by dip-coating is known to be affected by the withdrawal speed, the duration of the dipping and the concentration of the lubricant solution. The density and viscosity of the lubricant also affects the thickness of the layer in the coating. As all factors are kept constant for both lubricants, the thickness

of the lubricant film, and therefore the volume of lubricant, should theoretically be the same. However, it is the differences in viscosity and surface tension that cause MAC lubricant droplets to form, thus resulting in differing “film morphology” and eventually leading to different tribological properties when compared with PFPE. The surface tension also affects the lubricant’s cohesiveness and its ability to form a continuous layer under certain conditions, thereby providing better lubricity as contact is completely avoided.

Differences in the polished and unpolished Si surfaces tested between lubricants depend on the nature of the lubricant’s cohesiveness, controlled by the surface tension in particular. PFPE is believed to show lower friction coefficient on unpolished surfaces due to the collection of the lubricant in the valleys of the asperities, adding to the effectiveness of the self-replenishment property that PFPE is known for. This increases the lubricity of PFPE under these conditions, as there is a ready source of replenishment when the thin lubricant layer is swept away.

MAC lubricant, on the other hand, is extremely cohesive and therefore provides a layer between the two surfaces due to the high surface tension. This lubricant layer is most effective between two smooth surfaces where the lubricant is maintained as a complete layer, separating the surface from solid-solid contact during sliding. In the presence of asperities, this layer is broken up, with the tips of the asperities on the Si wafer coming into contact with each other. This solid-solid contact between the unpolished surfaces causes higher friction compared to smooth, polished surfaces as the lubricant layer is interrupted. The advantages of de-wetting of MAC on wear life may be reduced for unpolished surface as can be seen in the dip-coated/unpolished results for PFPE and MAC.

The reason why the initial and final coefficients of friction appear to be slightly lower at higher loads is unknown and bears further research.

## **5.5 Conclusion**

With improved friction and wear properties and a slightly differing lubrication mechanism, Multiple-Alkylated Cyclopentanes (MAC) lubricants have been shown to be a more effective lubricant than perfluoropolyethers (PFPE) under flat-on-flat reciprocating sliding wear conditions, particularly when using the “Loc-Lub” method. The improvement extends to all three areas of the tribological properties investigated – the initial coefficient of friction, the stable (in-use) coefficient of friction, and the overall wear life of the surfaces – and shows remarkable improvement on all accounts. Given that MAC lubricants also have very high thermal stability and possess the ability to lubricate various surfaces, as well as proven feasibility in the Loc-Lub method for application onto a local, small area, it presents itself to be a strong candidate for implementation in MEMS devices.

The use of MAC will then be further investigated in actual micro devices in sliding and reciprocating motion, particularly in liquid lubrication.

## **Chapter 6 - “Localized Lubrication” on Reciprocating MEMS Contacts**

*Having verified the practical use of the “Loc-Lub” method with different lubricants, the method is then applied to lubricate custom-made reciprocating MEMS devices. This chapter presents the tribological study of the use of the “Loc-Lub” method on custom-made MEMS tribometer devices, using both Multiply-Alkylated Cyclopentanes (MACs) and Perfluoropolyether (PFPE) lubricants. The wear lives of the devices are studied and the lubricating mechanisms for the two lubricants used investigated.*



## 6.1 Introduction

MEMS sidewall lubrication offers a tougher challenge than lubrication of plane surfaces in MEMS, due to the difference in surface properties, topography, and inaccessibility of the small gaps (Ashurst et al. 2003b). Furthermore, the characteristics of sidewalls are not documented in depth because of these restrictions, and may vary with factors such as fabrication methods or exposure to environment or etching media.

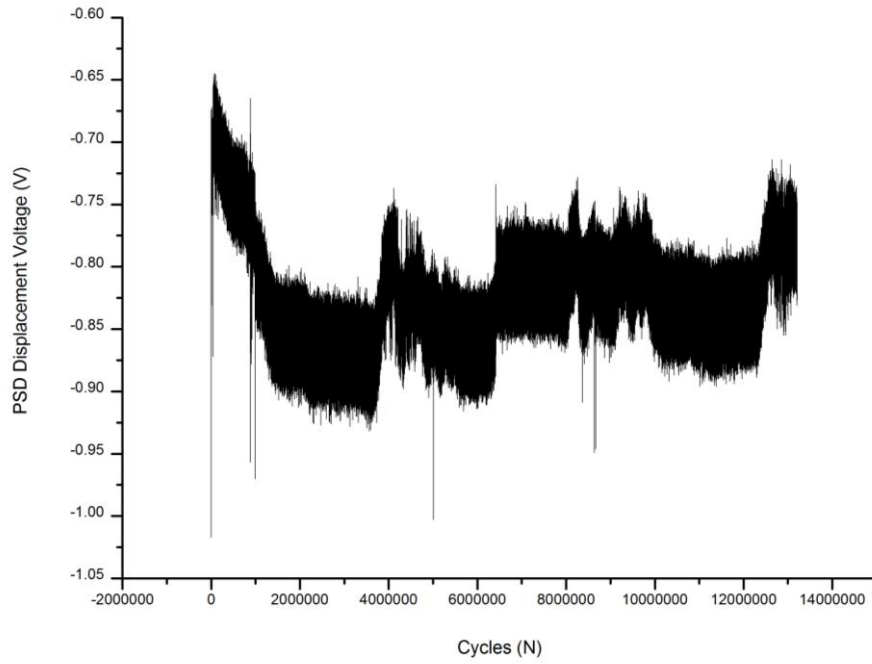
In addition to the feasibility tests and comparison of MACs and PFPE lubricants on silicon wafers described in the previous two chapters, tests were also carried out on the custom-designed reciprocating MEMS tribometer detailed in Chapter 3 (Figure 3-4 and 3-5) to ascertain the tribological effects of lubrication via the “Loc-Lub” method. Devices were tested either dry (unlubricated) or having been lubricated under the “Loc-Lub” method with a droplet of PFPE or MAC solution in H-Galden or n-hexane respectively. The concentrations of the lubricant solutions used were 4.0 wt%. Detailed experimental procedures are presented in Chapter 3.

The voltage output signal from the device is in the form of a high-frequency sinusoidal curve, representative of the frictional force experienced between components. As a wear test continues, friction slowly increases to the point where the reciprocating component can no longer slide against the contacting component. Device lifetime is considered to have been reached when the sinusoidal curve observed decreases to a straight line, resulting in a sudden drop in the displacement values measured from the diffraction grating.

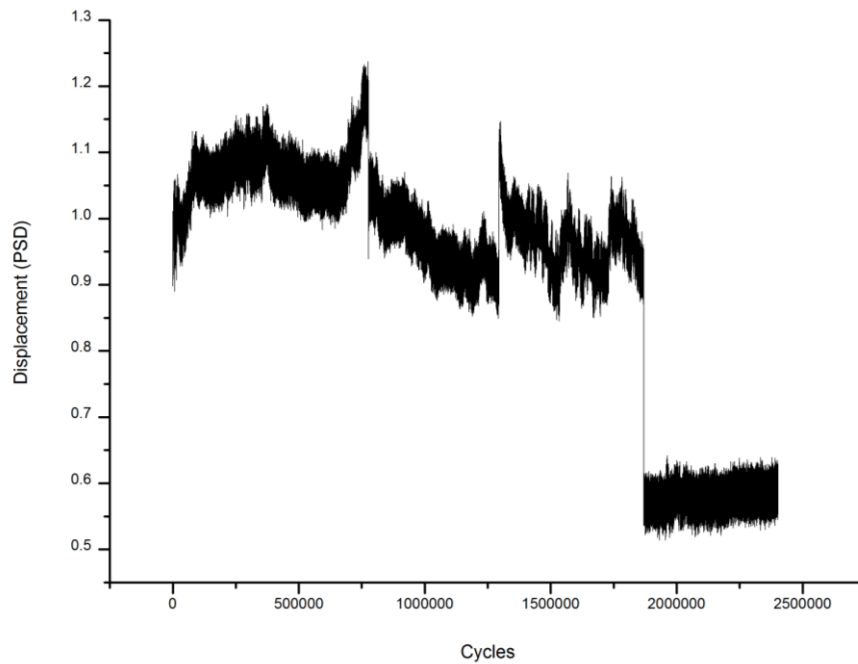
## **6.2 Results**

### **6.2.1 Wear Tests**

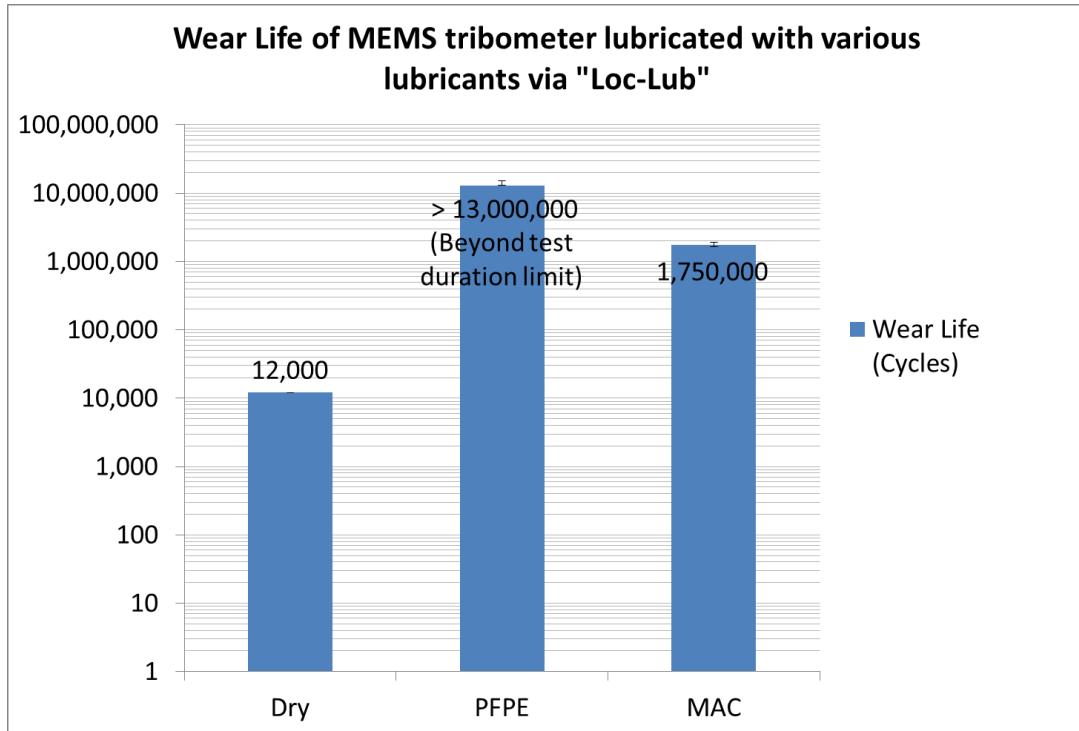
The friction tests conducted showed varying friction trends, making the comparison of the friction trends difficult – the discrepancies and difficulties will be discussed in a later section. Comparison of the device life, however, showed a consistent and striking increase in the device lifetime when lubricated with PFPE, and a slightly lower increase when lubricated with MAC lubricant, as compared to dry tests. Data sets for the PFPE and MAC lubricated tribometers are shown in Figures 6-1 and 6-2, and the results of the lifetimes are summarized in Figure 6-3. The voltage values (y-axis) in Figures 6-1 and 6-2 are arbitrary values and represent a nominal displacement of the diffraction fringes. As the positions of these fringes are not exactly the same, these values are not representative of the actual levels of friction, and merely indicate that there is motion. A sharp drop in the displacement voltage values, as shown in Figure 6-2, serves to indicate a sudden stop in the movement of the device (i.e. device failure).



**Figure 6-1:** Graph of PSD displacement voltage versus cycles for a PFPE-lubricated MEMS reciprocating tribometer. The device continued to move and therefore had not reached its lifetime even after 13,000,000 cycles.



**Figure 6-2:** Graph of PSD Displacement voltage versus cycles for a MAC-lubricated MEMS reciprocating tribometer. This device suddenly stopped moving, as evidenced by a sudden drop in the displacement voltage after a period of approximately 1,800,000 cycles.



**Figure 6-3: Device life of MEMS Reciprocating Tribometers when under dry conditions and lubricated via “Loc-Lub” with PFPE or MAC. Tests were repeated with at least three consistent values, and PFPE lubricated specimens did not fail within the duration of the test.**

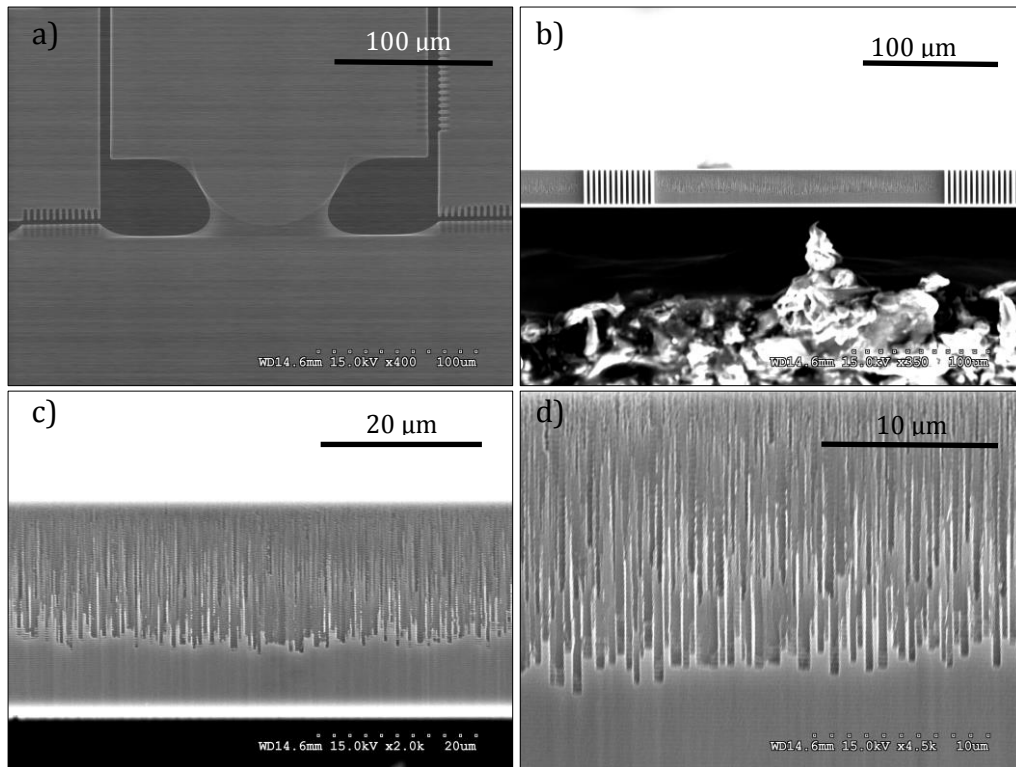
Despite previous work showing an improved wear life of silicon surfaces under MAC lubrication compared to PFPE lubrication for smooth flat surfaces (Figure 5-2, 5-3 and 5-4) the opposite is evident on the MEMS tribometer devices. With PFPE the devices operated for more than 3 days (more than 13,000,000 cycles) and experiments were halted without failure, whereas those lubricated with MAC last for only approximately 1,600,000 cycles. Tests were repeated with at least three consistent values and repeats were close, with scatter much less than the difference between the two lubricants, as shown in Figure 6-1. The differences in the behaviour of the two lubricants will be discussed shortly.

Surface analysis was conducted by FESEM and EDS examination of the contacts, to provide insight into the conditions of the contacts.

## 6.2.2 Surface analysis

### 6.2.2.1 FESEM/EDS

FESEM images taken of the sidewall contacts after testing are shown in Figure 6-4 for PFPE lubrication.



**Figure 6-4: FESEM images of the MEMS Tribometer device, showing a) contacts lubricated with PFPE (x400), b) sidewall of the flat contact at x450 magnification, c) x2000 magnification, and d) x4500 magnification**

The images show clearly that the sidewalls were not uniformly flat and had signs of etching from the fabrication and processing of the devices. These grooves were visible on dry, untested device sidewalls as well as on the lubricated and tested ones. Although not visible or detectable, it is also possible that the sidewalls are not perfectly vertical due to uncontrollable factors in the fabrication process, resulting in a lower contact area than designed. These features will affect the friction trends and possibly cause the variation in friction observed between devices. The effects of the

observed surface features on the tribological properties will be discussed in a later section.

For dry and MAC-lubricated specimens, no visible wear was observed on the surfaces, even after failure – this is due to the fact that the friction experienced by the device was strong enough to hinder and eventually halt the movement of the devices. This leads to a situation of complete stiction where the adhesive force between the surfaces is larger than that of the actuating force and all the movements of the actuator are accommodated by the elastic deformation of the structure. As such, the onset of wear has not occurred within the device lifetime. PFPE specimens also showed no wear debris, which is to be expected, as the devices do not fail within the experiment limit of 3 days.

The EDS mapping scans in Figure 6-5 and 6-6 show a significant amount of lubricant on surfaces that have been lubricated with PFPE prior to testing – this shows that the lubrication method is successful in delivering the lubricant to the sidewall surfaces, thereby extending the device life.

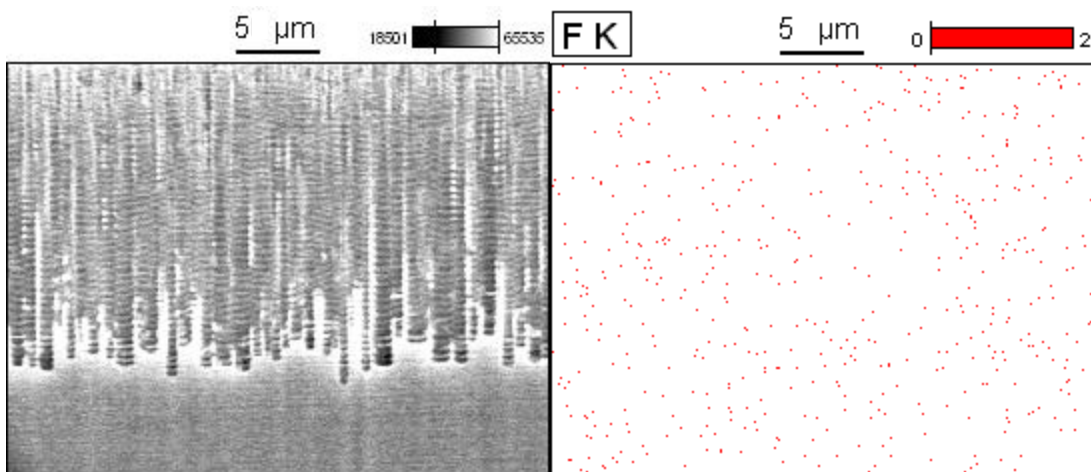


Figure 6-5: FESEM and EDS imaging scans on untested PFPE lubricated devices, with fluorine as the representative element of PFPE

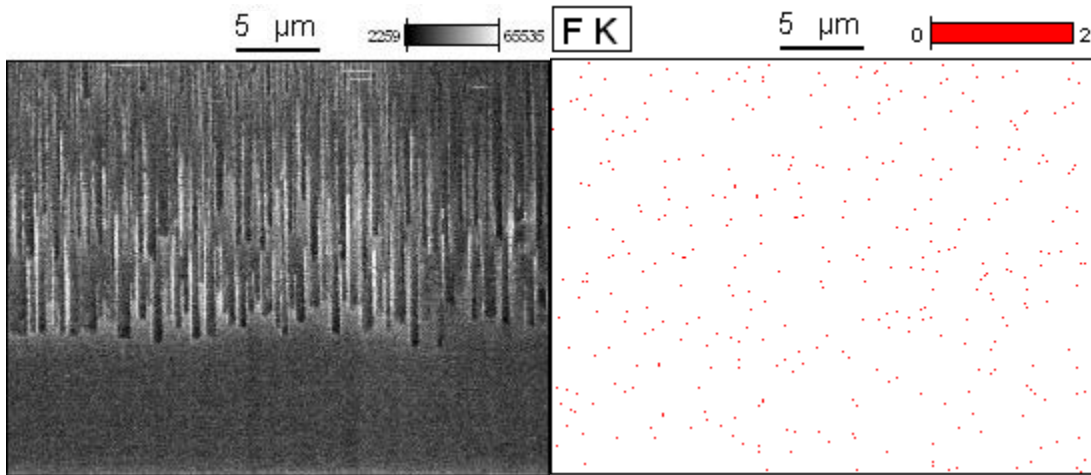


Figure 6-6: FESEM and EDS imaging scans for tested PFPE lubricated devices, with fluorine as the representative element of PFPE

After testing, component surfaces that had been lubricated with PFPE had a small amount of lubricant left on the surface relative to the amount on untested surfaces, as shown by the EDS mapping scans in Figures 6-5 and 6-6. This amount was sufficient to prevent device failure as the device did not stop (wear life exceeding 13 million cycles, Figure 6-1) due to friction/stiction during the duration of the test. The distribution and density of the element detected represents the presence of the PFPE lubricant on the surface, as explained in the previous chapters. This supports the device life measurements on such devices, which were found to not fail even after 3 days of testing (13,000,000 cycles), indicating that lubricant film did not fail or deplete sufficiently to allow adhesion and wear during this time.

Comparison between surfaces from tested and untested devices lubricated by MAC shows a notable difference in the levels and distribution of lubricant detected. A comparison of the sidewall images is shown in Figure 6-7.

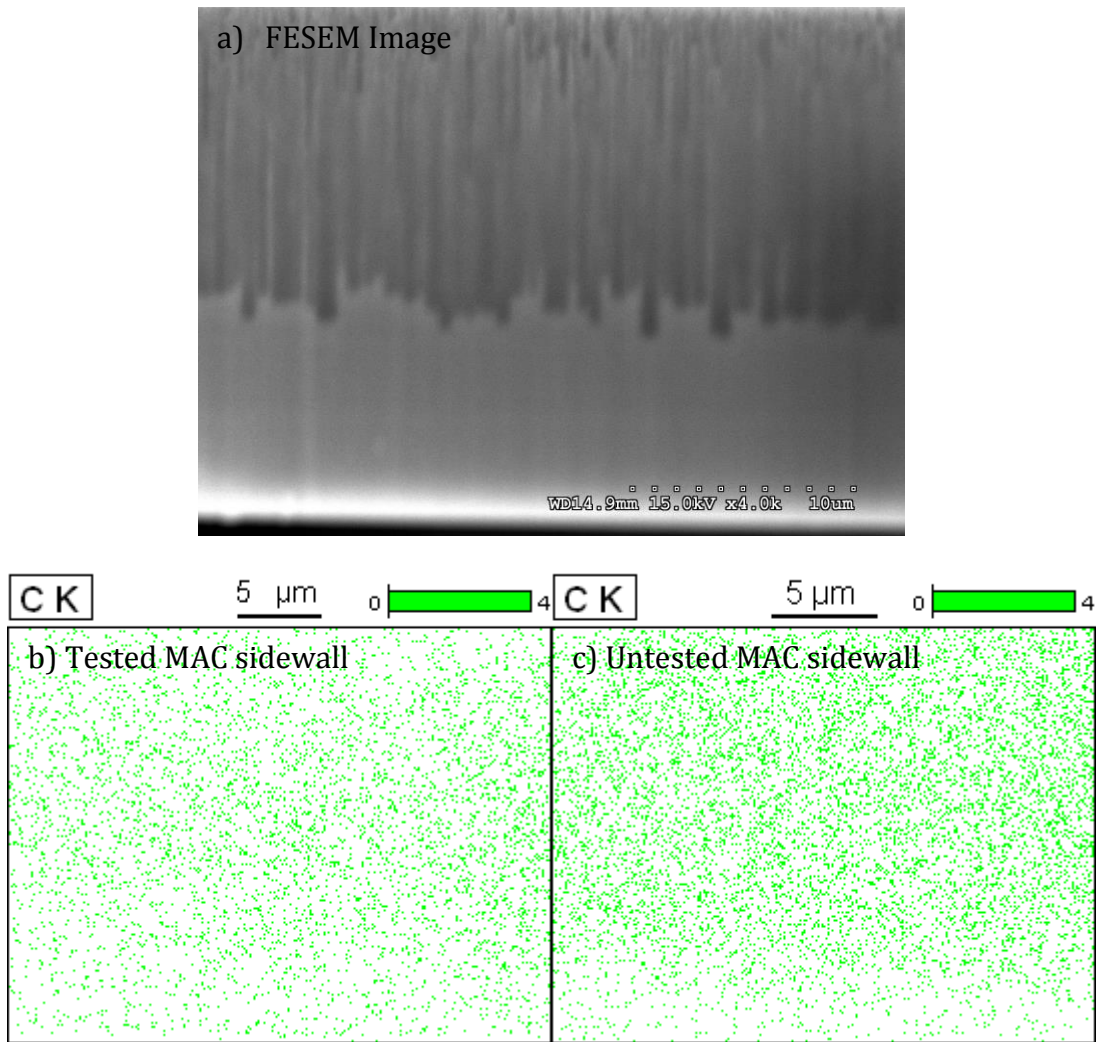


Figure 6-7: a) FESEM image for MAC-lubricated MEMS sidewalls, and EDS imaging scans for MAC lubricated devices, b) tested and c) untested

As can be seen in the density distribution map of carbon in Figure 6-7, representing the presence of the lubricant, the lubricant was slightly depleted after repeated sliding. Untested surfaces had levels of approximately 90 atom% and 80 wt% carbon while tested samples showed decreased levels of 80 atom% and 65 wt% carbon. This leads to one possible explanation of the limited device life when lubricated with MAC; that the lubricant film is worn off to levels at which it is not able to prevent the onset of friction or stiction. MAC was previously shown to have better wear properties and a longer wear life than PFPE when tested with silicon

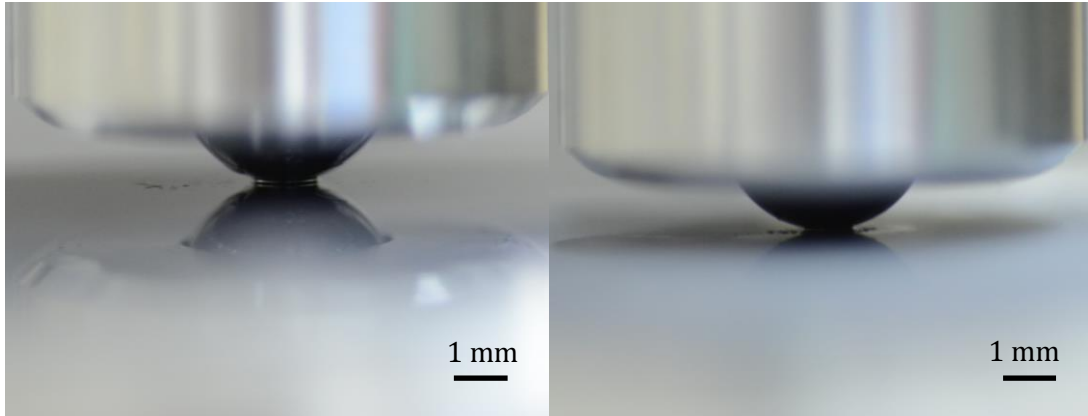


wafers under reciprocation. The discrepancies between the two tests will be discussed later.

It was observed that in all cases, lubricant was detected on the sidewall surfaces, despite the small amount of lubricant dispensed. This indicates the effectiveness of the “Loc-Lub” method of coating the sidewalls of MEMS devices with a liquid lubricant, without affecting the remaining portions of the device such as the comb drives and actuating components.

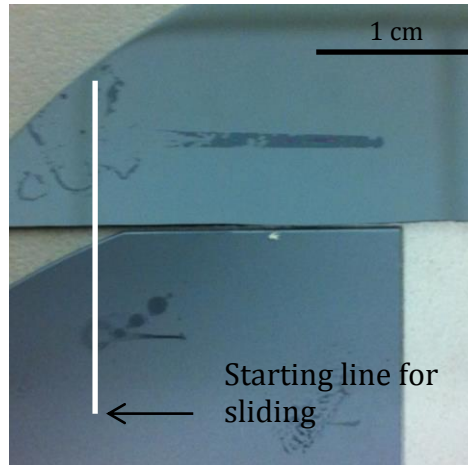
#### ***6.2.2.2 Effect of surface roughness***

It is possible that the rough surfaces of the sidewalls may have inhibited the formation of a sufficient meniscus bridge thereby reducing the ability of the MAC lubricant to sustain a coherent presence between the two contacts without asperity-to-asperity contact. Loy and Sinha (Loy et al. 2012) have investigated the variation of capillary bridges of liquid between surfaces using PFPE and MAC on smooth surfaces, so in this study a similar setup was used to investigate the meniscus presence between a rough flat Si surface and a point contact. Two types of Si wafer were used, one with roughness  $Ra$  616 nm, and the other roughness  $Ra$  16 nm, as measured using a Wyko NT1100 white-light interferometer (Veeco Instruments Inc.). A 2  $\mu$ l droplet of MAC at 4.0 wt% concentration was applied between the rough Si wafer surface and a 4 mm diameter silicon nitride ball. Optical images of the conjunctions are shown in Figure 6-8.



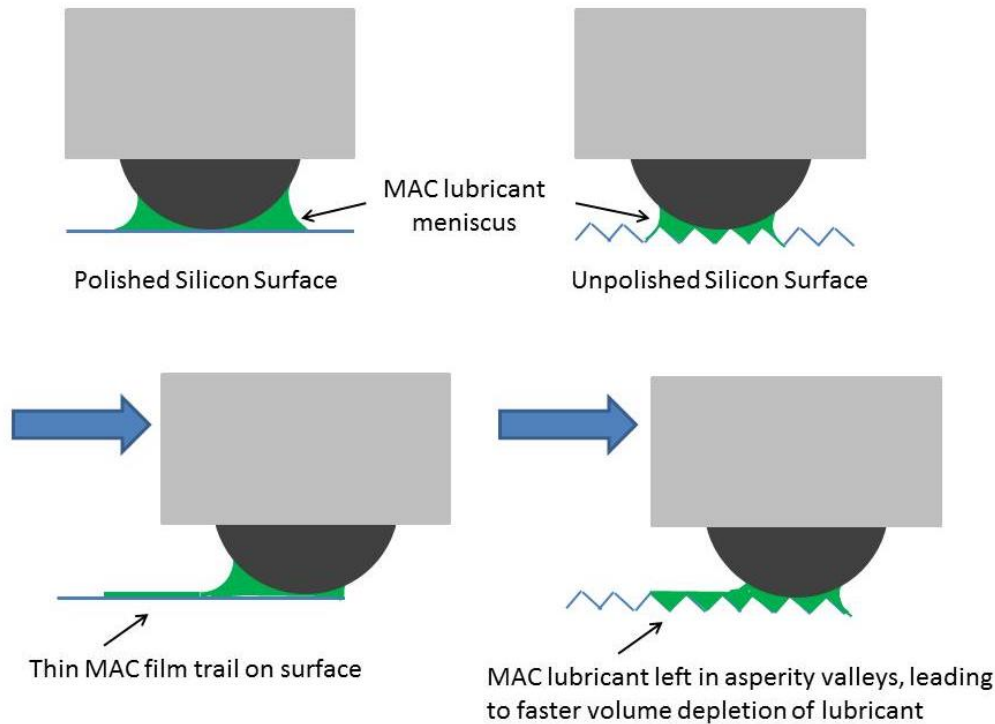
**Figure 6-8: Meniscus bridge of MAC lubricant between (left) silicon nitride ball and polished silicon wafer and (right) silicon nitride ball and unpolished silicon wafer, both just in contact. A visible meniscus is clearly seen on the polished silicon wafer, but none was visible on the unpolished silicon wafer.**

As reported by Loy and Sinha, a clear meniscus bridge was formed between the polished silicon wafer and the silicon nitride ball, as shown in Figure 6-8. However, on the rough silicon surface, the meniscus bridge was not so clearly visible at the point of application. This confirms reported literature (Frédéric et al. 2000; Ata et al. 2002; Butt et al. 2009; Noel et al. 2012) that the capillary forces between two surfaces are lowered when rough surfaces are involved. The lower capillary forces and smaller meniscus imply that less MAC is present at the point of contact between the two components, allowing for asperity contact in the setup shown in Figure 6-8, as well as in the MEMS tribometer contacts, leading to higher levels of friction and therefore quicker failure and shorter device life. To test this further, the above-mentioned ball-on-flat contacts were slid over a distance of 2 cm at a rate of 2 mm per sec, under just-in-contact conditions (approximately zero load), after being lubricated via “Loc-Lub” with 2  $\mu$ l of MAC lubricant solution. This sliding causes a lubricant trail to form behind the sliding ball, as shown in Figure 6-9.



**Figure 6-9:** Image of lubricant trails on a polished silicon surface (top) and an unpolished silicon surface (bottom), and a comparison of the two trails when placed together with an indicated starting line.

A comparison of the lengths of the lubricant trails on unpolished (rough) and polished (smooth) Si surfaces reveals that the lubricant depletes faster in the sliding contact on rough unpolished surfaces than on smooth surfaces. This is likely to be caused firstly by a smaller meniscus for the rough contact and secondly by the seeping of lubricant into the asperity valleys on the rough surfaces, reducing the volume dragged by capillary action at the contact point. In contrast, only a thin film is deposited on the smooth, polished silicon surface, allowing for a larger volume to remain at the contact point due to capillary meniscus and to be continually dragged over the entire sliding distance. A schematic of this mechanism is shown in Figure 6-10.



**Figure 6-10: Schematic of the proposed mechanism of depletion between the ball and flat contact upon sliding. The MAC lubricant can seep into or be left in asperity valleys upon sliding, leading to a larger volume left in the trail and therefore faster depletion. Sliding upon polished surfaces leaves only a thin film as a trail and so is less likely to deplete as quickly.**

The effect of roughness on the meniscus bridge (and resulting lubricant layer at the interface) will be discussed in the next section.

## 6.3 Discussion

### 6.3.1 Error in friction measurements

Friction trends were found to vary between device tests – such variations have been reported in other studies using MEMS tribometers, and are believed to be due primarily to limitations in their designs and manufacturing processes. This leads to significant device-to-device scatter, which makes it difficult to draw useful conclusions from quantitative friction measurements (Senft et al. 1997; Tas et al. 2003; Spengen et al. 2007; Timpe et al. 2007; Asay et al. 2008; Timpe et al. 2009; Ansari et al. 2012). The large variations in friction observed are considered to be due

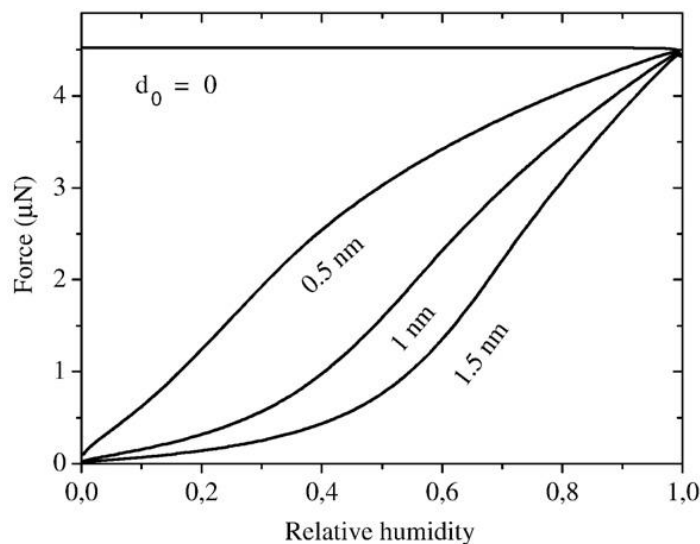
to a number of factors, the first of which is the design of the tribometer. As the springs in the components have a restoring force that changes the sliding parameters, the frictional forces recorded often are not representative of the assumed tested conditions. Furthermore, the restoring force as well as the spring constant was found to vary with the displacement of the component upon actuation with the comb drive, and this combination causes unpredictability in the speed and other parameters of the device. This variation in parameters and device configuration leads to a repeating cycle of increase and decrease of the parameters as the tests are run, leading to unpredictability of the instantaneous conditions, which directly affects friction. However, the device lives (i.e. when run till the friction forces are too large for the driving force to induce further motion) are thought to not be largely affected by the variations over the test duration, as the cycles are relatively short compared to the lifetime of the devices tested.

Another cause of the inconsistency of instantaneous friction measured is the fact that the conditions of the sidewalls prior to testing are unknown – it has been reported that the sidewall conditions are very different from that of the plane conditions and the effects of the fabrication and processing/storage environments are not well studied at this point of time. The effects of processing can also vary from device to device, or from batch to batch (Maboudian et al. 2002; Ashurst 2003; Ashurst et al. 2003b; Ansari et al. 2012). It is also observed in the FESEM images that the chemical etching in the processing and fabrication of the devices produces uneven texture across the sidewalls, both parallel to the sliding motion and through the thickness of the silicon wafer. Hence, it is unlikely that the sidewalls are all of the same roughness prior to testing, or even of the same condition of cleanliness. It is observed that the etched sidewalls have very uneven surfaces with asperities.

Despite these difficulties, it is still evident that the device lifetime is consistently extended by several orders of magnitude by the “Loc-Lub” method using PFPE as the lubricant. The effects of the varying parameters between devices bear further investigation.

### 6.3.2 Effect of Roughness on Tribological Behaviour

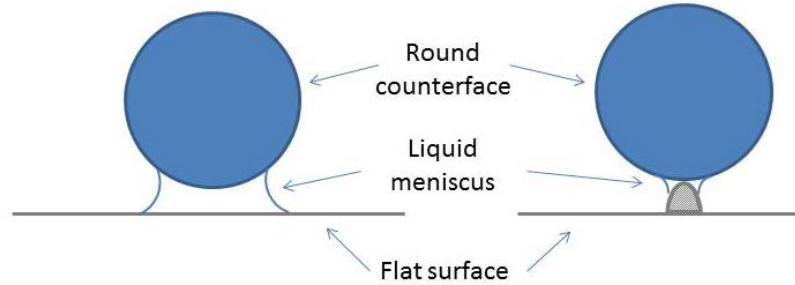
Butt and Kappl (Butt et al. 2009) showed that with an increase of surface roughness, a decrease of capillary forces between surfaces was observed. (Figure 6-11)



**Figure 6-11: Capillary forces due to condensation between surface, plotted for various roughness values and over varying humidity levels. Increasing roughness was found to reduce the capillary forces (Butt et al. 2009). Reprinted with permission.**

A similar effect was found by Ata and co-workers– an increase in the RMS roughness of a flat surface led to decreasing capillary adhesion forces, even in humid air (Ata et al. 2002). This reduction in adhesion forces was noted for both dry and humid situations, and the two values approached each other with increasing roughness, having almost equal trends at RMS values of 4 nm increasing to 12 nm. This was stated to result from the meniscus forming between the asperity and the

counterface, rather than the surface and the counterface – a schematic is shown in Figure 6-12 for illustration.



**Figure 6-12: Schematic for liquid meniscus behaviour against a flat surface and against asperities in a rough surface (Ata et al. 2002).**

The adhesion force in such a case is then determined by the radius of the asperity peak instead of the radius of the interacting sphere, as shown in Equation 6-1.

$$F_{ad} = 2\pi\gamma r_p (\cos \theta_1 + \cos \theta_2) \quad (6-1)$$

**Equation 6-1: Adhesion force model for a capillary meniscus between a rough sphere and a flat surface (Ata et al. 2002).**

where  $F_{ad}$  is the adhesion force,  $\gamma$  is the surface tension of the liquid,  $r_p$  is the asperity radius, and  $\theta_1$  and  $\theta_2$  are the contact angles that the liquid is supposed to form with the particle and the flat substrate respectively. The reduction in the thickness of the lubricant layer, coupled with the increased pressure exerted from the asperities instead of a perfectly flat surface, could have resulted in a lower device lives observed for devices lubricated with MAC lubricant, as the lubricant relies on the meniscus volume and capillary bridge to maintain a film between the contacts.

Restagno and co-workers investigated capillary condensation on rough surfaces, and found that an additional free-energy cost is required of the liquid bridges to overcome the defects in the surface (Frédéric et al. 2000). This free-energy cost ( $\Delta\Omega^\ddagger$ ) is given approximately by the following Equation 6-2:

$$\Delta\Omega^\dagger \equiv v_d \Delta\mu \Delta\rho \quad (6-2)$$

**Equation 6-2: Free energy cost required of liquid bridge to overcome defects in a surface in capillary condensation on rough surfaces (Frédéric et al. 2000).**

where  $v_d$  is the volume of the defect,  $\Delta\mu$  is the positive undersaturation in chemical potential of the gas, and  $\Delta\rho$  is the difference between the bulk densities of the liquid and the gas. It can be inferred that, since defects incur an additional free-energy cost for formation of a meniscus from liquid condensation, they can also have a similar effect for a liquid meniscus (similar to extremely humid conditions), thus reducing the volume at the contact point upon sliding. Little research has been published of liquid lubrication under round-on-flat conditions of sliding; so further research will be required to ascertain the validity of these models in this MEMS application.

It should be noted that rough surfaces were found to be detrimental only to MAC lubrication, which is considered to be due to the differing mechanisms in the two lubricant properties. This is discussed in the following section.

### **6.3.3 Differences in Lubricant Life and Behaviour**

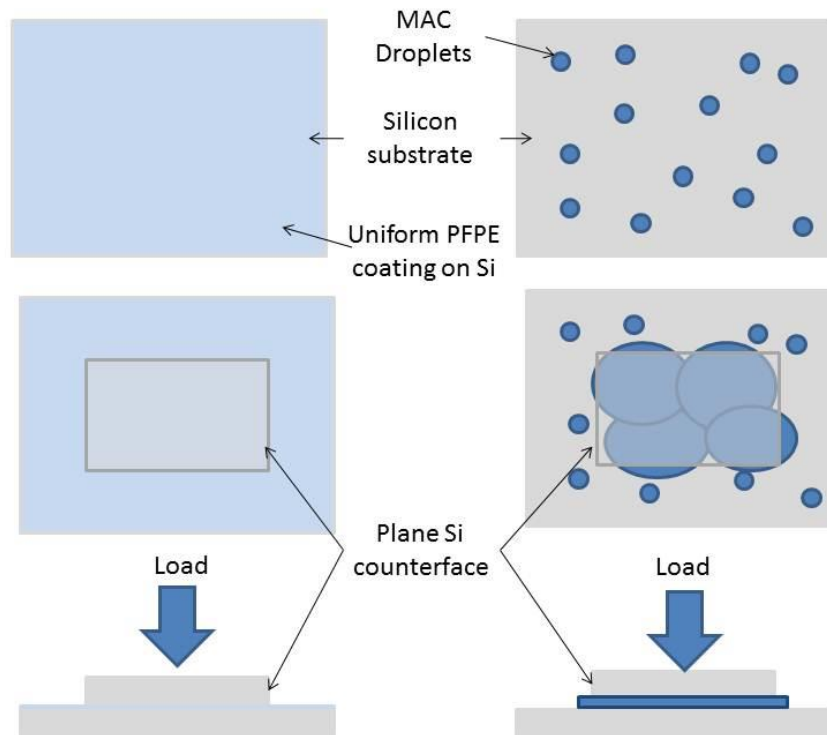
The work described in chapter 5 investigated the differences between the spreading and tribological behaviour of MAC and PFPE lubricant in a macro-scale contact. It was found that the cohesiveness of MAC lubricant improved the wear lives between smooth silicon surfaces by maintaining a consistent film between the surfaces. However, this depends heavily on the interaction between the surface tension of the liquid, and the capillary forces between the contacts. In the MEMS reciprocating tests described in the current chapter, the contact between a curved surface and a flat, reciprocating surface results in a line contact instead of an area contact, and it is possible that the surface area of the contact in the MEMS tribometer



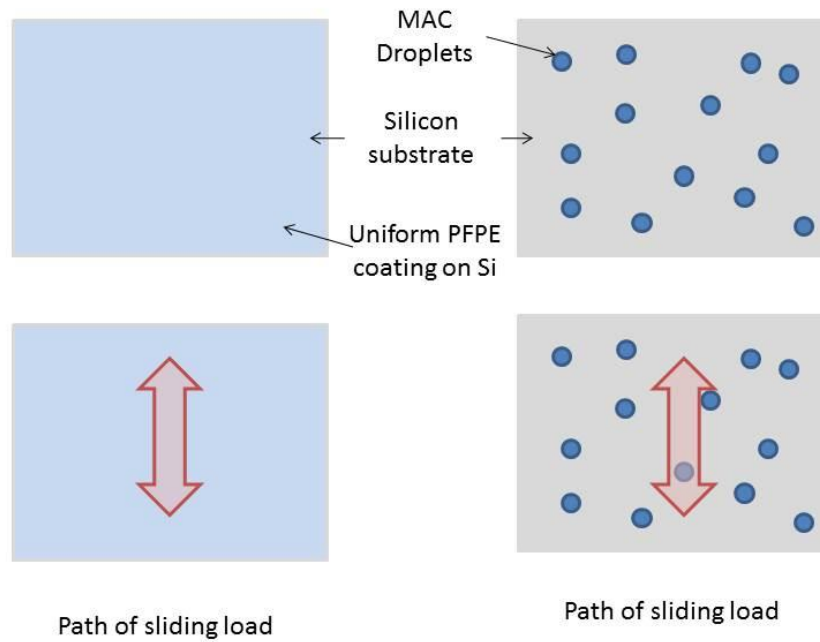
is too small to have enough capillary flow to maintain the MAC lubricant film between the interfaces, particularly for rough, sidewall surfaces. The smaller contact area combined with the higher frequency of oscillation compared to the macro-scale reciprocating wear tester would accentuate the lack of a meniscus of liquid at the contacts. The volume of the meniscus, if formed, is very small to have any lubrication effect. It is also highly possible that the lower capillary forces are unable to contain the liquid lubricant film, so the liquid is ejected from the contact. MAC lubricant may also be unable to seep uniformly or completely between the device sidewalls, resulting in dry contact at certain points within the line contact sliding. This will also lead to a quicker depletion of the lubricant film, and reduce the device life duration. Thus, the lack of a persistent film (as shown by the quicker depletion of the MAC lubricant film on rough silicon surfaces) previously observed in flat-on-flat contacts under reciprocating sliding, can be held responsible for the shorter device life in the MEMs tribometer.

By comparison, PFPE is likely to form a coherent film on the sidewall surface, as indicated by its spreading behaviour in Chapter 5. Since the mechanism of lubrication using PFPE does not involve a persistent liquid film between the contacts and relies instead on the dual-phase film deposited on the surface (Eapen et al. 2002; Satyanarayana et al. 2006), the effects previously discussed which will affect the film in MAC lubricant will not affect the PFPE lubricant in the same manner. PFPE remains as a uniform thin layer throughout the test (only a few nanometres thick). While this provided some protection for the surface, under flat-on-flat conditions, the PFPE lubricant mobile phase would be more easily swept aside due to a lower capillary force and smaller meniscus owing to lower surface tension of PFPE, leaving only the bonded layer on the surface, which provided very little wear protection. The

mechanisms of lubrication by PFPE have been heavily studied (Tani et al. 2001; Eapen et al. 2002; Satyanarayana et al. 2005; Satyanarayana et al. 2006; Ohno et al. 2010) and support this conclusion. A schematic of the different surface conditions as well as different mechanisms by which the various lubricants coat the surface are shown in Figures 6-13 and 6-14.



**Figure 6-13: Schematic of lubricant behaviour for PFPE (left column) and MAC (right column) under flat-on-flat reciprocal sliding. Both MAC and PFPE maintain a lubricant film between the surfaces as the surface area and capillary forces are large enough for MAC to form and maintain a film.**



**Figure 6-14: Schematic of point-on-flat sliding for PFPE coated (left) and MAC coated (right) specimens. The point of contact is not shown, as it is a line contact. An insufficient contact area, coupled with smaller capillary forces, render MAC less effective in maintaining a lubricant film compared to PFPE, which coats over the entire surface.**

However, in the case of the MEMS tribometer, the contact points are much smaller and are considered to be closer to the case illustrated in Figure 6-8 and 6-14, in which the contact slides across the surface with an extremely small contact area. PFPE then shows a continuous, dual layer lubricant film across the sliding distance as the entire surface is coated with a film, providing adequate protection between the two surfaces, with a bonded phase on the silicon oxide, as well as a mobile phase (Tani et al. 2001; Eapen et al. 2002). MAC, remaining as micro-droplets, may only intermittently supply the contact surface due to its dewetting nature on silicon, thus providing inadequate protection upon continuous testing. Furthermore, the small contact area is unlikely to provide a sufficient contact area for MAC to remain cohesive. This effect, coupled with the lower volume of MAC lubricant in the contact zones, as observed by the meniscus bridge, leads to a lower device life in the MEMS tribometer tests, even more so as there may be no available source for replenishment

along the sliding track. This factor would be accentuated in cases where the sidewalls were not perfectly vertical or parallel to each other, due to the uncontrollable processing environment effects.

It is therefore worth noting that the mechanisms of the two lubricants in reducing friction are extremely different. As the conditions tested in this setup do not favour the mechanisms of MAC lubricant, future work may be conducted under varying conditions to investigate the effectiveness of both lubricants.

## **6.4 Conclusions**

The “Loc-Lub” method that was tested in the reciprocating sliding against flat-on-flat silicon contacts has now been tested in a custom-made, MEMS reciprocating tribometer, with both PFPE and MAC lubricants. The following conclusions could be drawn.

1. The Loc-Lub method is effective in extending the device life of reciprocating sliding MEMS under the conditions tested.
2. In contrast to the flat-on-flat macro-scale contact, PFPE was found to be a better lubricant than MAC in the MEMS tribometer, exhibiting a considerably longer device life. The device did not fail even after 13 million reciprocating cycles for PFPE lubricated contacts.
3. The MAC lubricant, which remains as micro-droplets due to its dewetting nature on silicon, only intermittently supply the contact surface, thus providing inadequate protection. The roughnesses of the surfaces are also known to adversely affect the presence of a uniform liquid film between the contact surfaces and their asperities.

4. The delivery of lubricant using the “Loc-Lub” method is effective for MEMS sliding reciprocating devices, and thus may find possible application in commercial devices.

## **Chapter 7 - Hydrodynamic Lubrication in MEMS**

*Fluid film or hydrodynamic lubrication has been the traditional method of lubrication for many modern machines. Recent research has shown the efficacy of this method even for micro-machines. However, liquid lubrication of MEMS faces issues of high fluid film friction when relatively viscous liquids are used in the contacts, thus making it unfeasible. This chapter presents a method to reduce the hydrodynamic friction at high speed via additives – allowing for the potential use of liquid lubrication. Blends of hexadecane and multiply-alkylated cyclopentane (MAC) are compared to other blends of similar composition for verification, and a compound blend is investigated to reduce both the boundary and hydrodynamic friction in sliding.*

## 7.1 Introduction

Previous research has shown that boundary friction of liquid-lubricated, sliding silicon MEMS can be reduced when an additive is added into the base liquid as a friction modifier; studies show that amine additives (e.g. octadecylamine and dodecylamine) in particular are effective as their alkaline amine head group is weakly attracted to the acidic silica surfaces of the wafer. (Reddyhoff et al. 2011).

This chapter illustrates a series of experiments showing the reduction of hydrodynamic friction between smooth silicon surface MEMS contacts, lubricated by hexadecane with multiply-alkylated cyclopentane (MAC) as an additive. The results appear to show liquid slip similar to previously described occurrences described in the literature.

## 7.2 Materials and Experimental Procedures

Silicon MEMS pads (shown previously in Figure 3.8) were used in the rotating MEMS tribometer (details provided in Chapter 3, Section 3.2.4.4), with hexadecane as the base fluid. MAC was used as an additive at various concentrations and, later, in a compound blend with another previously-tested surface-active additive octadecylamine (ODA) mixed in hexadecane and with squalane. The base fluid used in this work was hexadecane, a linear alkane with the chemical formula  $C_{16}H_{34}$ . Concentrations of the various blends are indicated alongside the experimental results.

Friction tests were conducted on the silicon MEMS pads over speeds ranging from 10 to 15,000 RPM using the rotational MEMS tribometer, with friction measured continuously during the tests; test rig and method were detailed in Chapter 3.

## 7.3 Experimental Results

### 7.3.1 Test lubricants and additives

The base fluid hexadecane was mixed with a MAC lubricant at the concentrations shown in Table 7-1, which lists the viscosities and densities of the blends.

**Table 7-1: Viscosities of mixtures used in tests, measured with a Stabinger viscometer (model SVM 3000, Anton Paar, Graz, Austria). All viscosity measurements were taken at 25 °C**

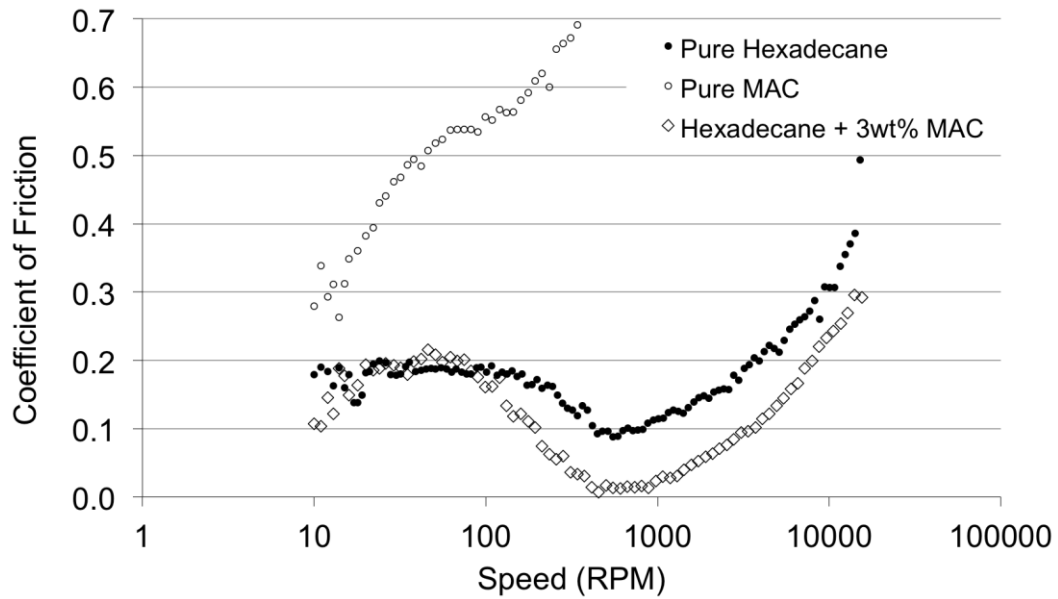
	<b>Dynamic Viscosity, <math>\eta</math> (cP)</b>	<b>Density, <math>\rho</math> (g/cm<sup>3</sup>)</b>
<b>Hexadecane</b>	3.138	0.7697
<b>Hexadecane + 0.5 wt% MAC</b>	3.139	0.7698
<b>Hexadecane + 1.0 wt% MAC</b>	3.162	0.7700
<b>Hexadecane + 2.0 wt% MAC</b>	3.306	0.7708
<b>Hexadecane + 3.0 wt% MAC</b>	3.345	0.7712
<b>Hexadecane + 4.0 wt% MAC</b>	3.473	0.7728
<b>Hexadecane + 7.0 wt% MAC</b>	3.703	0.7743
<b>Hexadecane + 20.0 wt% MAC</b>	4.807	0.7807
<b>MAC</b>	18.6	0.7730

### 7.3.2 Friction tests

#### 7.3.2.1 Hexadecane with MAC additive

Tests were carried out on the range of hexadecane and MAC blends detailed in Table 7-1, using the experimental setup and approach described in Chapter 3. Results are plotted as Stribeck curves of friction coefficient against rotational speed on a logarithmic scale.





**Figure 7-1: Friction coefficient versus speed for MEMS contacts lubricated with neat hexadecane, neat MAC, and a blend of 3 wt% MAC in hexadecane**

Figure 7-1 shows the variations in friction with respect to speed for a typical contact lubricated with neat hexadecane, neat MAC and a 3 wt% solution of MAC in hexadecane, showing the boundary, mixed, and hydrodynamic regimes previously mentioned. Boundary friction coefficient of contacts lubricated with neat hexadecane is approximately 0.2 and full hydrodynamic lubrication occurs above speeds of approximately 700 – 800 rpm; these values are consistent with previous research (Ku et al. 2010; Reddyhoff et al. 2011). The friction for neat MAC in MEMS contacts is also plotted on the same axis; in this case viscous friction increases dramatically at low speeds. In this case, because of the much higher viscosity of MAC (18.6 cP at 25 °C) compared to hexadecane (3.1383 cP), the contact operates in hydrodynamic lubrication down to the lowest speed tested, also showing very high hydrodynamic friction. For the 3 wt% MAC in hexadecane, despite higher viscosity of the blend compared to neat hexadecane, the blend shows reduced friction in both mixed and hydrodynamic regimes. A large number of these tests were carried out across different

calibrated platforms and specimens, and results were repeatable within less than 10% margin of error (Figure 7-2)

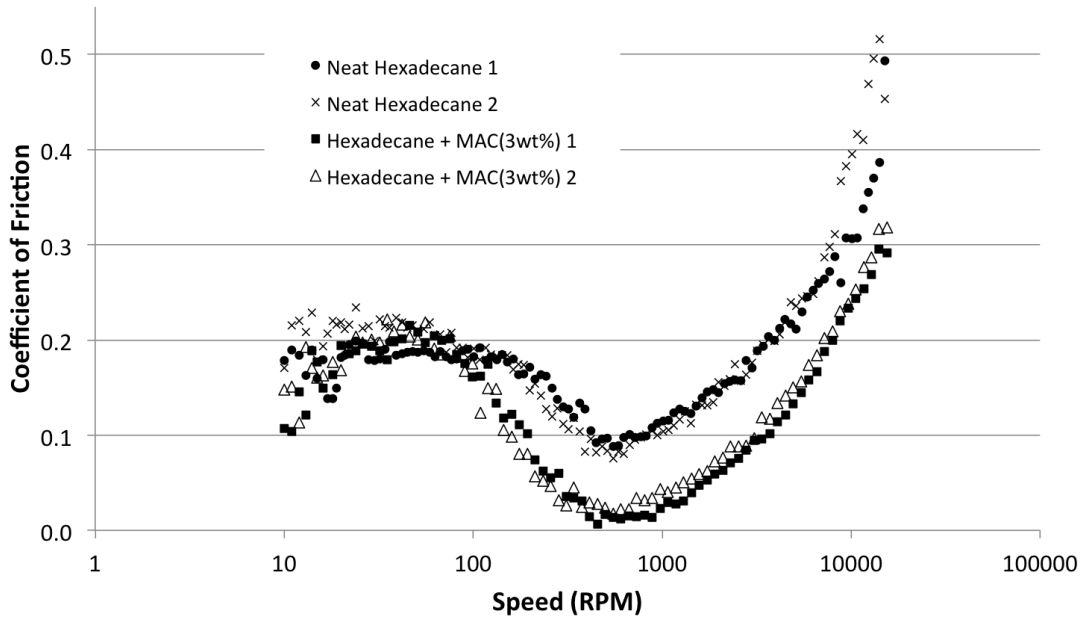


Figure 7-2: Repeatability of experimental results across tests, using different specimens.

Figure 7-3 shows the variation in friction coefficient with speed for concentrations of MAC in hexadecane ranging from 0 to 7 wt%. The optimum concentration was found to be 3 wt% of MAC in hexadecane, which reduces friction at 15,000 rpm from  $\approx 0.5$  to  $\approx 0.3$  when compared to neat hexadecane. Lower concentrations of MAC in hexadecane reduced the hydrodynamic friction to lesser extents, and for 0.5 wt% MAC in hexadecane the change is negligible. As the concentration of MAC increased above 3 wt%, hydrodynamic friction was observed to rise – this increase in friction with viscosity shows that above  $\approx 3.0$  wt%, the friction-reducing effect of MAC is outweighed by effects from its viscosity, though still lower than that predicted by hydrodynamic theory.

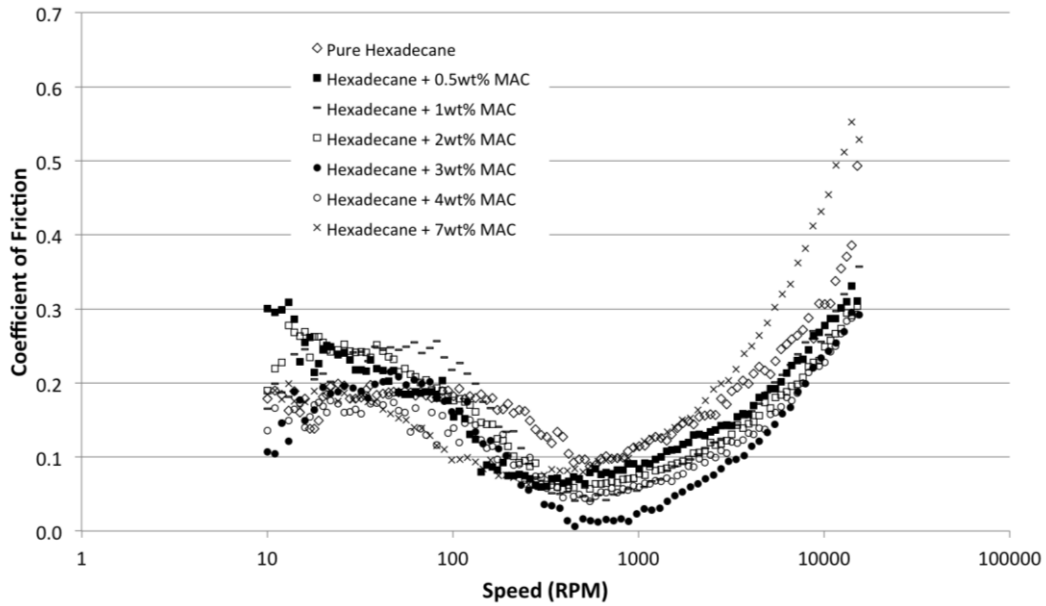


Figure 7-3: Friction coefficient versus speed for MEMS contacts lubricated with hexadecane with varying percentages of MAC as additive

Figure 7-4 plots the friction coefficient (CoF) at 15,000 rpm (high speed) and the minimum levels of friction coefficient values taken from Figure 7-3, plotted against the concentration of MAC blended in hexadecane. Also shown in this graph is how the dynamic viscosity (from Table 7-1) varies with MAC concentration, which clearly confirms the anomalous and unexpected friction behaviour with respect to an increase in viscosity. Below 4 wt% of MAC in hexadecane, friction falls with increasing concentration of MAC, while viscosity rises monotonically.

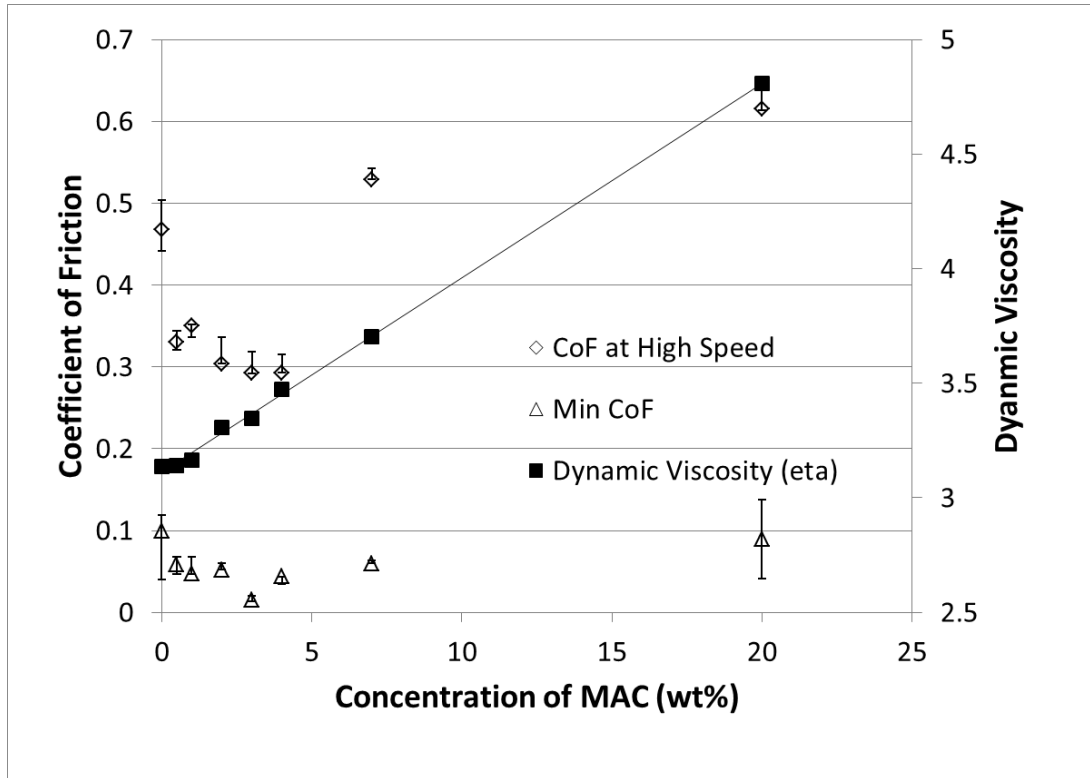


Figure 7-4: Plot of minimum coefficient of friction, friction measured at 15000 rpm and dynamic viscosity, all versus concentration of MAC additive in hexadecane.

One possible reason for this behaviour is the impact of heating effects due to increased viscosity. To test this, experiments were conducted using an alternative liquid with equal viscosity to that of 3 wt% MAC in hexadecane. This viscosity was obtained by mixing squalane and hexadecane in proportions suggested by ASTM D314 to produce a liquid of viscosity 3.3 cP, close to that of 3 wt% MAC in hexadecane (3.34 cP). The results are then plotted in a Stribeck curve (Figure 7-5). In this it is evident that the addition of squalane to hexadecane leads to an increase in hydrodynamic friction, in contrast to that of MAC as an additive, which reduces friction. Therefore, it is not simply the increase in liquid viscosity and consequent heating that is causing the anomalous reduction in friction, but some other change in property caused by the addition of MAC.

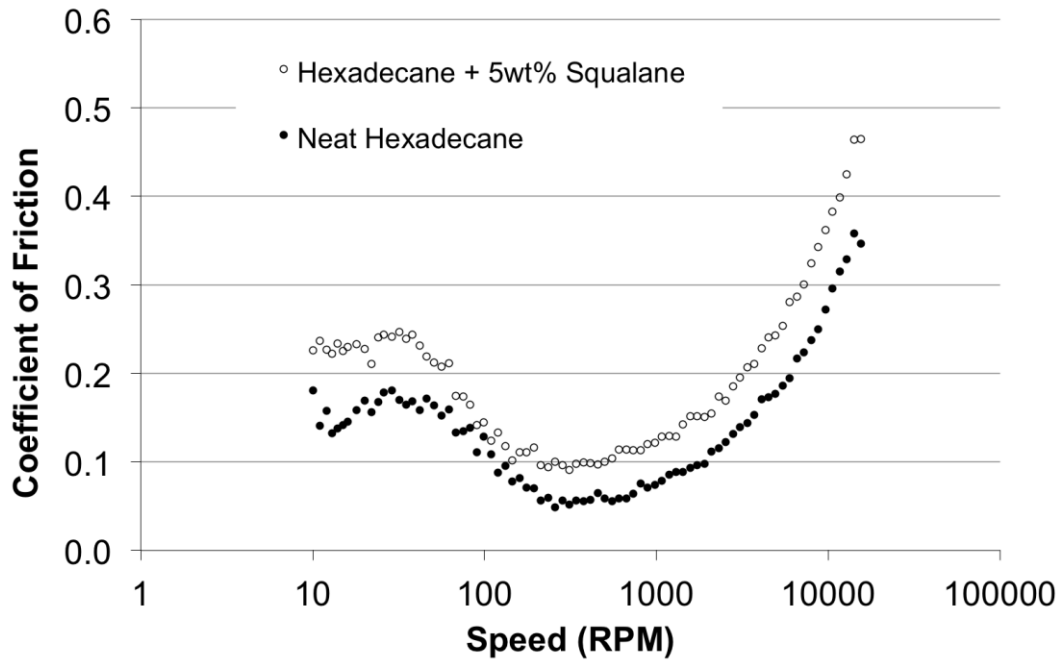


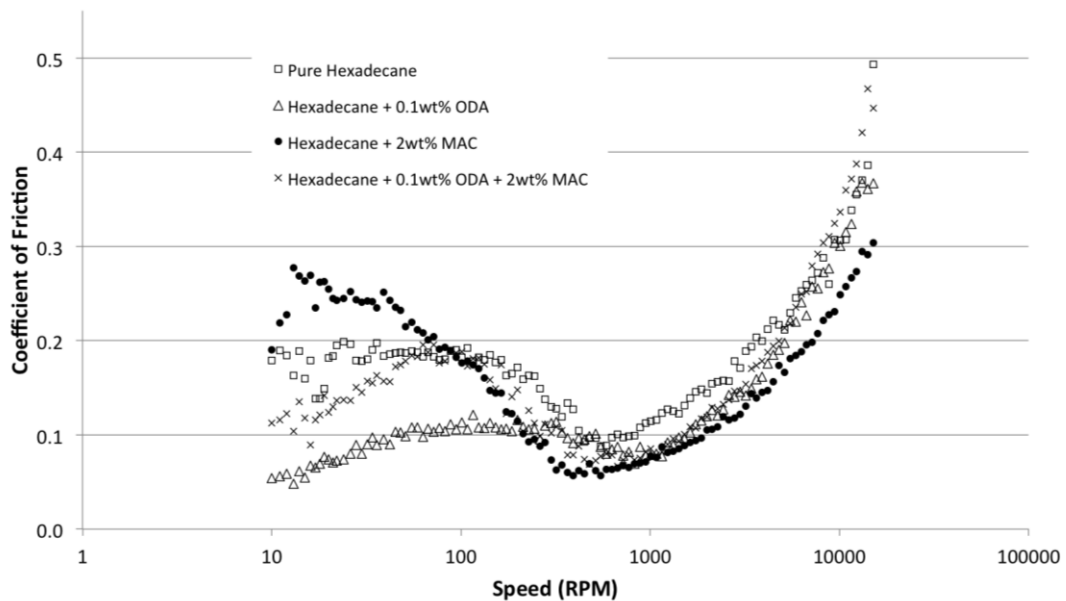
Figure 7-5: Coefficient of friction versus speed for neat hexadecane, and a blend of squalane and hexadecane of 3.3 cP dynamic viscosity to match the viscosity value of 3 wt% MAC in hexadecane

### 7.3.2.2 Compound blend of Hexadecane with Octadecylamine and MAC

A series of tests was carried out to establish if the reduction in friction resulted from phenomenon occurring close to the silicon surface of the specimens or within the lubricant bulk. In these tests, octadecylamine (ODA) was blended with the hexadecane-MAC blend since ODA was previously shown to act as a friction modifier additive that forms a boundary film on silica surfaces, thereby reducing friction at low speeds under the same conditions (Reddyhoff et al. 2011). Since ODA is surface-active on silica, its inclusion in the hexadecane-MAC blend is intended to probe whether the observed reduction in hydrodynamic friction can be attributed to a surface or bulk fluid phenomenon.

Figure 7-6 shows the variation of friction with the logarithm of sliding speed for four blends having hexadecane as the base fluid; neat hexadecane, hexadecane with 0.1 wt% ODA, hexadecane with 2 wt% MAC and hexadecane with 0.1 wt%

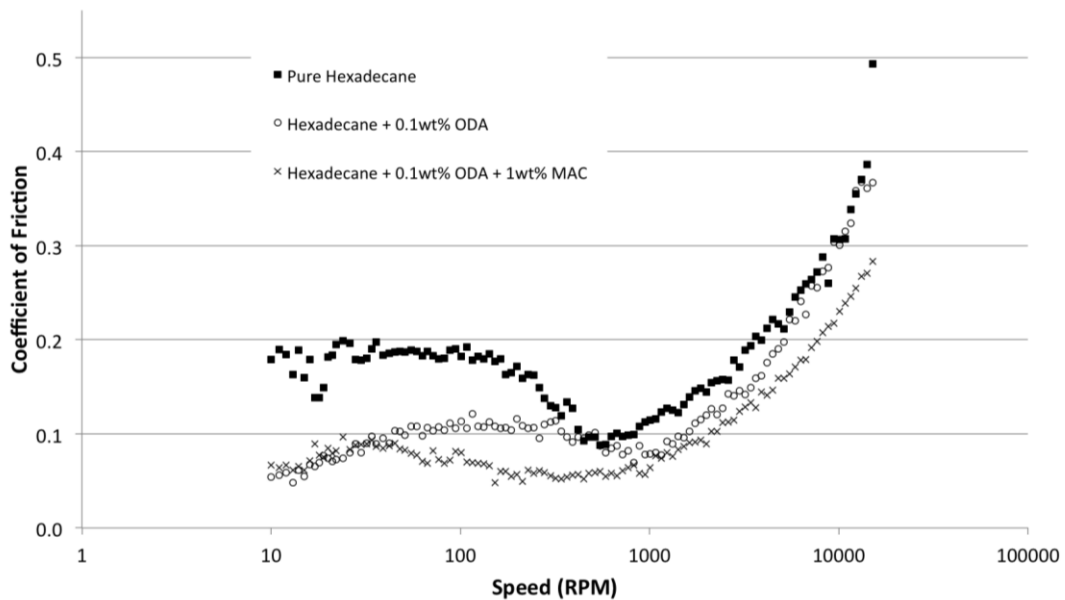
ODA and 2 wt% MAC. As previously discovered, the inclusion of 0.1 wt% ODA alone in hexadecane reduced boundary friction significantly (from  $\approx 0.2$  to  $< 0.1$ ), while the presence of the MAC alone reduces hydrodynamic friction. It can be seen that the friction reductions in the respective regimes for each additive were diminished when a blend of hexadecane including both additives is used. This suggests that the friction-reducing mechanisms associated with MAC and ODA are competing with each other, increasing the boundary and hydrodynamic friction compared to the individual blends of Hexadecane + 2 wt% MAC and Hexadecane + 0.1 wt% ODA. This suggests that the friction reducing behaviour from MAC is a phenomenon that also occurs close to or at the silicon surface.



**Figure 7-6: Coefficient of friction versus speed for individual blends of octadecylamine and 2 wt% MAC in hexadecane, including a blend with all three liquids**

It was noted that there is a slight difference between the friction values shown in the figures above and those observed in previous work (Reddyhoff et al. 2011). This is attributed to the different pad geometry used in the current work (as defined in Chapter 3) compared to those employed previously.

A series of tests were then conducted on compound blends in which the concentrations of MAC and ODA components were varied independently. The most effective blend in which friction was reduced in both boundary and hydrodynamic regimes consisted of hexadecane with 0.1 wt% ODA and 1 wt% MAC – a Stribeck curve obtained for this blend is shown in Figure 7-7, showing that the addition of both ODA and MAC to hexadecane acts to reduce both boundary and hydrodynamic friction. At these concentrations, the effect of slip induced by MAC is sufficiently present while not affecting the formation of the amine film adversely in preventing boundary friction. The increase to a concentration of 2 wt% MAC as shown in Figure 7-6 not only affects the amine layer formation enough to cause an increase in boundary friction, but the amine layer also interferes with the effect of slip in addition to the increased viscosity, leading to higher hydrodynamic friction.



**Figure 7-7: Coefficient of friction versus speed for MEMS contacts lubricated with pure hexadecane, hexadecane with 0.1 wt% octadecylamine (ODA), and a compound blend of hexadecane with 0.1 wt% ODA and 1 wt% MAC**

### 7.3.2.3 Squalane with MAC additive

The base liquid hexadecane is a linear molecule which has the propensity to exhibit liquid slip behaviour on very smooth oleophobic surfaces (Pit et al. 2000; Choo et al. 2007b). Non-linear hydrocarbons would not establish slip on sliding surfaces so easily due to their uneven molecular shape. In order to establish whether the addition of MAC would reduce friction when blended with a hydrocarbon base fluid that is non-linear in structure (which would imply that friction reduction is not due to slip), friction tests were conducted for the MEMS contact lubricated with both neat squalane and squalane blended with 2 wt% MAC. This concentration was used as it would show sufficient effect on the liquid if any were to be seen. As shown in Figure 7-8, the addition of 2 wt% MAC in squalane has negligible effect on friction compared to neat squalane. It should be noted that the viscosity of the blend of 2 wt% MAC in squalane was very similar to that of neat squalane.

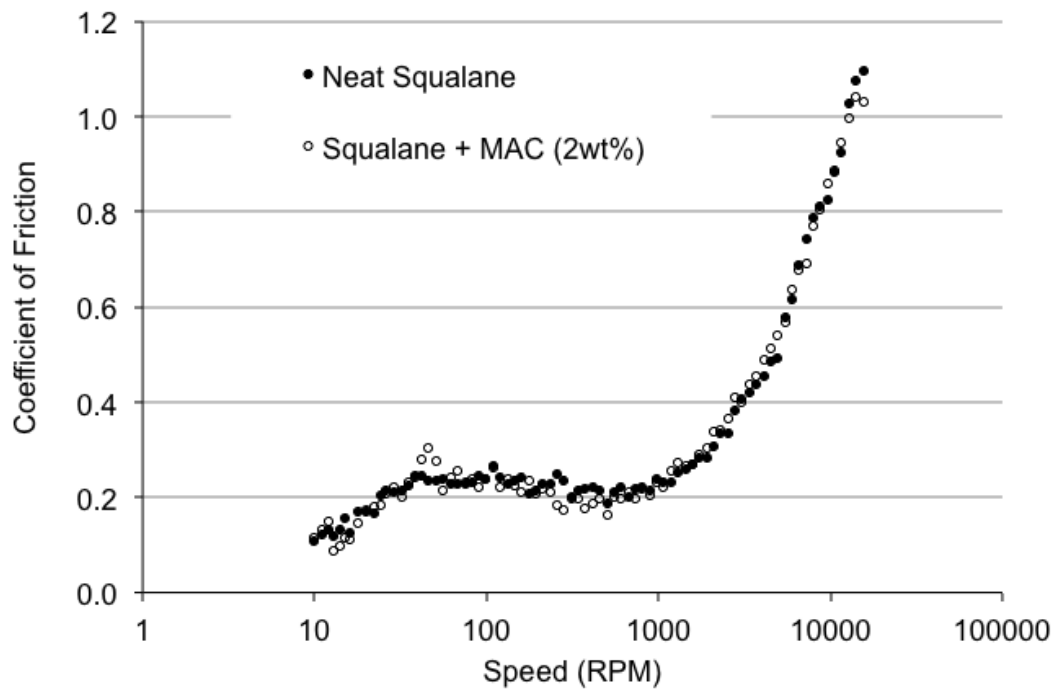


Figure 7-8: Coefficient of friction versus speed for neat squalane and squalane blended with 2 wt% MAC as additive



## 7.4 Discussion

### 7.4.1 Possible origins of observed friction reduction

The observed reduction in friction that occurs with an increase in fluid viscosity due to the addition of MAC in hexadecane is clearly contrary to conventional Reynolds' theory, which states that hydrodynamic friction  $\mu$  is approximately related to dynamic viscosity  $\eta$  by the following formula:

$$\mu \propto \left(\frac{\eta U}{W}\right)^{0.5} \quad (7-1)$$

**Equation 7-1: Relation of hydrodynamic friction to dynamic viscosity according to Reynolds's theory**

where  $U$  is the entrainment speed (equivalent to half the sliding speed of the contacts in the present study) and  $W$  is the load applied.

A tentative explanation for this behaviour is that a film of MAC forms on the silicon surface, causing hexadecane to slip, rather than shear against one or both of the surfaces – this slip of the liquid then reduces hydrodynamic friction at high speed sliding. Although the chemical composition of both di- and tri-(2-octyldodecyl)-cyclopentane, which are both unsaturated hydrocarbons, do not suggest any attraction to a silica surface, the following observations suggest that such a film is formed.

Firstly, the addition of ODA to the blend inhibits MAC friction reduction in the hydrodynamic regime, as seen in Figure 7-6 and 7-7 when compared to Figure 7-1. Since ODA is surface active on silica (Reddyhoff et al. 2011), this suggests that the friction-reducing mechanism of MAC additives occurs close to the silica surface. Furthermore, when MAC was blended with a squalane base fluid (which is also a

hydrocarbon) no corresponding friction reduction was observed. This observation suggests that slip has occurred with hexadecane since it would be expected to be seen with linear molecules such as hexadecane and not squalane (a branched molecule) due to the ability of linear molecules to orientate and align themselves, forming an ordered layer. The formation of an ordered film will also be promoted by the smooth nature of the silicon surfaces, with  $\approx 0.5$  nm Ra roughness (Pit et al. 2000; Zhu et al. 2001; Choo et al. 2007a; Choo et al. 2007b).

Slip has also been shown to occur more readily when liquids do not strongly wet the surfaces they are moving against. Contact angle measurements were therefore taken on surfaces and the results are listed in Table 7-2. A MAC-coated silicon wafer was produced by dip-coating a solution of 0.4 wt% MAC in n-hexane, before allowing the hexane to evaporate. This approach was necessary as neat MAC does not wet silica surfaces uniformly enough to form a film on which to measure contact angles.

**Table 7-2: Contact angles of 1  $\mu$ l of liquid on various surfaces. Values were measured at 25 °C**

<b>Liquid</b>	<b>Surface</b>	<b>Contact angle (°)</b>
Hexadecane	Bare silica	$\approx 0$
Hexadecane + 3.0 wt% MAC	Bare silica	19
Hexadecane	MAC-coated silica	23

It can be seen that the neat hexadecane wets the surface of the silicon specimens. However, if the surface has been coated with MAC prior to measurement, the contact angle increases from  $\approx 0$  to 23 °, showing that the wetting is reduced on the surface. A blend of hexadecane and MAC at 3.0 wt% yields a similar contact

angle of  $19^\circ$  when dropped on a silicon surface. If a similar non-wetting MAC layer is formed on the specimen surfaces during the testing process, it is possible that this dewetting property promotes slip.

Figure 7-1 showed that MAC in hexadecane reduces friction in both the mixed regime, occurring from  $\approx 100$  to 1000 RPM, as well as in the hydrodynamic regime. The reduction in mixed friction that occurs with the MAC blend has the effect of shifting the original Stribeck curve to the left. A reduction in the mixed regime has previously been attributed to formation of a viscous boundary layer, which increases fluid entrainment at intermediate speeds. Viscous fluid-like boundary films have been shown to occur in metal-metal elasto-hydrodynamic contacts (Smeeth et al. 1996). Here at low speeds, where the fluid film thickness is less than that of the adsorbed polymer film as investigated by Smeeth and co-workers, the fluid at the inlet is of higher viscosity than the bulk of the liquid. However, in contrast to the work by Smeeth and co-workers, this observed behaviour occurs in conformal silicon contact and the reduction of friction continues into the hydrodynamic regime.

A noteworthy point is that the optimum concentration of MAC in hexadecane ( $\approx 3$  wt%) is significantly higher than that of typical additive concentrations used. The reason for this is not entirely clear, but may suggest that MAC forms a layer that is several molecules thick on the surface.

## 7.5 Conclusion

Liquid lubrication has been found in previous research to be an effective method of reducing friction in MEMS applications. This approach requires low hydrodynamic friction, which can be obtained by using very low viscosity liquids.

A miniature test thrust pad bearing fabricated from silicon has been used to show that a blend of hexadecane and di- and tri-(2-octyldodecyl)-cyclopentane produces a lower level of friction in both the mixed and hydrodynamic regimes when compared to neat hexadecane alone. The reduction in hydrodynamic friction is contrary to what is expected from conventional Reynolds' lubrication theory, as the blend is of a higher viscosity than that of neat hexadecane. A number of observations seem to suggest that this reduction is due to a film formed on the silicon surfaces by the MAC additive, which causes hexadecane to slip against the surfaces. With an additional additive of octadecylamine in the blend, the boundary friction observed is lowered as well, leading to an overall decrease in friction over the speeds tested.

These observations have implications for the lubrication of MEMS devices which involve smooth silicon surfaces sliding under relatively low loads, as it may make liquid lubrication a more feasible method for controlling friction. This is because the very low viscosity liquids proposed to give acceptably low hydrodynamic friction in MEMs also tend to have very low volatility. The impact of MAC additive in reducing the hydrodynamic friction of hexadecane may enable to use of higher viscosity hydrocarbon fluids that previously considered.

## **Chapter 8 - Barrier Coatings for Local Containment of Lubricant**

*This chapter presents two methods of containing and preventing the spreading of lubricant on silicon surfaces, for application to MEMS contacts. These involve modification of the surface and modification of the liquid respectively. A novel spin test is used to ascertain that liquid containment results in a higher force being needed to force the liquid out of a predetermined area.*

## 8.1 Introduction

The use of specialized packaging for lubricant containment is cumbersome, limits the application of MEMS devices, and often makes common and commercial production of the device uneconomical. In the case of liquid lubrication, such packaging is made potentially more complex since depletion or spreading of the liquid becomes a concern. The presence of anti-spreading or anti-depletion surfaces and lubricants would help to promote the feasibility of using liquids in MEMS by reducing the severity of this problem. The scales of such devices make the building of physical containment walls into the device during the fabrication process unfeasible.

One of the objectives of the “Localized Lubrication” technique is to achieve application of lubricant on micro-devices at a precise location without affecting other components of the device or requiring specialized hermetic packaging. Even though the designed system can dispense a small amount of liquid lubricant ( $< 0.1 \mu\text{l}$ ), it is often observed that some spreading occurs on the surrounding region. It is anticipated that, by further limiting the spreading of the lubricant on the device surface, the technique will be improved, since the liquid will be clearly contained at specific locations during application. This would also allow for contained application of liquid lubricants such as hexadecane in reciprocating contacts.

Spreading can be prevented by two methods: modification of the surface to which the lubricant is applied, or modification of the liquid itself to make it non-spreading. On the surface, inducing a hydrophobic or oleophobic property helps to prevent spreading of a liquid droplet due to the reduction of surface tension of the surface against the liquid, with low surface energies causing the liquid not to wet the surface. However, another observation is also true – the non-wetting property of the hydrophobic or oleophobic surface will also allow the liquid droplet to slide off the

surface easily if prompted by an external force. Although SAMs and texturing have been known to give a hydrophobic or oleophobic surface as well as reduce adhesion in direct contact, such uniform coatings are less applicable for cases in which two surfaces are sliding against each other in relative motion, which would easily drag the droplet away from the contact area, or lead it to surfaces with a high propensity for wetting.

Modifications of the liquid to control spreading range from changing the liquid itself, to have a different viscosity or surface energy, to including additives in the liquid in order to induce anti-spreading properties. Unfortunately increasing the liquid viscosity is not a viable option in liquid-lubricated MEMS since although it will lead to a decrease spreading rate, as well as reduced volatility, it will also lead to unacceptably high hydrodynamic friction in high speeds contacts (Ku et al. 2012).

## 8.2 Materials and Experimental Procedures

Octadecyltrichlorosilane (OTS) was used to produce potential SAM hydrophobic barrier coating on silicon (Si) wafers (Si-OTS). Some of the resultant surfaces were then treated with oxygen plasma (Harrick Plasma cleaner) while protecting the surface with a PDMS mask. This enables the OTS to be removed from selected areas and thus produce localised and controlled hydrophilic regions (Si-OTS-mod) surrounded by hydrophobic borders. This method of selective modification of OTS has been used by Lin and co-workers to influence self-patterning of self-assembled monolayers (Lin et al. 2009). The exposure of the OTS layer to oxygen plasma converts the terminal methyl group ( $-\text{CH}_3$ ) to polar surface groups such as  $-\text{OH}$ ,  $-\text{CHO}$  and  $-\text{COOH}$ , thereby modifying the surface properties. The principle was to test whether lubricant could be contained within the produced hydrophilic region.

Octadecylamine (ODA) and dodecylamine (DDA) were used as additives in hexadecane to investigate possible changes of spreading behaviour by additives. Spin tests, contact angle measurements, droplet profiles and surface area calculations were conducted as outlined in Chapter 3.

## 8.3 Results

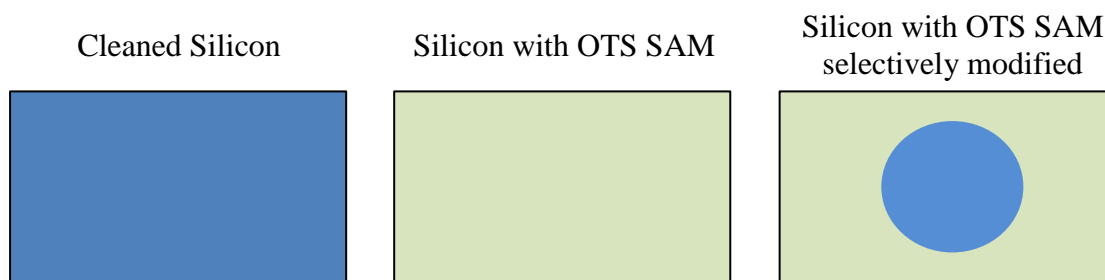
### 8.3.1 Contact Angle Measurements

Table 8-1: Contact angles performed on various silicon surfaces. Values measured at 25 °C

Surface	Water Contact Angle (°)	Hexadecane Contact Angle (°)
Plasma Cleaned Si	~ 0	~ 0
Si-OTS (without further treatment)	106	41
Si-OTS after plasma treatment	~ 0	~ 0
Unprotected area of Si-OTS after plasma treatment (Si-OTS-mod)	~ 0	~ 0
Protected area of Si-OTS after plasma treatment	105	39

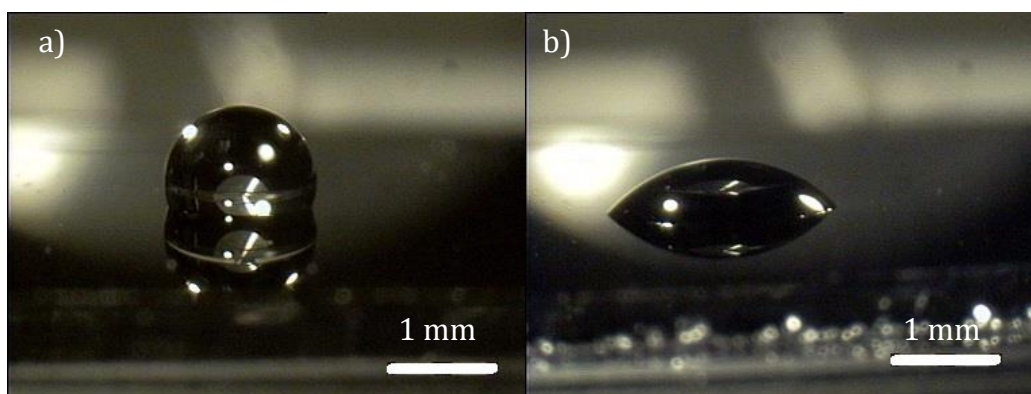
The contact angles taken on various silicon surfaces are summarized in Table 8-1. These show that the formation of an OTS SAM produced very hydrophobic surfaces which were removed by plasma treating to give a hydrophilic surface. Use of a PDMS conformal mask enabled localised hydrophilic surfaces to be formed in an OTS-coated while leaving the remainder of the surfaces still hydrophobic. A schematic of the surface conditions are shown in Figure 8-1.



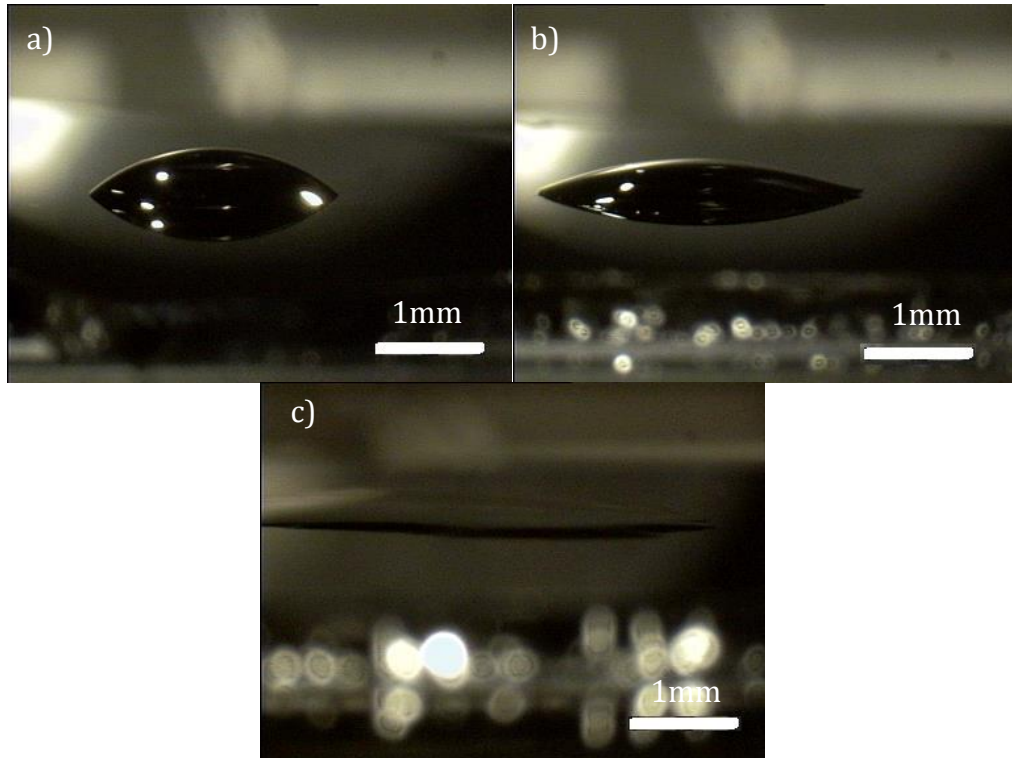


**Figure 8-1:** Schematic of silicon surfaces (left to right) after cleaning, after OTS SAM coating, and after selective modification using PDMS masking and plasma treatment

Droplets were placed on the different surfaces and observed via digital microscopy. The containment effects and the selective modification were clearly observed with water, as shown in Figure 8-2, in which the diameter of the wetting area is approximately the same diameter as the circle of modified hydrophilic surface (2 mm). The containment effect is not so clear in hexadecane (Figure 8-3) as it spreads more easily on the OTS layer, with a lower contact angle on OTS, compared to water (approximately  $40^\circ$  for hexadecane compared to approximately  $110^\circ$  for water), although the containment effects are more obvious when subject to the spin tests, in which the “throw off” force is compared.



**Figure 8-2:** 1  $\mu$ l water droplets on a) OTS coated silicon, and b) on the circle of plasma-treated silicon surface. Water was clearly contained within the 2 mm diameter of the area exposed to plasma treatment



**Figure 8-3: 1 µl hexadecane droplets on a) OTS coated silicon and b) on the plasma treated circle and c) on bare silicon. The containment of hexadecane is not as obvious when compared to OTS coated samples due to the lower repulsion between the liquid and surface, but is obvious when compared to bare cleaned silicon, in which spreading is evident**

### 8.3.2 Spin tests

A summary of the “throw-off forces” measured in the spin tests are shown in Figures 8-4 and 8-5, for radial distances of 40 mm and 20 mm respectively. Throw-off force was calculated from equation 3.2.

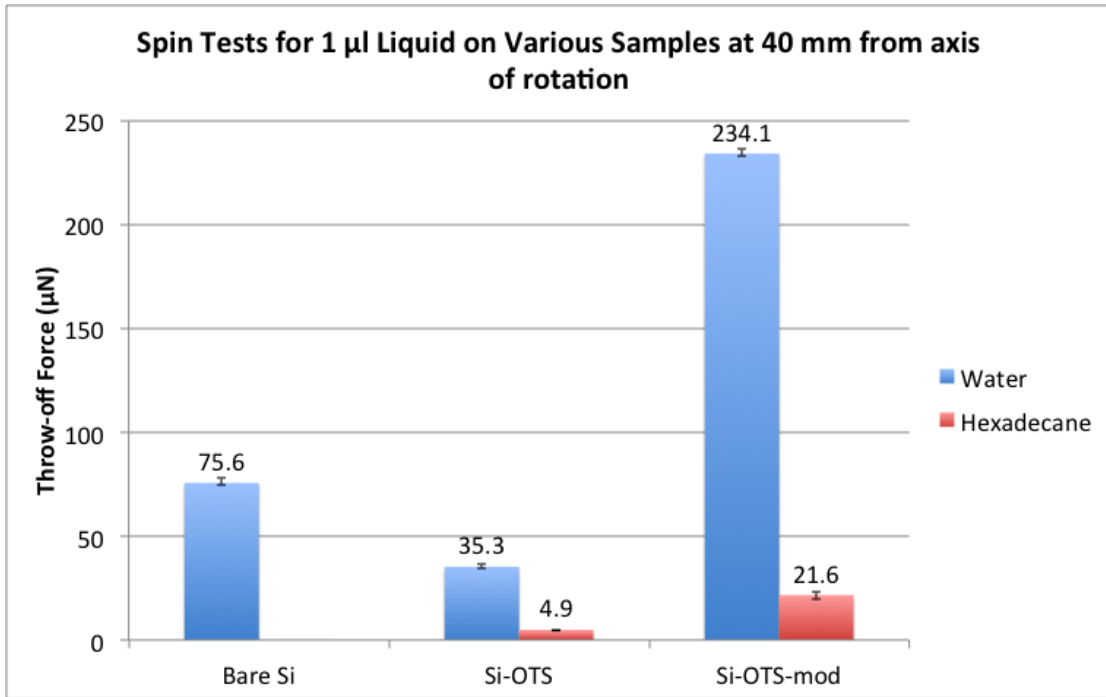


Figure 8-4: Throw-off Forces for Spin Tests conducted on cleaned bare Si, Si coated with an OTS SAM (Si-OTS), and Si with selective OTS removal after coating (Si-OTS-mod). Hexadecane spread readily on bare, cleaned silicon and so no value could be obtained.

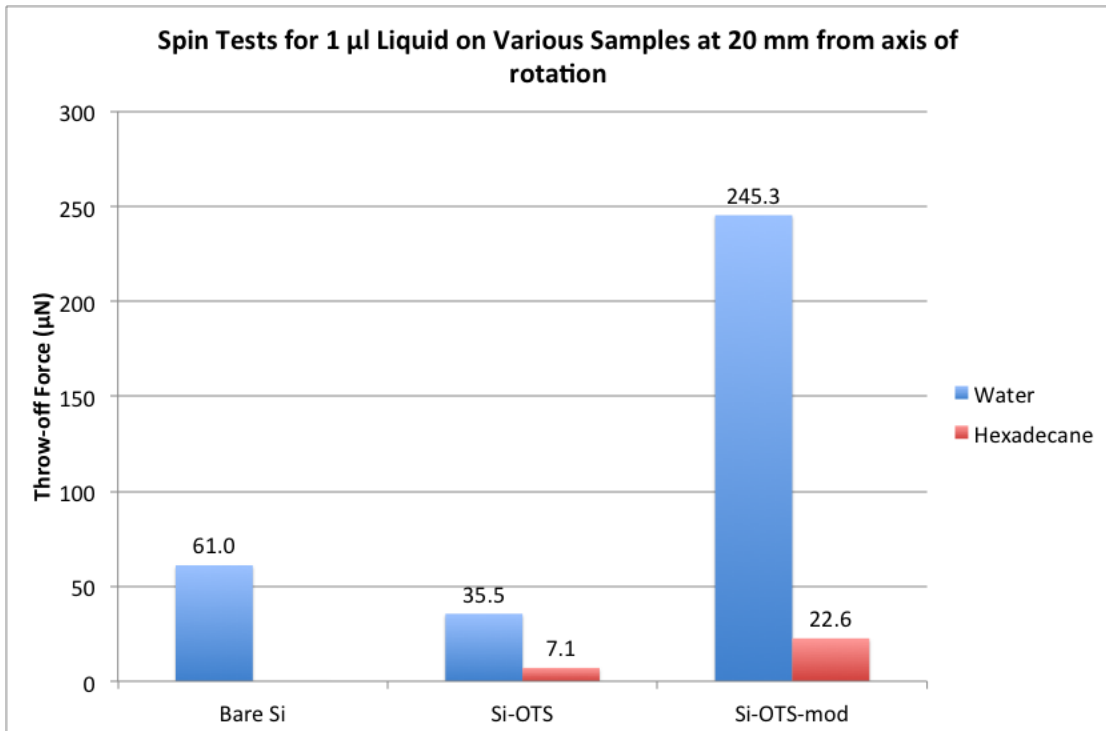


Figure 8-5: Throw-off forces for spin tests conducted on cleaned bare Si, Si coated with an OTS SAM (Si-OTS), and Si with selective OTS removal after coating (Si-OTS-mod). Hexadecane spread readily on bare, cleaned silicon and so no value could be obtained.

The results clearly show that the localised modification carried out on OTS-SAM coated surfaces by O<sub>2</sub> plasma treatment is effective in increasing the force required to move the lubricant from the location of application. These effects are clearly seen using water, and less prominently using hexadecane, as the repulsion between OTS and hexadecane is much less than that between OTS and water, as discussed earlier. However, the same trends are still evident.

Upon starting the spinning motion, water droplets on cleaned Si were observed to deviate from their original position slowly as the rotational speed reached the critical “throw-off” value. When tested with Si surfaces coated with an OTS SAM layer, droplet movement occurs at a much lower speed than that of cleaned Si, due to the low surface energies and non-wetting properties of the surface. In the case of Si coated with OTS SAM, the force required to overcome the initial resistance to movement was more than sufficient to move the droplet to the edge of the specimen, akin to a case in which the static friction of an object being pushed against a surface is much larger than that of the kinetic friction. The combination of the two effects explains the observed behaviour of the droplet being flung off the surface entirely as soon as any movement was detected.

Liquids are thus believed to be contained due to the step change in surface tension and surface energies on the selectively modified samples. The hydrophilic area attracts the droplet and prevents it from moving, while the surrounding hydrophobic areas repel the droplet and prevent it from wetting from the hydrophilic area. This successfully induces a mode of containment using surface modification.

Since SAMs such as OTS have been known to be applied on MEMS for reduction of friction and stiction, and PDMS moulds can be fabricated to form micro-channels, this method can in principle be further scaled down to provide containment

of lubricant at any particular location – either during application of the liquid or during sliding of components against each other – thereby preventing or delaying starvation of such contacts. This selective modification can also prevent lubricant from entering areas in which flooding would be detrimental to the functionality of the MEMS devices (e.g. comb drives), while keeping the relevant surfaces lubricated. Another potential use of such modified surfaces would be to hold a reservoir of lubricant at a separate location, for continual replenishment of lubricant upon depletion, by creating a channel to allow flow into the contact when required, without affecting the other device components.

### **8.3.3 Lubricant additives for non-spreading**

Spreading tests on bare silicon surfaces were carried out with a range of lubricants including additive-free hexadecane and solutions of DDA, ODA, MAC and squalane in hexadecane. In these, four main behaviours were observed by the various blends, corresponding to those mentioned by Cottington and co-workers (Cottington et al. 1964):

1. The droplet spreads normally,
2. The droplet initially spreads and then retracts towards its centre, reducing the surfaces area in contact between the droplet and the surface,
3. The droplet spreads initially, and then violently forms smaller droplets (or remains as a single droplet with a substantial contact angle) which moves rapidly away from the original location of the droplet and does not cross over any surface that it has previously flowed over,

4. The droplet remains non-spreading on the silicon surface, and exhibits a substantial contact angle.

Type 1 spreading was observed to occur only with neat hexadecane and relatively low concentrations of the additives compared to their saturation point. Only hexadecane with a 3 wt% MAC additive exhibited Type 4 behaviour, while all of the other blends exhibited either Type 2 or Type 3 behaviour. Extracted frames from a video of a blend that exhibited Type 3 spreading are shown in Figure 8-6, illustrating extensive movement of a single droplet over the surface as described. A summary of these results and the blends are presented in Table 8-2.

**Table 8-2: Categorization of the tested blends under the four types of spreading observed.**

<b>Type 1 (Normal)</b>	<b>Type 2 (Explosive)</b>	<b>Type 3 (Retraction)</b>	<b>Type 4 (Non-spreading)</b>
Neat hexadecane	Hex + 0.2wt% ODA	Hex + 0.1wt% ODA	Hex + 3.0wt% MAC
Hex + 0.1wt% DDA	High concentrations of amine additives	Hex + 0.5wt% DDA	
Hex + 0.2wt% DDA		Hex + 1.0wt% DDA	
Hex + 5wt% Squal			

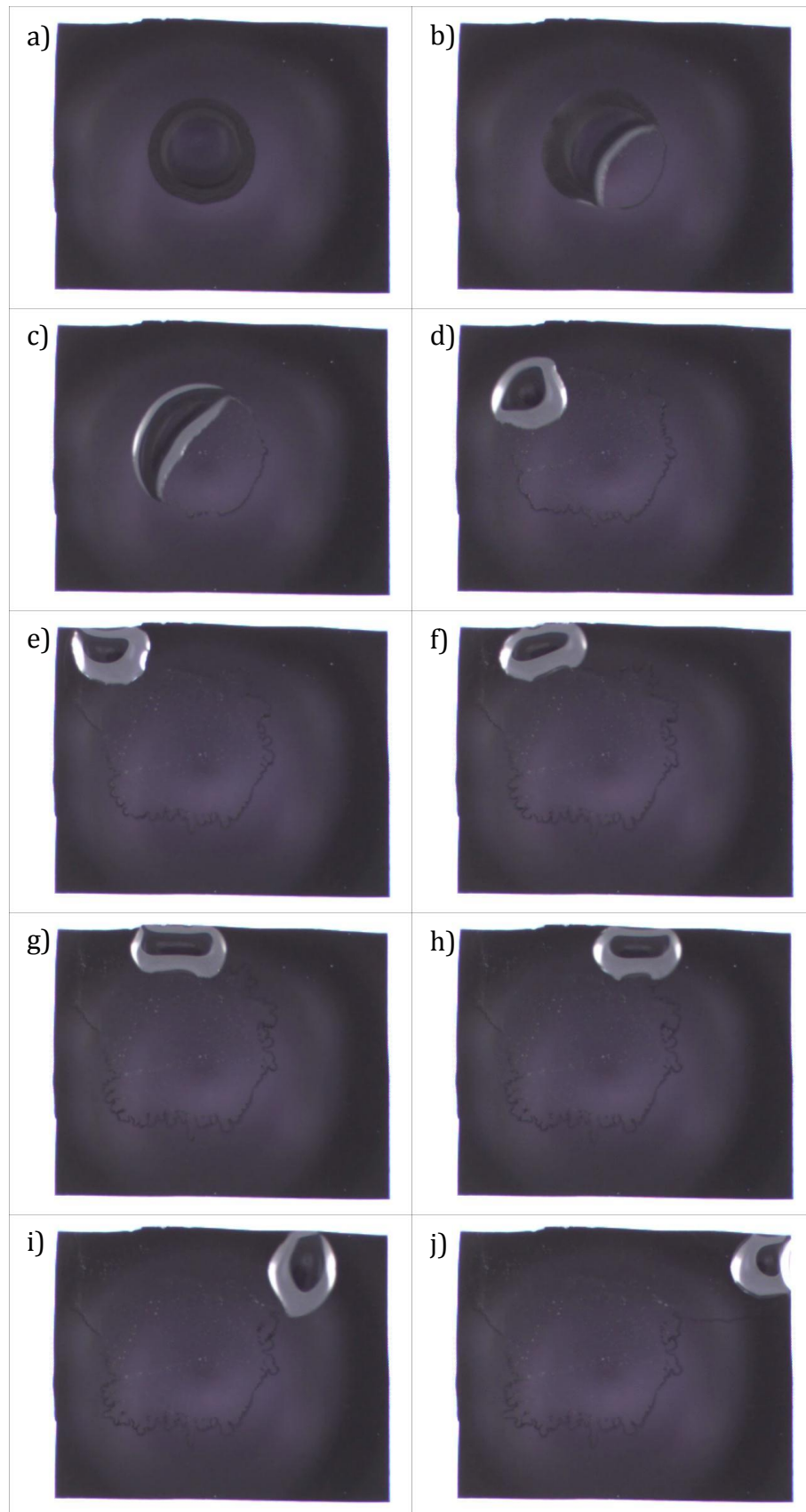


Figure 8-6: Frame captures from video taken at 30 fps of 0.2wt% ODA in hexadecane on a silicon surface, showing a) the droplet at application (frame 391), b) start of retraction at frame 511, c) frame 531, d) frame 541, e) frame 551, f) frame 561, g) frame 571, h) frame 581, i) frame 591, and j) frame 601. No further movement was observed after frame 601 as the droplet does not flow over areas twice.

Type 3 spreading behaviour can be explained with the formation of a film on the silicon surface, from the additives in the liquid, which modifies the surface properties of the silicon surface upon contact. This interaction between the surface and the additives has been mentioned as a factor in reducing boundary friction (Reddyhoff et al. 2011), but has not been investigated in terms of spreading. The movement of the droplet is caused by the difference in the surface tension between the trailing edge of the droplet and the advancing edge of the droplet; the film generated at the trailing edge of the drop has a lower surface tension than the surface at the advancing edge, thereby “pushing” the droplet. This mechanism also explains why droplets do not move further when meeting with a surface that they have already spread over, as the surface tension forces on either side would then be equal and no resultant force would occur. This same phenomenon is also described in the work conducted by Cottington and co-workers (Cottington et al. 1964), and the earlier section on surface modification uses a similar principle to induce containment of the liquids on the surface. Bigelow and co-workers (Bigelow et al. 1946) also provide a similar explanation for the phenomenon of sudden and rapid spreading at higher concentrations of additives. Although an oleophobic film is adsorbed on the silicon surface and the blend can thus be considered autophobic, the exact behaviour of the liquid observed is not favourable for application of lubricant at a specific location as random and rapid spreading occurs – it will be more suited for methods of pre-treatment. An example of a droplet retraction in the same location at which it has been applied (Type 2 behaviour) is shown in Figure 8-7.



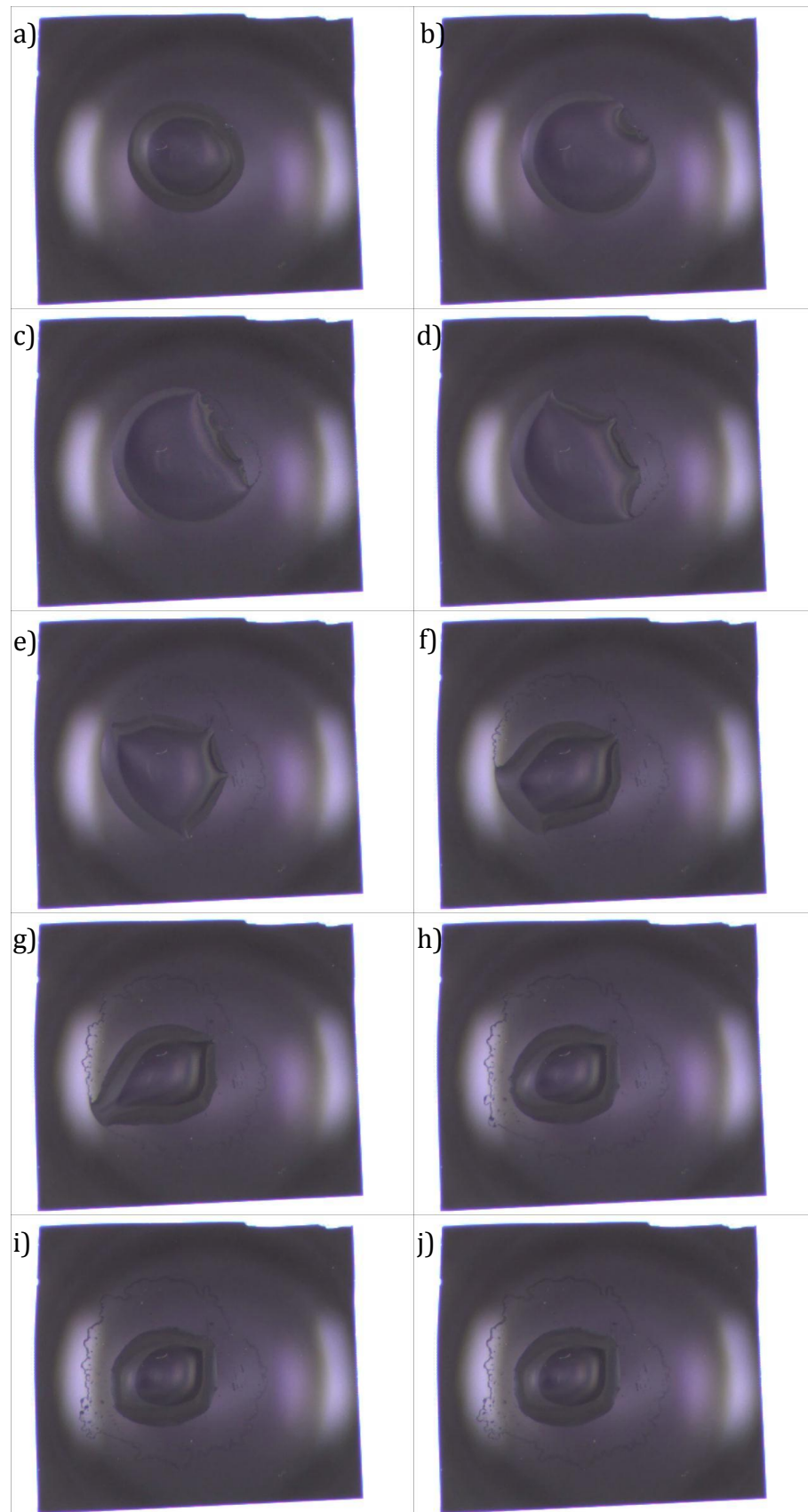
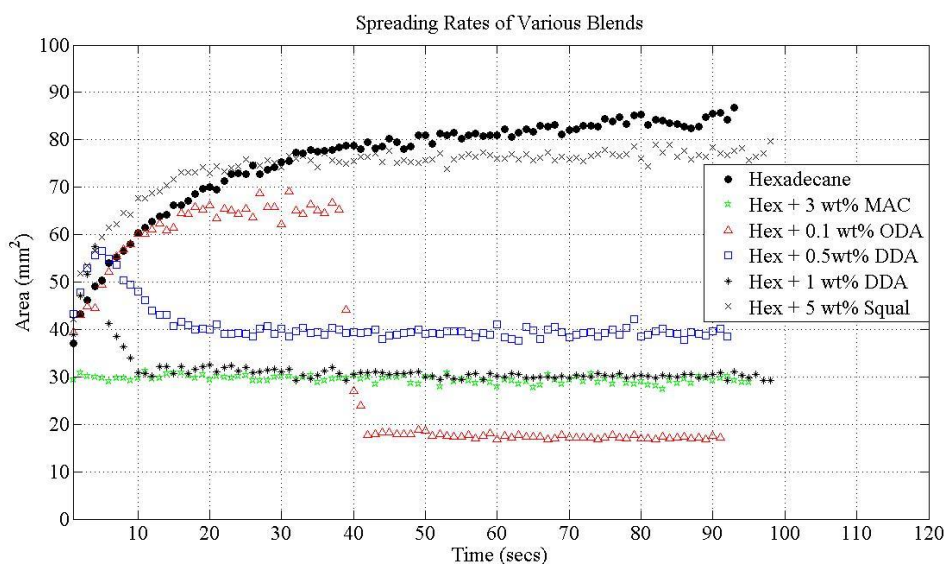
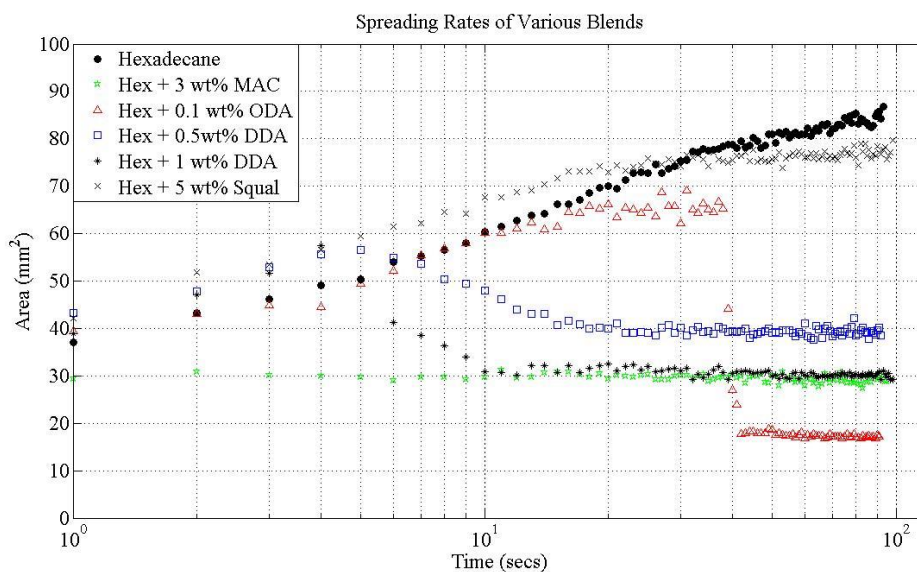


Figure 8-7: Frames from video taken at 30 fps of 1 wt% DDA in hexadecane on silicon, with a) droplet prior to retraction at frame 341, b) start of retraction at frame 441, c) continued retraction at frame 541, d) frame 641, e) frame 741, f) frame 841, g) frame 941, h) frame 1041, i) frame 1141, j) and approximate stabilization at frame 1241.

Due to the impracticality of such spreading behaviour, blends that exhibit Type 3, or “explosive”, behaviour (i.e. 0.2 wt% ODA in hexadecane) are excluded from consideration for practical application, and not presented in Figures 8-8 and 8-9, which show a summary of the spreading and/or retracting behaviour of the various blends. Lower concentrations that showed no change in spreading behaviour when compared to neat hexadecane are also excluded for brevity. A blend of hexadecane with 5 wt% squalane was also tested for viscosity comparison and will be elaborated shortly. Contact angles for the final conditions of the droplets are presented in Table 8-2.



**Figure 8-8: Plot of spreading area of the droplet vs. time for various blends of additives in hexadecane. 5  $\mu$ l of liquid was used in each blend application.**



**Figure 8-9: Plot of spreading area of the droplet vs. log(time) for various blends of additives in hexadecane. 5  $\mu$ l of liquid was used in each blend application.**

**Table 8-3: Contact angles of various blends on silicon after droplet retraction. 5  $\mu$ l of liquid was used in each blend application.**

Liquid blend used on Si surface	Contact angle of blend ( $^{\circ}$ )
Hexadecane + 3 wt% MAC	19.1
Hexadecane + 0.5 wt% DDA	7.00
Hexadecane + 1 wt% DDA	16.96
Hexadecane + 0.1 wt% ODA	30.60
Hexadecane + 0.2 wt% ODA	37.04

The graphs in Figures 8-8 and 8-9 were obtained by separating the frames of the video recordings (e.g. in Figures 8-6 and 8-7), and an image edge detection algorithm in MATLAB was used after image processing to detect the outline of the droplet on the surface, thereby relating the surface area (to a scale) of the liquid against the silicon surface. The effects of the various additives in the droplets behaviour are evident, especially in the cases of non-spreading droplets (3 wt% MAC additive), and retracting droplets (0.1 wt% ODA and 1 wt% DDA additives). All

blends except for the 3 wt% MAC were noted to have approximately the same behaviour at application, but with varying times and extents of retraction. The contact angles were also noted to be proportional to the surface area shown in Figures 8-8 and 8-9, as the same volume of liquid was used for each test.

The mechanism of retraction under Type 2 spreading is described in detail by Cottington and co-workers (Cottington et al. 1964), in which it is assumed that a “foot” or meniscus of oil turns outward at the base of the drop. In contrast to Cottington’s study, the adsorption of the additive in this case is quick and sufficient to make the critical surface tension of the surface less than that of the surface tension of the hexadecane blend, and cause the droplet to retract quickly and at its location on the wafer. If the adsorption is reasonably fast, immediate recession of the droplet would occur, having very little spreading. A slower adsorption rate would allow for more spreading to occur before retraction is observed. However, it is also possible that the adsorption of the additive is too slow to induce a retraction before most of the spreading has occurred. The random formation of the film results in a non-uniform film or lowers the critical surface tension of the surface insufficiently – in these cases, further spreading will occur at the drop margin onto areas where the film has not formed. The same principle, in a more extreme fashion, is responsible for the earlier described Type 3 spreading behaviour.

Bartell and co-workers, in studying the wetting of incomplete monomolecular layers (Bartell et al. 1956; Bartell et al. 1959), also noted that the variation of contact angles of hexadecane on both octadecylamine and dodecylamine films was largely affected by the completeness of the monolayer deposited on the surface. Their work also shows that the additives in hexadecane form a film on the solid surface, creating a consistent contact angle, as do Bigelow and co-workers (Bigelow et al. 1946). These

support the explanation that the additives in the liquid are responsible for film formation on the silicon surfaces, to an extent dependent on concentration. Failing such film formation, a lower contact angle and spreading will occur. A sharp drop in the contact angle was noted by Bartell and co-workers at about 50 % depletion of the adsorbed layer for ODA, and this agrees with other preliminary tests done with very low concentrations of 0.05 and 0.01 wt% of ODA which showed no reduction in spreading or retraction behaviour. It is likely that these low concentrations are insufficient to produce a consistent and complete film, so the defects in the film allow the blends to wet the surfaces. This effect of incomplete monolayers also accounts for the slightly lower contact angle observed in the blends investigated in this study (Table 8.2), as compared to other works (Bigelow et al. 1946; Bartell et al. 1956; Bartell et al. 1959). Bartell and co-workers, in particular, suggest that the lower surface area experienced after retraction is a combined result of the extent of the film completion and the difference in carbon chain length, the latter of which affects the extent of oleophobicity.

In the case of hexadecane with 3 wt% MAC as additive, no spreading at all was observed, even at the application of the droplet. Contact angles were conducted with hexadecane on silicon, comparing to that of the blend, and then neat hexadecane on MAC-coated silicon; these values are presented in Table 8-3.

**Table 8-4: Contact angles made when 1  $\mu$ l of test fluid is placed on bare and MAC-coated silicon wafers. Values were measured at 25 °C.**

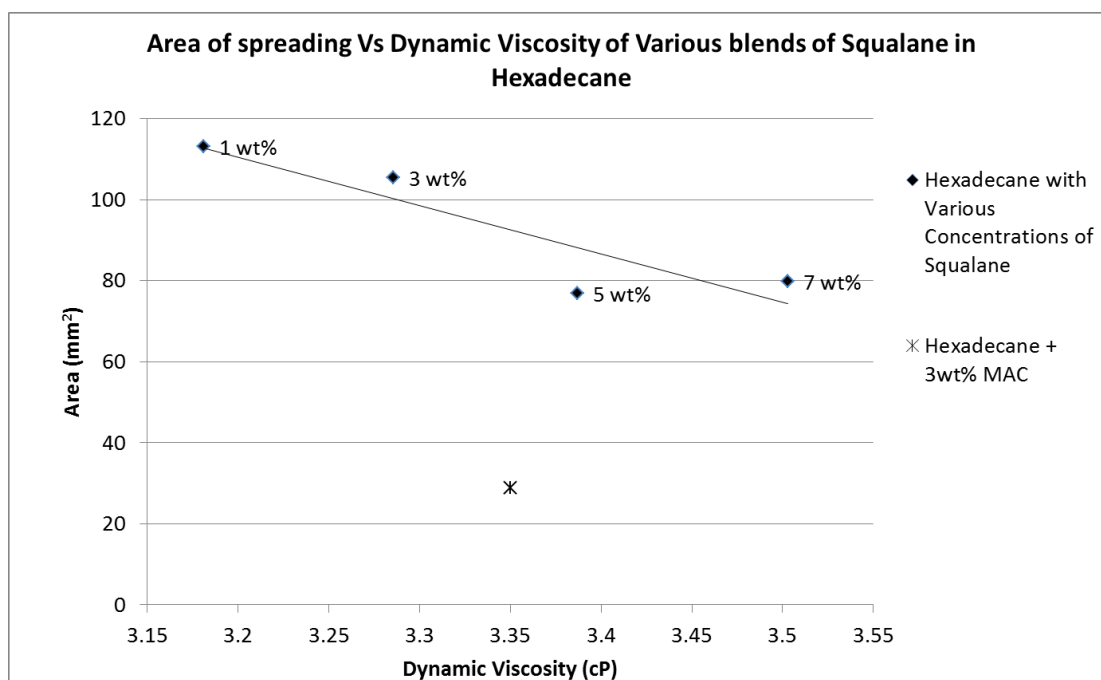
<b>Liquid</b>	<b>Surface</b>	<b>Contact angle (°)</b>
Hexadecane	Bare silica	~0
Blend of hexadecane + 3.0 wt% MAC	Bare silica	19.1
Hexadecane	MAC-coated silica	23.0

As contact angles are observed to be relatively high on MAC-coated silicon and the blend of hexadecane and MAC, this would imply that the non-spreading effect is due to the dewetting of the liquid on the surface. It should be noted that as MAC does not wet a silicon surface uniformly, a reduced concentration of 0.4 wt% MAC in n-hexane was used to form a film coating on the silicon surface prior to application of hexadecane and measuring of the contact angle. MAC is also known to induce a hydrophobic property on silicon surface (Wang et al. 2010b), which supports this conclusion.

In order to confirm that the non-spreading behaviour was only due to that of the additive and not an effect of the increased viscosity, spreading tests were also done with blends of various concentrations of squalane in hexadecane, compared to 3 wt% MAC in hexadecane. Squalane was used as it is a hydrocarbon molecule, similar to MAC and hexadecane, but does not have a dewetting effect like MAC. Dynamic viscosity measurements of 3 wt% MAC and various concentrations of squalane in hexadecane are shown in Table 8-4 and an approximate viscosity equivalent to 3 wt% MAC in hexadecane was obtained with 5 wt% squalane in hexadecane. The final stable surface areas of the blends are also plotted and presented in Figure 8-10.

**Table 8-5: Dynamic viscosities of 3wt% MAC in hexadecane and various concentrations of squalane in hexadecane.**

Blend Description	Dynamic Viscosity (cP)
Hexadecane + 3 wt% MAC	3.35
Hexadecane + 1 wt% squalane	3.18
Hexadecane + 3 wt% squalane	3.29
Hexadecane + 5 wt% squalane	3.38
Hexadecane + 7 wt% squalane	3.50

**Figure 8-10: Plot of stable spread area versus dynamic viscosity for various concentrations of squalane and 3wt% MAC in hexadecane. Blend with 3wt% MAC shows much lower spreading despite having viscosity comparable with the squalane blends.**

As can be seen, 3 wt% MAC in hexadecane spreads considerably less than the blends of squalane in hexadecane, even of squalane blends with higher viscosities than the 3 wt% MAC blend. This implies that the small amount of spreading observed in the 3 wt% MAC blend in hexadecane is due to effects other than the slightly increased viscosity, and suggests that the dewetting effect mentioned earlier is the

main factor. It is believed that the MAC blend forms a film on the silicon surface on which the blend itself is not able to spread and therefore stays as a consistent droplet. In light of this, it is concluded that the dewetting property of the MAC additive is primarily responsible for the non-spreading behaviour.

## **8.4 Discussion**

### **8.4.1 Differences between liquid behaviour in spin tests**

The observed “throw-off force” between different liquids were noted to be very different for the two liquids; water and hexadecane. This is due to a number of factors – firstly, the densities and the viscosities of the liquids are quite different, and these affect the intrinsic spreading and moving ability of the liquid. The second and more prominent factor is that the repulsion between the OTS SAM and the liquids are very different. OTS is known to be hydrophobic, producing a contact angle of  $> 90^\circ$  with water. However, the contact angle observed with hexadecane is only about  $40^\circ$  - this implies that OTS is not nominally oleophobic as the contact angle is less than  $90^\circ$ , but still induces non-wetting between the liquid and the surface, and is sufficient to note a difference when used for containment effects in our study. In short, the different levels of repulsion produce different levels of containment using the same selective modification process, when comparing different liquids.

It is possible to recreate the same containment strength for oils, using properly-made oleophobic surfaces achieved from various films or other fabrication processes (Bigelow et al. 1946; Zisman W 1964; Sagiv 1980; Juhue et al. 2003; Tuteja et al. 2007; Liu et al. 2010). In principle, the containment process and mechanism should still remain the same.



Despite limitations of the experimental setup and procedures, lubricant containment was observed on the modified surfaces due to the step in surface tensions and wettability of the surface at the modified/non-modified OTS-SAM junction.

#### **8.4.2 Practical use of additives for non-spreading liquids**

The study conducted in this Chapter differs from other referenced work in various aspects – here silicon is used as the substrate due to its common use in fabrication of MEMS, instead of stainless steel and other metals. Different liquids were also investigated, as the interaction between solids and liquids change between materials. Although both spreading and non-spreading behaviour was observed in this study as well as other referenced works, the modes and observations reported vary significantly. Comparisons were also made in this work between reduction of spreading/non-spreading behaviour induced by increase of viscosity and that induced by additives, as applications of liquid containment should be suitable for MEMS devices use.

There are competing factors in the successful use of such additives for anti-spreading – the strength of repulsion, the speed of film formation and the resilience of the adsorbed film to solvent attack. Surface film formation should ideally be fast, so as to prevent excessive spreading from occurring, if any. The film should also form uniformly, so as not to create a surface energy or surface tension gradient over the circumference of the droplet, thereby causing it to continuously move over the surface (i.e. Type 3 Spreading, as shown in Figure 8-6).

Although the concentration of the additive in the lubricants can be increased to strengthen the repulsion or retraction effect, practical uses of additives must be limited to small concentrations as mentioned earlier (Cottington et al. 1964) and are also limited by the solubility limit of the additive in the lubricant.

In view of this, it is suggested that 0.1 wt ODA or 1 wt% DDA would be an idea concentration for practical applications in anti-spreading of hydrocarbons on Si surfaces. Since both additives have also been studied for use in lubrication of micro-devices under different conditions and found to reduce boundary friction (Reddyhoff et al. 2011), these spreading methods are highly feasible for actual application and testing on MEMS devices.

## **8.5 Conclusion**

Various methods of lubrication of micro-machines have been investigated in previous research – the practical application of which all face a potential issue of starvation and depletion of adequate lubrication in contacts. Two methods of lubricant containment and anti-spreading are presented in this chapter – one by modifying the surface and another by modifying the liquid. Both methods have been found to successfully contain liquid lubricants on silicon surfaces. Both surface modification and the use of additives have also been applied in previous works on MEMS to reduce adhesion and friction between contacts, which suggests that extension of such procedures to control spreading may be feasible.

## **Chapter 9 - Conclusions and Future Work**

*This chapter summarizes the conclusions found from the work described above. It briefly describes the achievements and the successes of the Loc-Lub method of lubrication, and extends the feasibility of using liquid lubrication to lubricate MEMS by reducing hydrodynamic lubrication using additives and also containing the lubricant at specified locations.*

## **9.1 Conclusions**

### **9.1.1 “Localized Lubrication” Method**

The “Loc-Lub” method has been investigated initially on silicon wafers as a feasibility study, using both PFPE and MAC lubricants. The following conclusions can be drawn.

1. The “Loc-Lub” method shows more effective lubricant application than dip-coating and vapour deposition techniques, extending the wear life of tested silicon wafers by several magnitudes and reducing friction.
2. Due to the cohesive properties of MAC lubricant, wear is further reduced due to a persistent lubricant film of MAC lubricant, with silicon wafers under reciprocating wear testing in flat-on-flat contact geometry.
3. The “Localized Lubrication” method has been found to successfully lubricate the sidewalls of MEMS device components, lowering the static and kinetic friction values, as well as reducing adhesion between the components. Wear tests have also revealed a higher wear life than that of unlubricated specimens. This discovery has considerable potential for enabling new designs and applications of MEMS devices, as sidewalls can now be lubricated and made to slide against each other for a significant device lifetime.

### **9.1.2 Reduction of Hydrodynamic friction**

The effects of MAC and octadecylamine as friction modifier additives were investigated over a range of speeds using a custom-made MEMS tribometer, with the following main conclusions:

1. An optimum concentration of 3 wt% MAC in hexadecane shows a reduction in the hydrodynamic friction at high speeds, clearly visible in the Stribeck curves plotted.
2. Comparison with other liquids of similar composition and viscosity shows that the effect is not due to a viscosity change but due to surface effects of the additive. Further investigation suggests that it may result from liquid slip at the surfaces. This is supported by comparing the behaviour of squalane and by the dewetting effect of MACs on a silicon surface. The effect is akin to that of the “half wetted bearing” (Spikes 2003a; Spikes 2003b).
3. This behaviour has implications for liquid lubrication of MEMS devices involving smooth silicon surfaces sliding under low load since it may allow for the use of higher viscosity lubricants with lower volatility, while still retaining acceptably low hydrodynamic friction at high speeds.

### **9.1.3 Lubricant Containment**

The feasibility of using modifications to both surfaces and liquid lubricants to prevent spreading and induce containment of the lubricant at the location of application has been investigated. The following conclusions can be drawn from this work:

1. Silicon surfaces were modified by (i) using an OTS SAM layer to make them hydrophobic, followed by (ii) localised oxygen plasma treatment of the coating through a PDMS mask to create localised regions which are hydrophilic. Lubricant located at the treated, hydrophilic regions had higher “throw-off” force of a liquid droplet, compared to bare silicon or silicon uniformly coated with OTS SAM.

2. The same trends were noted for both water and hexadecane, although at different magnitudes, due to the different extents of hydrophobicity and oleophobicity of the surface.
3. An optimum concentration of additives can be used in hexadecane to induce autophobicity, causing the droplet to retract at the location of application.
4. Liquids can be made autophobic by dissolving amine surfactant additives in the liquid, causing the latter to dewet or have non-spreading properties on their own surface-adsorbed film. Depending on the behaviour, this may not always be practical for actual application of lubricant, but can be used as a pre-treatment prior to actual application.
5. Use of such amine additives have been previously investigated as friction modifier additives, and might therefore be feasible for actual MEMS applications.

## **9.2 Future work**

### **9.2.1 “Localized Lubrication” on MEMS devices**

The “Loc-Lub” method of lubricating silicon surfaces, MEMS devices and sidewalls has been proven to show extended wear/device life and reduce friction and adhesion. To perfect the technique, a few considerations of some further development should be carried out;

1. Use of the “Loc-Lub” method in other rubbing conditions, such as ball-on-disc or pin-on-disc conditions, to simulate various forms of practical rubbing contact.

2. Investigation of other lubricants for use with the method, and the compatibility of the lubricating mechanisms. A comparison of optimal lubricant properties for material surfaces would also be beneficial as various materials are now being used for MEMS devices (e.g. SU-8 and other polymers) in addition to silicon.

### **9.2.2 Hydrodynamic friction reduction in MEMS**

The use of MAC as an additive was found to reduce hydrodynamic friction in high speed sliding MEMS. This was attributed to a slip at the silicon surface, thereby changing the factors involved in the friction observed, as illustrated in the “half-wetted bearing” effect. Further work that could be carried out are as follows:

1. The extent and effect of slip on the surface could be investigated using fluorescence or other methods.
2. Other methods of inducing slip at the silicon surface could be investigated, such as coatings on the silicon devices or other forms of additives that are soluble in such liquids.
3. The impact of roughening of one of the pair of silicon surfaces, to inhibit slip at this surface but not at the other surface, should be investigated.

### **9.2.3 Anti-spreading methods and lubricant containment**

The use of additives and surface modification was shown to successfully prevent spreading of lubricants, inducing autophobicity, and increasing the amount of force required to move a droplet off a surface. To perfect the method, further developments should be investigated:

1. The use of actual oleophobic surfaces (with contact angles of more than  $90^\circ$  for hexadecane or other oils) should be tested with the selective modification principle, particularly with surface texturing effects. Other surface modifications can also be investigated.
2. Film formation mechanism can be investigated, as well as the chemical and physical bonding strength between the film and the surfaces. Film properties can also be investigated.
3. Tribological testing of these contained areas can be carried out and compared to non-contained surfaces, to see if wear lives and friction properties are improved after the treatment or additives are included.



## References

- Abdul Samad, M., Satyanarayana, N. and Sinha, S. K. (2010). "Tribology of UHMWPE film on air-plasma treated tool steel and the effect of PFPE overcoat." Surface and Coatings Technology **204** (9-10): 1330-1338.
- Ansari, N. and Ashurst, W. R. (2012). "Single-crystal-silicon-based microinstrument to study friction and wear at MEMS sidewall interfaces." Journal of Micromechanics and Microengineering **22** (2): 025008.
- Asay, D., Dugger, M. and Kim, S. (2008). "In-situ Vapor-Phase Lubrication of MEMS." Tribology Letters **29** (1): 67-74.
- Asay, D. B., Dugger, M. T., Ohlhausen, J. A. and Kim, S. H. (2007). "Macro- to Nanoscale Wear Prevention via Molecular Adsorption." Langmuir **24** (1): 155-159.
- Ashurst, W. R. (2003). Surface Engineering for MEMS reliability. Berkeley, CA, University of California. **Ph.D. Dissertation.**
- Ashurst, W. R., Carraro, C. and Maboudian, R. (2003a). "Vapor phase anti-stiction coatings for MEMS." IEEE Transactions on Device and Materials Reliability **3** (4): 173-178.
- Ashurst, W. R., de Boer, M. P., Carraro, C. and Maboudian, R. (2003b). "An investigation of sidewall adhesion in MEMS." Applied Surface Science **212-213**: 735-741.
- Ata, A., Rabinovich, Y. I. and Singh, R. K. (2002). "Role of surface roughness in capillary adhesion." Journal of Adhesion Science and Technology **16** (4): 337-346.

- Bartell, L. S. and Ruch, R. J. (1956). "The Wetting of Incomplete Monomolecular Layers." The Journal of Physical Chemistry **60** (9): 1231-1234.
- Bartell, L. S. and Ruch, R. J. (1959). "The Wetting of Incomplete Monomolecular Layers. II. Correlation with Molecular Size and Shape." The Journal of Physical Chemistry **63** (7): 1045-1049.
- Benítez, J. J., Kopta, S., Díez-Pérez, I., Sanz, F., Ogletree, D. F. and Salmeron, M. (2002a). "Molecular Packing Changes of Octadecylamine Monolayers on Mica Induced by Pressure and Humidity." Langmuir **19** (3): 762-765.
- Benítez, J. J., Kopta, S., Ogletree, D. F. and Salmeron, M. (2002b). "Preparation and Characterization of Self-Assembled Monolayers of Octadecylamine on Mica Using Hydrophobic Solvents." Langmuir **18** (16): 6096-6100.
- Bernett, M. K. and Zisman, W. A. (1964). Prevention of Liquid Spreading or Creeping. Contact Angle, Wettability, and Adhesion AMERICAN CHEMICAL SOCIETY. **43**: 332-340.
- Bhushan, B. (1990). "Tribology and Mechanics of Magnetic Storage Devices." Springer-Verlag, New York.
- Bhushan, B. (2007). Nanotribology and Materials Characterization of MEMS/NEMS and BioMEMS/BioNEMS Materials and Devices. Springer Handbook of Nanotechnology. Bhushan, B., Springer Berlin Heidelberg: 1575-1638.
- Bhushan, B., Israelachvili, J. N. and Landman, U. (1995). "Nanotribology: friction, wear and lubrication at the atomic scale." Nature **374** (6523): 607-616.
- Bhushan, B., Palacio, M. and Kinzig, B. (2008). "AFM-based nanotribological and electrical characterization of ultrathin wear-resistant ionic liquid films." Journal of Colloid and Interface Science **317** (1): 275-287.

- Biebuyck, H. A. and Whitesides, G. M. (1994). "Autophobic Pinning of Drops of Alkanethiols on Gold." Langmuir **10** (12): 4581-4587.
- Bigelow, W. C., Pickett, D. L. and Zisman, W. A. (1946). "Oleophobic monolayers : I. Films adsorbed from solution in non-polar liquids." Journal of Colloid Science **1** (6): 513-538.
- Bulkley, R. and Snyder, G. H. S. (1933). "Spreading of Liquids on Solid Surfaces. The Anomalous Behavior of Fatty Oils and Fatty Acids with Experiments Leading to a Tentative Explanation." Journal of the American Chemical Society **55** (1): 194-208.
- Butt, H.-J. and Kappl, M. (2009). "Normal capillary forces." Advances in Colloid and Interface Science **146** (1-2): 48-60.
- Buttafava, P., Bretti, V., Ciardiello, G., Piano, M., Caporiccio, G. and Scarati, A. (1985). "Lubrication and wear problems of perpendicular recording thin film flexible media." Magnetics, IEEE Transactions on **21** (5): 1533-1535.
- Cabuz, C., Cabuz, E. I., Ohnstein, T. R., Neus, J. and Maboudian, R. (2000). "Factors enhancing the reliability of touch-mode electrostatic actuators." Sensors and Actuators A: Physical **79** (3): 245-250.
- Cassie, A. B. D. and Baxter, S. (1944). "Wettability of porous surfaces." Transactions of the Faraday Society **40**: 546-551.
- Chau, K. H. L. and Sulouff, R. E. (1998). "Technology for the high-volume manufacturing of integrated surface-micromachined accelerometer products." Microelectronics Journal (Incorporating Journal of Semicustom ICs) **29** (9): 579-586.
- Chen, C.-Y., Bogy, D. and Bhatia, C. S. (2001). "Effect of lubricant bonding fraction at the head-disk interface." Tribology Letters **10** (4): 195-201.

- Choo, J.-H., Forrest, A. and Spikes, H. (2007a). "Influence of Organic Friction Modifier on Liquid Slip: A New Mechanism of Organic Friction Modifier Action." Tribology Letters **27** (2): 239-244.
- Choo, J. H., Glovnea, R. P., Forrest, A. K. and Spikes, H. A. (2007b). "A Low Friction Bearing Based on Liquid Slip at the Wall." Journal of Tribology **129** (3): 611-620.
- Chun, S. W., Talke, F. E., Kang, H. J. and Kim, W. K. (2003). "Thermal Characteristics of Multiply Alkylated Cyclopentane and Perfluoropolyether." Tribology Transactions **46** (1): 70 - 75.
- Cottingham, R. L., Murphy, C. M. and Singleterry, C. R. (1964). Effect of Polar-Nonpolar Additives on Oil Spreading on Solids, with Applications to Nonspreading Oils. Contact Angle, Wettability, and Adhesion AMERICAN CHEMICAL SOCIETY. **43**: 341-354.
- Deng, K., Collins, R. J., Mehregany, M. and Sukenik, C. N. (1995). "Performance Impact of Monolayer Coating of Polysilicon Micromotors." Journal of The Electrochemical Society **142** (4): 1278-1285.
- Doms, M., Feindt, H., Kuipers, W. J., Shewtanasoontorn, D., Matar, A. S., Brinkhues, S., Welton, R. H. and Mueller, J. (2008). "Hydrophobic coatings for MEMS applications." Journal of Micromechanics and Microengineering **18** (5): 055030.
- Dube, M. J., Bollea, D., Jones, W. R., Marchetti, M. and Jansen, M. J. (2003). "A New Synthetic Hydrocarbon Liquid Lubricant for Space Applications." Tribology Letters **15** (1): 3-8.

- Eapen, K., Patton, S. and Zabinski, J. (2002). "Lubrication of Microelectromechanical Systems (MEMS) Using Bound and Mobile Phases of Fomblin Zdol®." Tribology Letters **12** (1): 35-41.
- Eaton, W. P. and Smith, J. H. (1997). "Micromachined pressure sensors: review and recent developments." Smart Materials and Structures **6** (5): 530.
- Frédéric, R., Lydéric, B., Thierry, B. and Élisabeth, C. (2000). "Thermally activated dynamics of capillary condensation." Journal of Physics: Condensed Matter **12** (8A): A419.
- Gao, C., Lee, Y. C., Chao, J. and Russak, M. (1995). "Dip-coating of ultra-thin liquid lubricant and its control for thin-film magnetic hard disks." Magnetics, IEEE Transactions on **31** (6): 2982-2984.
- Girbau, D., Pradell, L., Lazaro, A. and Nebot, A. (2007). "Electrothermally Actuated RF MEMS Switches Suspended on a Low-Resistivity Substrate." Journal of Microelectromechanical Systems **16** (5): 1061-1070.
- Guangya, Z. and Fook Siong, C. (2006). "Micromachined Vibratory Diffraction Grating Scanner for Multiwavelength Collinear Laser Scanning." Journal of Microelectromechanical Systems **15** (6): 1777-1788.
- Guangya, Z., Logeeswaran, V. J., Fook Siong, C. and Tay, F. E. H. (2004). "Micromachined in-plane vibrating diffraction grating laser scanner." Photonics Technology Letters, IEEE **16** (10): 2293-2295.
- Guckel, H., Sniegowski, J. J., Christenson, T. R., Mohny, S. and Kelly, T. F. (1989). "Fabrication of micromechanical devices from polysilicon films with smooth surfaces." Sensors and Actuators **20** (1-2): 117-122.
- Hare, E. F. and Zisman, W. A. (1955). "Autophobic Liquids and the Properties of their Adsorbed Films." The Journal of Physical Chemistry **59** (4): 335-340.

- Helmick, L., Liang, J. and Ream, B. (1998). "The decomposition reaction path of a linear PFPAE under tribological conditions." Tribology Letters **4** (3): 287-292.
- Hongbin, Y., Guangya, Z., Sinha, S. K., Leong, J. Y. and Fook Siong, C. (2011). "Characterization and Reduction of MEMS Sidewall Friction Using Novel Microtribometer and Localized Lubrication Method." Journal of Microelectromechanical Systems **20** (4): 991-1000.
- Hurst, K. M. (2010). "Nanoparticle-Based Surface Modifications for Microtribology Control and Superhydrophobicity." Dissertation, Auburn University.
- Jones, W. R., Poslowski, A. K., Shogrin, B. A., Herrera-Fierro, P. and Jansen, M. J. (1999). "Evaluation of Several Space Lubricants Using a Vacuum Four-Ball Tribometer." Tribology Transactions **42** (2): 317 - 323.
- Juhue, D., Pabon, M., N'Zudie, D. T., Corpart, J.-M. and Lina, M.-J. (2003). Fluorocopolymers for the hydrophobic and oleophobic treatment of various substrates. U.S. , E. I. du Pont de Nemours and Company.
- Katano, T., Oka, M., Nakazawa, S., Aramaki, T. and Kusakawa, K. (2003). "Characteristics of dual lubricant layers." Magnetics, IEEE Transactions on **39** (5): 2489-2491.
- Keren, D., Ramanathan, G. P. and Mehregany, M. (1994). "Micromotor dynamics in lubricating fluids." Journal of Micromechanics and Microengineering **4** (4): 266.
- Kim, H., Jang, C., Kim, D., Kim, Y., Choa, S. and Hong, S. (2009). "Effects of Self-Assembled Monolayer and PFPE Lubricant on Wear Characteristics of Flat Silicon Tips." Tribology Letters **34** (1): 61-73.

- Kim, S. H., Asay, D. B. and Dugger, M. T. (2007). "Nanotribology and MEMS." Nano Today **2** (5): 22-29.
- Koinkar, V. N. and Bhushan, B. (1996). "Microtribological studies of unlubricated and lubricated surfaces using atomic force/friction force microscopy." Journal of Vacuum Science & Technology A: Vacuum, Surfaces, and Films **14** (4): 2378-2391.
- Komvopoulos, K. (1996). "Surface engineering and microtribology for microelectromechanical systems." Wear **200** (1-2): 305-327.
- Krupka, I., Poliscuk, R. and Hartl, M. (2009). "Behavior of thin viscous boundary films in lubricated contacts between micro-textured surfaces." Tribology International **42** (4): 535-541.
- Ku, I. S. Y., Reddyhoff, T., Choo, J. H., Holmes, A. S. and Spikes, H. A. (2010). "A novel tribometer for the measurement of friction in MEMS." Tribology International **43** (5-6): 1087-1090.
- Ku, I. S. Y., Reddyhoff, T., Holmes, A. S. and Spikes, H. A. (2011). "Wear of silicon surfaces in MEMS." Wear **271** (7-8): 1050-1058.
- Ku, I. S. Y., Reddyhoff, T., Wayte, R., Choo, J. H., Holmes, A. S. and Spikes, H. A. (2012). "Lubrication of Microelectromechanical Devices Using Liquids of Different Viscosities." Journal of Tribology **134** (1): 012002-012007.
- Lacroix, L.-M., Lejeune, M., Ceriotti, L., Kormunda, M., Meziani, T., Colpo, P. and Rossi, F. (2005). "Tuneable rough surfaces: A new approach for elaboration of superhydrophobic films." Surface Science **592** (1-3): 182-188.
- Legtenberg, R., Tilmans, H. A. C., Elders, J. and Elwenspoek, M. (1994). "Stiction of surface micromachined structures after rinsing and drying: model and

- investigation of adhesion mechanisms." Sensors and Actuators A: Physical **43** (1-3): 230-238.
- Lei, R. Z., Gellman, A. J. and Jones, P. (2001). "Thermal Stability of Fomblin Z and Fomblin Zdol Thin Films on Amorphous Hydrogenated Carbon." Tribology Letters **11** (1): 1-5.
- Li, N., Meng, Y. and Bogy, D. (2011). "Effects of PFPE Lubricant Properties on the Critical Clearance and Rate of the Lubricant Transfer from Disk Surface to Slider." Tribology Letters: 1-12.
- Lin, M.-H., Chen, C.-F., Shiu, H.-W., Chen, C.-H. and Gwo, S. (2009). "Multilength-Scale Chemical Patterning of Self-Assembled Monolayers by Spatially Controlled Plasma Exposure: Nanometer to Centimeter Range." Journal of the American Chemical Society **131** (31): 10984-10991.
- Liu, H. and Bhushan, B. (2003). "Nanotribological characterization of molecularly thick lubricant films for applications to MEMS/NEMS by AFM." Ultramicroscopy **97** (1-4): 321-340.
- Liu, Y., Xiu, Y., Hess, D. W. and Wong, C. P. (2010). "Silicon Surface Structure-Controlled Oleophobicity." Langmuir **26** (11): 8908-8913.
- Loy, X. Z. K. and Sinha, S. K. (2012). "Lubrication of polyether ether ketone (PEEK) surface by liquid ultrathin films for high wear durability." Wear **296** (1-2): 681-692.
- Ma, J., Liu, J., Mo, Y. and Bai, M. (2007). "Effect of multiply-alkylated cyclopentane (MAC) on durability and load-carrying capacity of self-assembled monolayers on silicon wafer " Colloids and Surfaces A: Physicochemical and Engineering Aspects **301** (1-3): 481-489.



- Maboudian, R., Ashurst, W. R. and Carraro, C. (2000). "Self-assembled monolayers as anti-stiction coatings for MEMS: characteristics and recent developments." Sensors and Actuators A: Physical **82** (1-3): 219-223.
- Maboudian, R., Ashurst, W. R. and Carraro, C. (2002). "Tribological Challenges in Micromechanical Systems." Tribology Letters **12** (2): 95-100.
- Madou, M. (1997). Fundamentals of Microfabrication. CRC Press.
- Marchetto, D., Rota, A., Calabri, L., Gazzadi, G. C., Menozzi, C. and Valeri, S. (2010). "Hydrophobic effect of surface patterning on Si surface." Wear **268** (3-4): 488-492.
- Mastrangelo, C. H. and Hsu, C. H. (1993). "Mechanical stability and adhesion of microstructures under capillary forces. I. Basic theory." Journal of Microelectromechanical Systems **2** (1): 33-43.
- Mate, C. M. (2007). "Tribology on the Small Scale - A Bottom Up Approach To Friction, Lubrication and Wear." Oxford: Oxford University Press.
- Mehregany, M. and Dhuler, V. R. (1992). "Operation of electrostatic micromotors in liquid environments." Journal of Micromechanics and Microengineering **2** (1): 1.
- Myo, M., Jonathan, L. Y. and Sinha, S. K. (2008). "Effects of interfacial energy modifications on the tribology of UHMWPE coated Si." Journal of Physics D: Applied Physics **41** (5): 055307.
- Nainaparampil, J. J., Eapen, K. C., Sanders, J. H. and Voevodin, A. A. (2007). "Ionic-Liquid Lubrication of Sliding MEMS Contacts: Comparison of AFM Liquid Cell and Device-Level Tests." Microelectromechanical Systems, Journal of **16** (4): 836-843.

- Nainaparampil, J. J., Phillips, B. S., Eapen, K. C. and Zabinski, J. S. (2005). "Micro-nano behaviour of DMBI-PF 6 ionic liquid nanocrystals: large and small-scale interfaces." Nanotechnology **16** (11): 2474.
- Nakayama, K. and Mirza, S. M. (2006). "Verification of the Decomposition of Perfluoropolyether Fluid Due to Tribomicroplasma." Tribology Transactions **49** (1): 17 - 25.
- Noel, O., Mazeran, P.-E. and Nasrallah, H. (2012). "Sliding Velocity Dependence of Adhesion in a Nanometer-Sized Contact." Physical Review Letters **108** (1): 015503.
- Novotny, V. J. and Marmur, A. (1991). "Wetting autophobicity." Journal of Colloid and Interface Science **145** (2): 355-361.
- Ohno, N., Mia, S., Morita, S. and Obara, S. (2010). "Friction and Wear Characteristics of Advanced Space Lubricants." Tribology Transactions **53** (2): 249 - 255.
- Palacio, M. and Bhushan, B. (2008). "Ultrathin Wear-Resistant Ionic Liquid Films for Novel MEMS/NEMS Applications." Advanced Materials **20** (6): 1194-1198.
- Patton, S. T., Eapen, K. C. and Zabinski, J. S. (2001). "Effects of adsorbed water and sample aging in air on the  $\mu$  N level adhesion force between Si(100) and silicon nitride." Tribology International **34** (7): 481-491.
- Patton, S. T. and Zabinski, J. S. (2002). "Failure mechanisms of a MEMS actuator in very high vacuum." Tribology International **35** (6): 373-379.
- Pepper, S. V. and Kingsbury, E. P. (2003a). "Spiral Orbit Tribometry - Part I: Description of the Tribometer." Tribology Transactions **46** (1): 57-64.

- Pepper, S. V. and Kingsbury, E. P. (2003b). "Spiral Orbit Tribometry - Part II: Evaluation of Three Liquid Lubricants in Vacuum." Tribology Transactions **46** (1): 65-69.
- Peterangelo, S. C., Gschwender, L., Snyder, C. E., Jones, W. R., Nguyen, Q. and Jansen, M. J. (2008). "Improved additives for multiply alkylated cyclopentane-based lubricants." Journal of Synthetic Lubrication **25** (1): 31-41.
- Pit, R., Hervet, H. and Léger, L. (2000). "Direct Experimental Evidence of Slip in Hexadecane: Solid Interfaces." Physical Review Letters **85** (5): 980-983.
- Potter, C. N. (2005). Hermetic MEMS Package and Method of Manufacture. U.S. Patent No. 7,358,106 B2. Austin, TX, Stellar MicroDevices, Inc., Austin, TX.
- Reddyhoff, T., Ku, I., Holmes, A. and Spikes, H. (2011). "Friction Modifier Behaviour in Lubricated MEMS Devices." Tribology Letters **41** (1): 239-246.
- Rymuza, Z. (1999). "Control tribological and mechanical properties of MEMS surfaces. Part 1: critical review." Microsystem Technologies **5** (4): 173-180.
- Sagiv, J. (1980). "Organized monolayers by adsorption. 1. Formation and structure of oleophobic mixed monolayers on solid surfaces." Journal of the American Chemical Society **102** (1): 92-98.
- Satyanarayana, N. and Sinha, S. K. (2005). "Tribology of PFPE overcoated self-assembled monolayers deposited on Si surface." Journal of Physics D: Applied Physics **38** (18): 3512.
- Satyanarayana, N., Sinha, S. K. and Ong, B. H. (2006). "Tribology of a novel UHMWPE/PFPE dual-film coated onto Si surface." Sensors and Actuators A: Physical **128** (1): 98-108.

- Senft, D. C. and Dugger, M. T. (1997). "Friction and wear in surface-micromachined tribological test devices." 31-38.
- Singh, R. A., Satyanarayana, N. and Sinha, S. K. (2011). "Surface chemical modification for exceptional wear life of MEMS materials." AIP Advances **1** (4): 042141-042148.
- Sinha, S. K., Jonathan, L. Y., Satyanarayana, N., Yu, H., Harikumar, V. and Zhou, G. (2010). "Method of applying a lubricant to a micromechanical device." U.S. Provisional Patent, 61/314,627.
- Sinha, S. K., Kawaguchi, M., Kato, T. and Kennedy, F. E. (2003). "Wear durability studies of ultra-thin perfluoropolyether lubricant on magnetic hard disks." Tribology International **36** (4-6): 217-225.
- Smallwood, S. A., Eapen, K. C., Patton, S. T. and Zabinski, J. S. (2006). "Performance results of MEMS coated with a conformal DLC." Wear **260** (11-12): 1179-1189.
- Smeeth, M., Spikes, H. and Gungel, S. (1996). "Boundary Film Formation by Viscosity Index Improvers." Tribology Transactions **39** (3): 726-734.
- Spengen, W. M. and Frenken, J. M. (2007). "The Leiden MEMS Tribometer: Real Time Dynamic Friction Loop Measurements With an On-Chip Tribometer." Tribology Letters **28** (2): 149-156.
- Spikes, H. A. (2003a). "The half-wetted bearing. Part 1: Extended Reynolds equation." Proceedings of the Institution of Mechanical Engineers, Part J: Journal of Engineering Tribology **217** (1): 1-14.
- Spikes, H. A. (2003b). "The half-wetted bearing. Part 2: Potential application in low load contacts." Proceedings of the Institution of Mechanical Engineers, Part J: Journal of Engineering Tribology **217** (1): 15-26.

- Srinivasan, U., Foster, J. D., Habib, U., Howe, R. T., Maboudian, R., Senft, D. C. and Dugger, M. T. (1998a). Lubrication of polysilicon micromechanisms with self-assembled monolayers. Conference: 1998 solid state sensor and actuator workshop, Hilton Head, SC (United States), 1 Jun 1998
- Srinivasan, U., Houston, M. R., Howe, R. T. and Maboudian, R. (1998b). "Alkyltrichlorosilane-based self-assembled monolayer films for stiction reduction in silicon micromachines." Journal of Microelectromechanical Systems **7** (2): 252-260.
- Srinivasan, U., Houston, M. R., Rowe, R. T. and Maboudian, R. (1997). Self-assembled fluorocarbon films for enhanced stiction reduction. Solid State Sensors and Actuators, 1997. TRANSDUCERS '97 Chicago., 1997 International Conference on.
- Streator, J. L., Bhushan, B. and Bogy, D. B. (1991). "Lubricant Performance in Magnetic Thin Film Disks With Carbon Overcoat - Part I: Dynamic and Static Friction." Journal of Tribology **113** (1): 22-31.
- Syms, R. R. A., Zou, H., Stagg, J. and Veladi, H. (2004). "Sliding-blade MEMS iris and variable optical attenuator." Journal of Micromechanics and Microengineering **14** (12): 1700.
- Tagawa, M., Ikemura, M., Nakayama, Y. and Ohmae, N. (2004). "Effect of Water Adsorption on Microtribological Properties of Hydrogenated Diamond-Like Carbon Films." Tribology Letters **17** (3): 575-580.
- Talke, F. E. (2000). An overview of current tribology problems in magnetic disk recording rechnology. Tribology and Interface Engineering Series. Dowson, D., Priest, M., Taylor, C. M., Ehret, P., Childs, T. H. C., Dalmaz, G.,

- Lubrecht, A. A., Berthier, Y., Flamand, L. and Georges, J. M., Elsevier.  
**Volume 38:** 15-24.
- Tan, A. H. and Wei Cheng, S. (2006). "A novel textured design for hard disk tribology improvement." Tribology International **39** (6): 506-511.
- Tani, H. and Matsumoto, H. (2001). "Spreading Mechanism of PFPE Lubricant on the Magnetic Disks." Journal of Tribology **123** (3): 533-540.
- Tanner, D. M. (2000). Reliability of surface micromachined MicroElectroMechanical actuators. Microelectronics, 2000. Proceedings. 2000 22nd International Conference on.
- Tanner, D. M., Miller, W. M., Peterson, K. A., Dugger, M. T., Eaton, W. P., Irwin, L. W., Senft, D. C., Smith, N. F., Tangyunyong, P. and Miller, S. L. (1999). "Frequency dependence of the lifetime of a surface micromachined microengine driving a load." Microelectronics Reliability **39** (3): 401-414.
- Tas, N. R., Gui, C. and Elwenspoek, M. (2003). "Static friction in elastic adhesion contacts in MEMS." Journal of Adhesion Science and Technology **17** (4): 547-561.
- Tay, N., Minn, M. and Sinha, S. (2011). "A Tribological Study of SU-8 Micro-Dot Patterns Printed on Si Surface in a Flat-on-Flat Reciprocating Sliding Test." Tribology Letters **44** (2): 167-176.
- Timmons, C. O. and Zisman, W. A. (1964). "A Study of Autophobic Liquids on Platinum by the Contact Potential Method." The Journal of Physical Chemistry **68** (6): 1336-1342.
- Timpe, S. J., Alsem, D. H., Hook, D. A., Dugger, M. T. and Komvopoulos, K. (2009). "Wear of Polysilicon Surface Micromachines Operated in High Vacuum." Journal of Microelectromechanical Systems **18** (2): 229-238.

- Timpe, S. J. and Komvopoulos, K. (2007). "Microdevice for measuring friction and adhesion properties of sidewall contact interfaces of microelectromechanical systems." Review of Scientific Instruments **78** (6): 065106-065109.
- Tuteja, A., Choi, W., Ma, M., Mabry, J. M., Mazzella, S. A., Rutledge, G. C., McKinley, G. H. and Cohen, R. E. (2007). "Designing Superoleophobic Surfaces." Science **318** (5856): 1618-1622.
- Ulman, A. (1991). Introduction to Thin Organic Films. San Diego, CA, Academic.
- Venier, C. G. and Casserly, E. W. (1991). "Multiply-alkylated cyclopentanes (MACs): a new class of synthesized hydrocarbon fluids." Lubrication Engineering **47** (7): 586-591.
- Wade, W. H. and Blake, T. D. (1971). "Adsorption on flat surfaces. I. Gas phase autophobicity." The Journal of Physical Chemistry **75** (12): 1887-1892.
- Waltman, R. J., Khurshudov, A. and Tyndall, G. W. (2002). "Autophobic Dewetting of Perfluoropolyether Films on Amorphous-Nitrogenated Carbon Surfaces." Tribology Letters **12** (3): 163-169.
- Wang, M., Miyake, S. and Matsunuma, S. (2005). "Nanowear studies of PFPE lubricant on magnetic perpendicular recording DLC-film-coated disk by lateral oscillation test." Wear **259** (7-12): 1332-1342.
- Wang, W., Wang, Y., Bao, H., Xiong, B. and Bao, M. (2002). "Friction and wear properties in MEMS." Sensors and Actuators A: Physical **97-98** (0): 486-491.
- Wang, Y. and Baia, M. (2010a). Wettability Study of Multiply-Alkylated Cyclopentanes (MACs) on Silicon Substrates. Advanced Tribology. Luo, J., Meng, Y., Shao, T. and Zhao, Q., Springer Berlin Heidelberg: 102-103.

- Wang, Y., Mo, Y., Zhu, M. and Bai, M. (2010b). "Wettability and Nanotribological Property of Multiply Alkylated Cyclopentanes (MACs) on Silicon Substrates." Tribology Transactions **53** (2): 219 - 223.
- Wang, Y., Wang, L., Mo, Y. and Xue, Q. (2011). "Fabrication and Tribological Behavior of Patterned Multiply-Alkylated Cyclopentanes (MACs)–Octadecyltrichlorosilane (OTS) Dual-Component Film by a Soft Lithographic Approach." Tribology Letters **41** (1): 163-170.
- Wei, J., Fong, W., Bogy, D. and Bhatia, C. (1998). "The decomposition mechanisms of a perfluoropolyether at the head/disk interface of hard disk drives." Tribology Letters **5** (2): 203-209.
- Wenzel, R. N. (1936). "Resistance of Solid Surfaces to Wetting By Water." Industrial & Engineering Chemistry **28** (8): 988-994.
- Williams, J. A. (2001). "Friction and wear of rotating pivots in MEMS and other small scale devices." Wear **251** (1-12): 965-972.
- Yu, D., Guangya, Z., Koon Lin, C., Qingxin, Z., Hanhua, F. and Fook Siong, C. (2009). "A 2-DOF Circular-Resonator-Driven In-Plane Vibratory Grating Laser Scanner." Journal of Microelectromechanical Systems **18** (4): 892-904.
- Zhou, G., Cheo, K. K. L., Du, Y., Chau, F. S., Feng, H. and Zhang, Q. (2009a). "Hyperspectral imaging using a microelectrical-mechanical-systems-based in-plane vibratory grating scanner with a single photodetector." Opt. Lett. **34** (6): 764-766.
- Zhou, G., Logeeswaran, V. J. and Chau, F. S. (2009b). "Optical scanning using vibratory diffraction gratings." U. S. Patent 7542188.
- Zhu, Y. and Granick, S. (2001). "Rate-Dependent Slip of Newtonian Liquid at Smooth Surfaces." Physical Review Letters **87** (9): 096105.



Zisman W, A. (1964). Relation of the Equilibrium Contact Angle to Liquid and Solid Constitution. Contact Angle, Wettability, and Adhesion AMERICAN CHEMICAL SOCIETY. **43**: 1-51.